Addis Ababa University

Addis Ababa Institute of Technology

African Railway Centre of Excellence

MSc in Railway Engineering (Traction and Train Control)

Master's Thesis

On

Study of multiphase induction motor applicability in dc electrified conventional railway

By

Odette MANIRAMBONA

ID Number: GSR/3109/11

Advisor: Dr.Mengesha Mamo

Submission date:30/3/2022

Declaration

I, **Odette MANIRAMBONA**, declare that this research is my own work except where the acknowledgement was made in the text and that it has never to the best of my knowledge been submitted for an prior academic award or qualification.

Signed:  Date: 25/3/2022

Odette MANIRAMBONA

Email:manirambonaodette@gmail.com

Approval

The undersigned have examined the Thesis entitled **'Study of multiphase induction motor applicability in dc electrified conventional railway** 'Presented by **Odette MANIRAMBONA** a candidate for the degree of Master of Science in Railway Engineering (Traction and Train Control) and hereby certify that it is worth of acceptance.

Submitted by:

Odette Manirambona		30/3/2022
Student	Signature	Date

Approved by:

Mengesha Mamo (PhD)		31-3-22
Advisor	Signature	Date
Mr.Getu Gabisa		31/03/22
Examiner 1	Signature	Date
Chala Meiga (PhD)		02/Apr/2022
Examiner 2	Signature	Date
Mr.Birhanu Reesom Bistrat		02-Apr-2022
Chairperson	Signature	Date

Abstract

Power transmission to electric locomotives and railway vehicles can be carried out using DC or single-phase AC networks. The utility company supplies the railway company with AC voltage which can be used as either DC voltage or AC voltage depending on the different factors. Propulsion is provided by induction (AC) motors in both cases.

Conventional three-phase induction motor have been seen as the standard for electrical alternating current drives for industry and transport, although they have an inherent setback in terms of performance with regards to the loss of phase conditions. In view of this loss of phase, the three-phase induction engine does not provide sufficient operation, such as power output and torque, as required in electrical traction and other applications. Thus, the Multiphase machine has several advantages over the conventional three-phase motor such as cost-effectiveness, reduced torque pulsation, reduced harmonic current per rotor phase, high reliability and high fault tolerance.

The same machine parameters were used to simulate the system in Matlab/Simulink software using mathematical models to create the Simulink blocks in order to test the output of both three and six phase induction motors in DC traditional railway traction system. The study of the economical aspect of multiphase induction motor compared to three phase motor was also carried out. The V/F motor speed control technique was employed, in which the frequency and voltage decrease proportionally (their ratio remaining constant), while peak torque remains constant, resulting in speed control and an increase in starting torque up to the motor's maximum torque.

The distortion was shown to be higher in three phase motors than in six phase motors. The torque in six phase IM was seen to be 1.86 times that of three phase induction motor while the speed in three phase induction motor is 2.6 times that of six phase induction motor. The overall impact of multi-phase systems yields in a small reduction in price (-11%) according to the economic analysis of both motors.

As a result, using a multiphase induction motor in a DC railway would improve energy efficiency, and cost savings, as well as help to increase traditional railway capacity i.e. the number of trains that can travel over a given section of line during a given period of time.

Key words: *railway, three phase induction motor, voltage source inverter(VSI), six phase induction motor, v/f control technic.*

Acknowledgment

I would like to express my gratitude to all those who helped me in the course of my Master studies and the writing of this thesis. My sincere gratitude goes to my supervisor Dr. Mengesha Mamo for his helpful advice and suggestions during my research. His support and feedback has been instrumental in completing this research.

I also wish to express my gratitude to the Inter-University Council for East Africa(IUCEA) for the financial support to pursue this Master degree.

I offer my sincere thanks to my parents, especially my mother and siblings for their unwavering support and confidence in me all through these years.

My special thanks go to all my family, especially I dedicate this thesis to my Lovely husband

Munyaneza Pierre for his encouragement and patience throughout my study as well as my kids Ganza Keefa Frank and Shimwa Daniella for their unconditional love and patience.

Last but not least, I thank the Almighty God for His guidance and protection all through these years.

Table of content

LIST OF TABLES

LIST OF FIGURES

Abbreviations and Acronyms

Term	Explanation / Meaning / Definition
AC	Alternating current
AALRT	Addis Ababa Light Rail Transit
DC	Direct Current
DTIM	Dual three-phase winding induction motor
EMF	Electromotive Force
EMU	Electric Multiple Unit
HV	High Voltage
HPO	High Phase Order
IGBT	Insulated Gate Bipolar Transistor
IM	Induction Motor
IS	International Standard
IUCEA	Inter University Council for East Africa
MMF	Magneto Motive Force
PWM	Pulse Width Modulation
PMSM	permanent magnet synchronous machines
RMS	Root Mean Square
SVPWM	Space vector pulse width modulation

Term	**Explanation / Meaning / Definition**
AC	Alternating current
AALRT	Addis Ababa Light Rail Transit
SPIM	Six Phase Induction Motor
SRMs	self-reluctance motors
TPIM	Three phase induction motor
SPWM	Sine Pulse Width Modulation
VF	Voltage Frequency
VSI	Voltage Source Inverter

CHAPTER 1: INTRODUCTION

1.1 Background

The idea of rail electrification for propulsion purposes is not new; it began in 1804 with the invention of the steam locomotive, which was built in the United Kingdom by Richard Trevithick, and was followed by the invention of the diesel locomotive, which was followed by the invention of the battery-powered locomotive in 1837, but its widespread use was halted due to battery power's limited capacity. The tramway locomotive driven by the running rail was also introduced on 180Vdc. With the introduction of multiple-unit train control by Sprague in 1897, electricity soon became the preferred power source for subways.

In the early 1900s, the majority of street railways were electrified. The first practical AC electric locomotive was designed by Charles Brown, who then worked for Oerlikon in Zürich. In 1891, Brown used a three-phase AC to illustrate long-distance power transmission. [1].

The capacity and efficiency of the propulsion system (motor), which is the heart of the train, must be increased as the world's population grows. An electric vehicle's motor generates the necessary force to move the vehicle, making it the vehicle's core. [2].

As power semiconductor devices and digital controllers progress, multiphase machines are becoming more popular and gaining more scientific interest. In 1969, a five-phase voltage source inverter-fed induction motor drive was suggested [4], which was the first record of a multiphase motor drive. There was a steady but small interest in multiphase motor drives over the next 20 years.

The footstep started to accelerate in the 1990s, owing to advancements in electric ship propulsion, traction (including electric and hybrid electric vehicles), and the idea of a "more-electric" aircraft [3] . Electric vehicle manufacturers are able to overcome their traditional shortcomings as technology advances, making them more and more suitable for modern transportation.

Multiphase devices have many benefits, including improved magneto motive force (MMF) waveforms, lower supply voltages, and higher efficiencies, but they also have decreased torque bursts, lower losses, lower acoustic noise, and lower supply converter power ratings [6]. The DC conventional railway reliability and power will be improved by introducing six-phase

induction motor technology, as railway traction motors must meet higher efficiency, lower mass, longevity, and a wide range of speed controllability.

1.2 Advantages of multiphase induction machine drives

In high-power applications, multi-phase induction machine drives have many benefits over traditional three-phase induction machine drives:

a. Improved reliability, i.e. Since the two neutrals are held open, if one inverter fails, the motor continues to operate (but at a lower rating) while the continuity of operation is maintained.
b. Performance increases as losses are minimised and there are no circulating currents due to the harmonic reduction caused by the 30^{o} phase shift.
c. By using 30 degrees' phase displacement with the same air gap flux, the inverter dc bus voltage is decreased by about half (voltage connections are like star-delta because of 30 degrees' displacement) [6].

Six-phase motors have the greatest current effect on magneto motive force of all multiphase motors [15]. Six phase motors can be produced on the base of three-phase motor

1.3 Features distinguishing a railway traction drive from a standard industrial drive system

a. Environmental conditions (temperature, humidity, shock, vibration): Extreme weather events have an impact on all railway infrastructure components, including tracks, catenary, bridges, embankments, and tracks. In some circumstances, such as on the track, higher/lower temperatures, precipitation, and snowstorms may cause traffic problems and, in the worst-case scenario, track damage. As a result, an appropriate understanding of weather occurrences must be assessed during the planning, design, operation, and maintenance of railway infrastructure in order to increase the serviceability and life of the assets [4].

b. Supply system conditions (voltage level, "weak" line, line voltage tolerances): The standard procedure in railway power supply system investment planning is to forecast future traffic first, and then ensure that the power system is strong enough (the ability to keep the forecasted timetables, or to keep the minimum or average voltage levels above some threshold) for that specific traffic.

Forecasts, however, are not certain, and even if they were, it may be smarter to build the power supply to be more robust in the long run. On other cases, it may be prudent to limit future traffic levels due to overpriced power supply components. The entire planning process includes the selection of catenary type, the use of high voltage lines if applicable, the capacity of each converter station and the inter-converter-station distances.

c. Restrictions on space (e.g. low floor installations for EMUs) i.e. A better power-per volume ratio will allow more efficient vehicle design with more space for passengers but also more flexibility regarding, for example space requirements for cross border operation due to safety and control systems.

d. Restrictions on axle weight load [5] i.e. A better power-per-weight ratio is the path to go in order to provide less axle load and the basis for a more efficient vehicle design.

1.4 Problem statement

As previously stated, the utility company provides AC voltage to the railway company, which decides whether to use DC or AC voltage based on a variety of factors. In both cases, conventional three-phase induction engines have been used as the standard for electrical alternating current drives for industries and transportation over the years, despite the fact that they have an inherent setback in terms of efficiency with regards to the loss of phase conditions. The three-phase induction engine does not provide adequate operation, such as output power and torque, as needed in electrical traction and other applications, when loss of phase occurs.

As a result, multiphase machines can overcome these drawbacks as they have many advantages over traditional three-phase motors (which are currently used in railway traction systems), including reduced torque pulsation, lower per-phase rotor harmonic current, high reliability, and high fault tolerance [9]. i.e.

i. in a multiphase machine, stator excitation generates a field with a lower space-harmonic content, resulting in higher efficiency than in a three-phase machine.
ii. multiphase machines have a higher fault tolerance than three-phase machines, which ensures that if one phase of a three-phase system fails, the machine

becomes two-phase. It can continue to run, but it will need some external assistance to get started, and it will need to be massively de-rated. But if one or three phase of a six-phase system is open circuited, it can self-start and operate with only minor de-rating.

iii. multiphase machines are less vulnerable to time-harmonic components in the excitation waveform than their three-phase counterparts. Pulsating torques are generated by such excitation components at even multiples of the fundamental excitation frequency.

As a result of all of these features, noise characteristics are better when compared to three-phase motor drives [5]. As compared to a three-phase motor drive, using multiphase motor variable-speed drives allows for a reduction in the necessary rating of power electronic components for a given motor output power, an aspect that becomes extremely important in high power drives [10]. Therefore, employing multiphase induction motor in DC railway will enhance the railway energy efficiency as well as the reduction in energy bill and help to boost the conventional railway capacity.

1.5 Objectives

1.5.1 General Objectives

The main objective of this research is to study the applicability of multiphase induction motor technology in DC electrified railway.

1.5.2 Specific Objectives

i. To establish the matlab blocks for both six phase and three phase induction motor drives and simulate the system.
ii. To compare the two induction motor drives in terms of performance.
iii. To perform an economic analysis of both three phase and six phase induction motors in DC railway systems.

1.6 Scope

This study focused on establishing mathematical models for three and six-phase induction motors, as well as modelling three-phase and multiphase inverter-fed induction motor blocks.

The performance of a six-phase induction motor was compared to that of a three-phase induction motor currently in use, and the results were discussed in order to determine what could be used in a railway propulsion system.

1.7 Structure of the Thesis

The first phase of this thesis involved establishment of mathematical model for both three and six phase induction motors, which was then used to create a matlab model. The tinycad software was used to assist in circuit drawings by using a mathematical model. The model was simulated in Matlab/Simulink by inserting motor specifications, and the results were discussed.

The thesis is divided into five chapters, which are as follows:
Chapter 1 of the thesis is the introduction. It describes the research's background, the problem statement, and presents the goals of the study in terms of General and Specific Objectives.

Chapter 2 provides a review of the current literature in this field of study. It describes the operating principles of both Induction motors (three and six phase motors), variable speed drives feature as well as their control technics. Finally, this chapter discusses some related works as well as research gaps that have been identified.

Chapter 3 presents the methodology and procedures used to achieve the objectives described in Chapter 1. It entails system modelling according to the mathematical models, and data collection.

Chapter 4 provides a detailed analysis and discussion of the study's findings in relation to the objectives and methodologies described in the previous chapters.
The conclusion, and recommendations are presented in Chapter 5.

CHAPTER 2: LITERATURE REVIEW

2.1 Introduction

Multiphase induction motors have received a lot of attention in the manufacturing world because they have a lot of advantages over three phase motors. Studying its application in the railway industry by developing and simulating models and comparing their results would improve its reliability, performance, energy bill reduction, and railway capacity. Six-phase motors are divided into two types: symmetrical and asymmetrical winding configurations.

A six-phase machine can be thought of as two separate three-phase machines connected in series for asymmetrical winding configuration, and it can be controlled like a traditional three-phase machine and symmetrical machines can have six phase stator windings with three or six phase rotor windings. In industrial applications where high efficiency is needed, a multi-phase induction motor is used instead of a traditional three-phase induction motor. The most common kind of multiphase machine is the six-phase induction motor.

2.2 Six phase induction motor working principle

Their operating theory is as follows: Six phase induction motors, like three phase induction motors, operate by applying Faraday's law and Lorentz force to the conductor. When the stator winding receives a six-phase ac supply, a spinning magnetic field is formed that rotates at synchronous speed. When a short circuited rotor (squirrel cage) is placed in a rotating magnetic field, electromagnetic induction induces an electromotive force (EMF) in the rotor conductor [6]. Current continues to circulate in the rotor conductor as a result of the EMF, which produces its own magnetic field. The interaction between these two magnetic fields generates a force that rotates the conductor. The induction motor's field winding is installed in the stator, which is excited by a six-leg inverter as shown in the figure 2.1 below. The stator winding of an n-phase machine can be built in such a way that the spatial displacement between any two successive stator phases equals, $\alpha = 2\pi/n$ in the case of a symmetrical multiphase machine.

In a symmetrical multiphase machine, the two sets of three phase windings are 60^o apart, and in an unsymmetrical configuration, they are 30^o apart [7] .

In split phase electric machines [13], two similar stator windings share the same magnetic circuit, with two, three phase winding groups separated by 30°, i.e. the 60^0 phase belt is split into two parts, each spanning 30^0, which eliminates (6n +1) order harmonics (torque and air gap flux) as well as rotor copper losses where n=1,3,5, etc. [8]

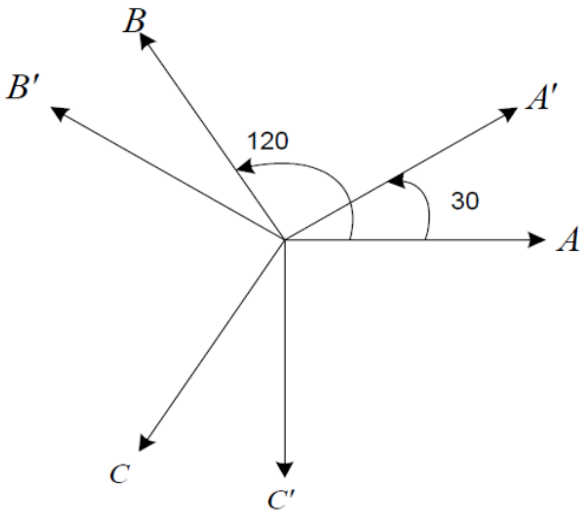

Figure 2.1Split phase motor phasor diagram

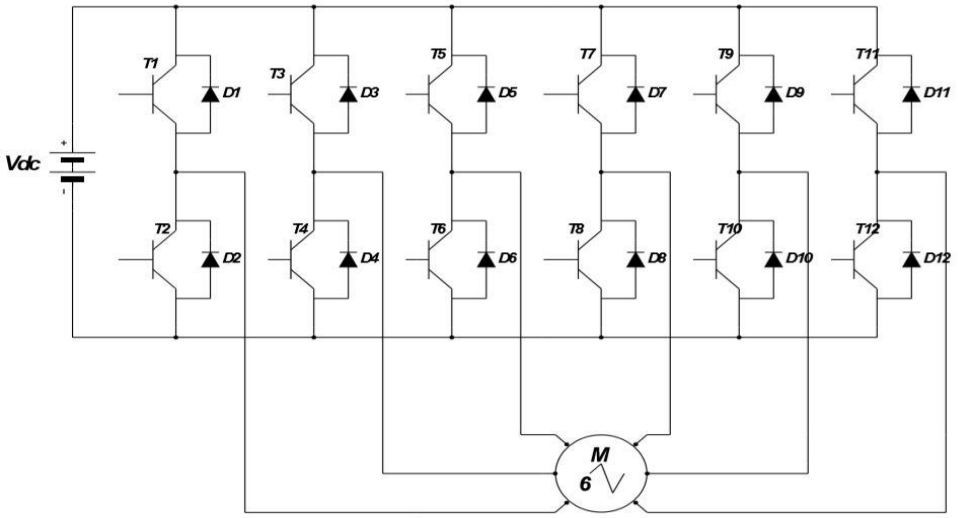

Figure 2.2. Six phase VSI fed induction motor

2.3 Multiphase variable-speed drives feature

a. For a given machine's output power, using more than three phases allows the power to be split over a greater number of inverter legs, allowing lower-rated semiconductor switches to be used.

b. Multiphase machines have a much higher fault tolerance than three-phase machines due to their greater number of phases, which becomes impossible if one phase of a three-phase system becomes open-circuited, but it is not a problem in a multiphase machine as long as no more than (n - 3) phases are faulted. Where n represents the number of phases [9]. Independent flux and torque control necessitates the ability to control two currents independently.

2.4 Related works

Archana et al. [6] as part of their research on "Control of Planned Developed Six Phase Induction Motor," they decided to design and construct a six phase prototype induction motor free of third harmonic current injection for torque improvement." The objective of their research was to use vector control to control the speed of a prototype six-phase induction motor with arbitrary phase displacement. In a nutshell, their study focused on the design, development, and testing of a six-phase prototype induction motor, followed by the control of the same motor. During the prototype's testing, they concluded that there is no standard test for six phase induction motors. This is because the same repetitive checks that are performed on their three phase prototype are also performed on their six phase prototype. That is the equivalent of two three-phase induction motors with the same magnetic circuit and shaft, but electrically separated. As a result, routine assessments were carried out in compliance with IS requirements, one by one, using two three-phase sets (for example, ABC and XYZ).

The prototype was put through a number of tests, including a high-voltage test, an insulation resistance test, a no-load test, a blocked rotor test, a temperature rise test, and a load test. Both of these experiments were passed by the prototype six-phase induction motor. The motor was tested with a single three-phase Voltage Source Inverter for speed control. This was done to see if the built six-phase motor was suitable for variable-frequency operation. The current waveforms in three and six phases were obtained and compared. The current in a six-phase system is double that of a three-phase system. Two inverters were used for the actual power, but they were synchronised. It was discovered at the end of their research that no third harmonic current injection or current sensor was needed for torque improvement. The torque of this prototype six phase induction motor was discovered to be 1.6 times that of a three phase induction motor.

Other advantages of a prototype six-phase induction motor include increased reliability (if one inverter fails, the motor continues to operate at a lower rating, maintaining operation continuity while the two neutrals are held open) and reduced losses (i.e., efficiency is improved since there are no circulating currents due to harmonic reduction because of 30 degrees.) Control was cost-effective since sensorless vector control was used. It is critical to recognise that motor design is incomplete unless the speed can be controlled, which was achieved in their study. The study had two significant drawbacks: for higher ratings, the motor and thus the inverter must be much larger, potentially raising the total cost.

Second, while sensorless vector control is cost-effective, the parameter variation issue, particularly near zero speed, imposes a challenge to speed estimation accuracy.

E. Levi, et al [3] in their research on "Multiphase induction motor drives-a technology status review," The advantages of multiphase induction machines, such as the use of multiphase motor variable-speed drives, were shown compared to a three-phase motor drive, to reduce the necessary power electronic component rating for the provided motor output power and to increase the noise characteristics of the motor output power. Multi-phase induction machines were modelled, as well as simple vector control and direct torque control systems, and multi-phase voltage source inverter PWM control.

A comprehensive description of control methods for five-phase and asymmetrical six-phase induction motor drives has been included by the authors. The experimental results revealed that as the number of phases increased, the order of the m.m.f harmonics generated by the stator excitation, also known as phase belt harmonics, increased as well. The magnitude of these harmonic components was also found to be inversely proportional to the number of poles, implying that the size of the motor decreases as the number of poles increases.

Renato et al [10] In their research on “Torque density improvement in a six-phase induction motor with third harmonic current injection” the torque density enhancement strategy was applied by injecting current to overcome the third harmonic component, i.e. injecting third harmonic zero sequence current components into the phase currents, which greatly increases the system torque density. Analytical, finite element, and experimental findings were presented to illustrate the device's function as well as the rise in torque density. The suggested scheme was tested experimentally to demonstrate the expected torque increase. It is shown that the current sharing between the two three-phase classes is unequal for voltage-fed systems and can cause problems.

This methodology has shown that with the same peak flux distribution as a traditional three-phase method, a gain of up to 40% in torque output can be estimated using analytical analysis, assuming the saturation of the stator teeth as the flux density constraint.

Finite element analysis was used to show the behaviour of the air gap and core flux with third harmonic currents. This research is especially critical for accurately mapping the action of a machine's flux in places where direct calculation is difficult.

The experimental findings show that by increasing the fundamental portion of current and flux, the torque can be increased with the third harmonic current injection with the same air gap peak flux density. These observations help the theoretical study and promote further studies into the system.

Apsley et al [11] in their research on “Analysis of multi-phase induction machines with winding faults” presented generalised harmonic analysis techniques for simulating the steady-state behaviour of a multi-phase squirrel cage induction motor with some kind of stator winding open-circuit or short-circuit fault. A 4-pole machine with a 48-slot stator was used to verify the analytical model. Each coil of this machine's stator winding was connected to a patch-board, allowing for single-phase, two-phase, three-phase, four-phase, six-phase, or twelve-phase excitation configurations of the stator. The experimental findings were compared to computer forecasts for a six-phase machine with both open-circuit and short-circuit faults.
Generalized harmonic analysis approaches have been shown to provide reliable performance forecasts in multi-phase cage induction machines for some kind of stator open circuit or short-circuit fault. Simple motor architecture solutions to improve fault tolerance have been evaluated using the model. The inherent fault-tolerance of the multiphase motor was shown in the case of an open-circuit fault, as the current in adjacent phases increased to compensate for the mmf that should have been generated by the faulted phase.

P. Venter et al [12]in their research on “Realization of a “3 & 6 Phase” Induction Machine” High phase order (HPO) machines have shown to have many advantages over their three phase counterparts, including decreased torque ripple, smaller current per phase with the same rating, and, most importantly, fault tolerance. HPO induction machines' ability to operate in the event of a single or even two-phase open circuit fault allows for a safe "limp home" operation, which is very useful in train and ship propulsion.
As the name implies, a symmetrical six phase induction machine (SPIM) has six phase windings symmetrically displaced at 60° angle around the stator diameter. This is a unique structure that can be used to operate as three-phase or six-phase systems. The unit can be used as a six phase induction motor with a sinusoidal six phase voltage source or a six phase inverter when designed in its usual configuration. In the case of inverter-fed drives, it is usually preferred to feed the system with six single-phase inverters, which improves the drive's reliability. The angle of winding between each second winding is 120°.

This means that the original six-phase structure can be separated into two three-phase winding sets, making for a wider variety of applications.

As a consequence, this system can be used to build several three-phase systems, such as a three-phase motor, a three-phase motor with reactive power injection, a three-phase transformer, and a simultaneous three-phase motor and transformer. The three phase stator winding of a traditional three phase system can be removed and a newly constructed six phase winding wound in the stator slots to develop a prototype of this "3 & 6 phase" induction machine. The six windings must be terminated externally on both sides. This will allow the system to be configured as various devices by adjusting the stator winding terminal configurations. A 120° displacement occurs between the second winding of an SPIM machine. This means that a symmetrical six-phase machine's stator windings can be divided into two three-phase windings with a 60-degree separation between them.

In their study "Modeling and Analysis of Asymmetrically wound 6-phase Induction Motor for Improved Performance," Prabhat Kumar et al [19] presented a dynamic model of the motor in a d-q asynchronously rotating reference frame in which they assumed that there is no friction and winding loss in the system, no core losses and magnetic saturation in the core, and the air gap is uniform and winding are sinusoidally distributed around the air gap.

They developed a mathematical model for three and six phase induction motors and simulated them in Matlab/Simulink software, assessing electromagnetic torque response under full load, speed response under full load, and per phase stator current response under full load. The below are the advantages of a six-phase induction motor over a three-phase induction motor:

i. The per-phase stator current amplitude is decreased without raising the per-phase voltage.
ii. The efficiency of a six-phase induction motor is higher than that of a three-phase induction motor.
iii. The torque per ampere is increased as the required power is split into several phases, increasing the power handling capacity.
iv. Harmonic distortion is lower in stator current.
v. The speed variation from no load to full load is less than for a three-phase induction motor.
vi. In the stator winding, there is less copper loss per phase. The settling time is shorter than for a three-phase induction motor, which means the transient duration is shorter.

Hanan Mikhael D et al. [20] found that three phase induction motors are the most commonly used for industrial control and automation in their study "Speed Control of Induction Motor Using PI and V/F Scalar Vector Controllers." Because of their robustness, reliability, low maintenance, and high durability, induction motor are usually referred to as the workhorse of the motion industries. The two main types of IM variable frequency control methods are scalar control and vector control approaches. Scalar control, also known as V/F control, is a very simplistic structure that is usually used without speed feedback. However, due to the fact that the stator flux and torque are not directly controlled, this controller does not achieve good accuracy in both speed and torque responses. The key aim of the control system is to independently control the torque and flux, much as in separately exited DC machines. This is achieved by selecting a d-q rotating reference frame that rotates synchronously with the rotor flux space vector.

A voltage source inverter (VSI) should have a stiff voltage source at the input, which means the thevenin impedance should be as low as possible. A big capacitor could be attached at the input if the voltage source is not stiff. The inverter is operated by a DC voltage source (either a battery or a diode-based bridge rectifier) via an LC or C filter and consists of power bridge devices with three output legs, each consisting of two power switches and two freewheeling diodes. The PWM control scheme used was SVPWM. The Space Vector Pulse Width Modulation (SVPWM) approach is a sophisticated, computationally intensive PWM technique that could be the best of all PWM techniques for variable frequency drive applications. It has a high dc-bus voltage usage and low overall harmonic distortion(THD) as opposed to other PWM approaches. SVPWM is more suited for digital application in the linear modulation spectrum and will increase the overall output voltage, with the maximum line voltage reaching 70.7 percent of the DC link voltage.

In addition, the use of V/F scalar vector and PI controllers to control induction motor speed was demonstrated. Many techniques, such as scalar controller (V/F) and vector controller (Field oriented control and direct torque control) using PI, intelligent controller, and so on, can be used to improve the output of an induction motor drive. The V/F control is dependent on the presence of voltage derivatives in the stator. They found that closed loop V/F control provides a better response and outcome than open loop V/F control of an induction motor based on their experiments and findings.

With a variable Voltage-Variable Frequency (V/F) base torque-speed control, a three phase induction motor fed by a PWM Voltage Source Inverter was simulated. The pulse width modulated output signals of a 2-Level Voltage Source Inverter driving a three phase induction motor were generated using the PWM technique, which involves modulating a standard sinusoidal reference signal with a triangular carrier to produce pulse width modulated output signals. As a result, the output of a three-phase induction motor fed by a PWM voltage source inverter was simulated in terms of inverter phase current, rotor and stator current, rpm, and inverter electromagnetic torque. Simulation findings showed the reliability and feasibility of a constant V/F induction motor drive. The actual speed follows the reference speed, and as the speed changes from high to low and low to high, the voltage and current profiles adjust appropriately.

The overall V/F control implementation methodology has been given. The PWM Inverter is one of the scheme's most fundamental needs. PWM inverters were modelled and their outputs were fed to the Induction Motor drives in their research. The induction motor's uncontrolled transient and steady state responses have been obtained and analysed. The research also revealed that there are two control methods: scalar control and vector control, all of which have benefits and drawbacks. Scalar control is a low-cost, easy-to-implement method. Many systems in the industry use this control technique because of its benefits and simplicity. However, owing of its slow response to transients, it is insufficient for controlling dynamic drives.

This is the case because the V/f constant technique controls frequency and voltages rather than the phase and amplitude of currents. It is a low-performance control approach that is also stable. The field oriented control approach regulates currents, allowing for quicker responses. This approach meets the requirements of dynamic drives that require fast response. It is a great control method for dealing with transients. Its drawback is its complexity, as well as the high cost of the driver circuit. It is, however, a high-performance control technique. Both techniques can be used at the nominal speed without reducing torque.

In their study “An Overview on Performance improvement of an Induction Motors (IM) – A Review,” Vijayakumar.R et.al [21] addressed Improvements in IM efficiency, IM torque control techniques, and IM speed control approaches. Even if an induction motor has already been designed, it is feasible to increase efficiency in a Variable Speed Drive (VSD) application by properly controlling the magnetic flux (Voltage/frequency ratio) to reduce overall losses to a minimum, especially at low speeds.

The cost of the motor seems to rise as the cost of each individual loss is reduced. Temperature rise can also be improved in certain situations to minimise mechanical losses. Start current, torque, and power factor are all influenced in some circumstances. As a result, induction motor designers and researchers face a difficult task in reducing losses while keeping prices low and increasing total motor performance, which includes noise, vibration, temperature rise, starting current and torque, and power factor, among other things.

The two most common sensor-less torque control methods in IM are field oriented control (FOC) and direct torque control. Unlike FOC, DTC does not need coordinate transformation, PWM signal generators, current controllers, or a position encoder, all of which introduce delays and require the usage of a mechanical transducer. Despite its simplicity, DTC enables rapid instantaneous torque control in the steady state and under transient operating conditions using a basic control structure. Since an electric vehicle drive system must have a rapid torque response, affordable cost, reliability, and durability, the DTC of IM seems to be highly useful for electric vehicle applications. DTC is a low-cost technique since no mechanical speed sensors are required at the motor shaft. Voltages and currents measured at the motor terminal are used to estimate rotor speed.

As a consequence, it can minimise the drive machine's hardware complexity and size, eliminate the sensor cable, enhance noise invulnerability, improve reliability, and minimise maintenance costs in electric vehicle applications. Despite its simplicity, the basic DTC scheme based on hysteresis controllers has a number of significant disadvantages, including variable inverter switching frequency, high torque ripple, and the requirement for a high-speed processor. The two speed control methods for induction motors are scalar and vector control, with the v/f form being the most commonly used scalar control system, in which the motor is fed with variable frequency signals provided by PWM control from an inverter. The V/f ratio is kept constant in the operating range to ensure constant torque. The term scalar control comes from the fact that only the magnitudes of the input variable-frequency and voltage are controlled.

Ahmed Fathy Abouzeid et.al [13] in their research on ‘Strategies for Induction Motors in Railway Traction Applications’ According to the study, the VSI fed IM drive is currently the preferred choice in traction systems for railways due to benefits such as improved robustness, lower cost, and lower maintenance requirements. Furthermore, precise control of the IM torque-speed is now possible thanks to the invention of modern power devices and digital signal processors, as well as advancements in AC-driven control methods.

The electric motor and the inverter are the two most important components of a traction mechanism. The number of traction motors, motor capacity, inverter rating strength, cooling system, and other factors that go into developing a cost-effective traction system for a specific application are all determined by a complex, iterative process.

The control and modulation techniques must be established after the physical elements of the traction mechanism that have been defined. Furthermore, since the traction system must meet a variety of specifications, a dynamic iterative procedure might be needed in that situation. These include those imposed by desired train performance (e.g., torque-speed characteristic, maximum torque and speed, acceleration/deceleration times, and so on), electric drive performance (e.g., machine and inverter efficiency, temperature limits, maximum torque ripple, and so on), existing standards (e.g., electromagnetic interference, acoustic noise, and so on), and so on.

These objectives, however, can always conflict. Low switching frequencies are utilised to decrease inverter losses, however this results in increased losses and severe torque pulsations in the motor, as well as affecting dynamic response and drive stability.

There are two sorts of control methods for induction motors:

Induction motor scalar based control

i. Open loop V/F

It changes the amplitude of the voltage proportionally to the frequency. As a consequence, there is an almost constant flux. Its drawback is that due to slip, the rotor speed cannot be precisely controlled. Furthermore, an inappropriate voltage to frequency ratio, voltage decrease in stator resistance, and variation in the DC link voltage feeding the inverter can result in incorrect flux values, causing the machine's operating point to deviate from the desired value.

ii. V/F with feedback control

In IM traction drives, closed-loop speed control with slip regulation is commonly used. Speed error generates the slip command through a proportional-integrator (PI) controller, which when added to the measured speed produces the stator voltage's angular frequency.

Induction motor vector based control

Vector control methods are designed to manipulate the IM fields and torque directly. These approaches are focused on well-known d-q models.

In a synchronous reference frame, FOC represents flux and torque as a function of stator currents, with high bandwidth current regulators supplying the voltage command to the inverter. Direct torque control (DTC) techniques, on the other hand, use torque and flux controllers to give the inverter with IGBT gate signals without the need for particular stator current control.

In their research on "modelling approaches for an asymmetrical six-phase machine," M.zabaleta et al. [23] focused on model transformation in ac machines to obtain a new set of equations, typically less in number and less complex in nature, that accurately represented the machine's behavior as the original equations. The model transformation, which was first used on three-phase machines, involves referring the equations to a new reference frame made up of three mutually orthogonal axes. Two of them are placed in the machine's cross-sectional plane and are often referred to as α-β (Stationary axis) or d-q (Synchronously rotating axis). They are the flux/torque generating subspace (α-β subspace hereinafter), which represents electromagnetic energy transfer across the air gap. The zero sequence components are represented by the third axis, which is typically denoted as 0, which is seldom used since the neutral point of ac rotating machines is usually left isolated. Extensive research on multiphase machine applications in electric vehicles, aerospace, and ship propulsion has recently revealed some of the advantages of multiphase machines and drives.

The basic concept of the model transformations is kept the same in multiphase machines with near-sinusoidal magnetomotive force (m.m.f.) distributions, but due to the increase in the dimension of the system, it adds additional degrees of freedom. The electromagnetic energy flow through the airgap is represented by a - subspace once more, but there are additional, mutually orthogonal subspaces whose components do not contribute to the energy transfer (x-y subspaces).

Multiphase machines with near sinusoidal m.m.f can be divided into two categories, regardless of whether they are synchronous or induction machines:

a. Machines having a prime number of phases, a single neutral point, and a spatial shift equal to 2p/n between any two subsequent phases.
b. Machines with an odd number of phases or a composite odd number of phases, built with k windings, each with a phase and a single or k neutral point. There might be a spatial shift between the first phases of k windings with phases equal to 2π/n (symmetrical machines) or π/n (asymmetrical machines) in such machines.

A situation with a = 3, in which the total number of phases is n = 3k, is a common design that is normally of interest.

They examined an asymmetrical six-phase machine with a 30° spatial shift between two three-phase windings (n = 6, k = 2, a = 3) in a typical configuration with two independent neutral points (n = 6, k = 2, a = 3).

The double d-q transformation was derived directly from that of three-phase machines, and its implementation was simple and straightforward. In the other hand, since it treats each of the three-phase systems independently, it has several disadvantages. This establishes two parallel subspaces to which all information is mapped, making it impossible to isolate mutual interactions between them; as a result, compensation becomes complicated.

Kamalesh Hatua et.al [14] in their work "Direct Torque Control Schemes for Split-phase Induction Machine(SPIM)," they developed two types of direct torque control for split phase induction machines: resultant flux control technique and individual flux control method. The torque ripple in SPIM could be greatly decreased without raising the switching frequency, according to the findings. Because of the lower switching frequency of operation in current source inverter (CSI) application, sixth harmonic torque pulsations were prominent in early eighties. Sixth harmonic torque pulsations are produced by the interaction of the fundamental flux with the fifth and seventh harmonic rotor currents. To eliminate sixth harmonic torque pulsations, a split phase induction machine (SPIM) configuration was developed. SPIM is equipped with two three-phase winding pairs.

In this design, sixth harmonic torque pulsations produced by the two sets of windings are in phase opposition. As a result, SPIM lacks sixth harmonic torque pulsations. The SPIM is powered by two voltage source inverters that operate independently of one another. Because of the invention of the IGBT, inverters now switch at considerably higher frequencies than fundamental. As a result, low-order harmonics are almost non-existent in induction machine drive. As a consequence, sixth harmonic torque pulsations have been eliminated. SPIM has the following advantages:

i. In the SPIM, full flux linkage may be achieved by supplying about half the rated voltage of the original three phase machine to each half winding. This functionality is appropriate for high-power, traction, and electric vehicle applications.
ii. As compared to a three-phase induction machine, the M.m.f profile of SPIM is smoother.

iii. When compared to a three-phase induction machine, the SPIM has more control possibilities. The control options of SPIM were properly used in this paper to develop the DTC technique. Torque ripple was observed to be greatly decreased in SPIM.

The split phase induction motor drive is constructed in such a way that SPIM generates two sets of stator coils divided by thirty degrees electrically. A2B2C2 winding group's supply is thirty degrees ahead of A1B1C1 winding group's supply. Individual m.m.fs produced by each set of windings can algebraically add up to produce resultant m.m.fs when SPIM is used in this manner. Because of the split winding design, if there are any 5th and 7th harmonic components in the voltage, no 5th and 7th harmonic rotor currents will be created. This equipment is capable of almost eliminating sixth harmonic torque pulsations. In the present DTC designs, the system is powered by two independent two-level voltage source inverters. They use the same D.C. bus. Both sets of windings' neutrals are kept isolated as represented in figure 2.3 below.

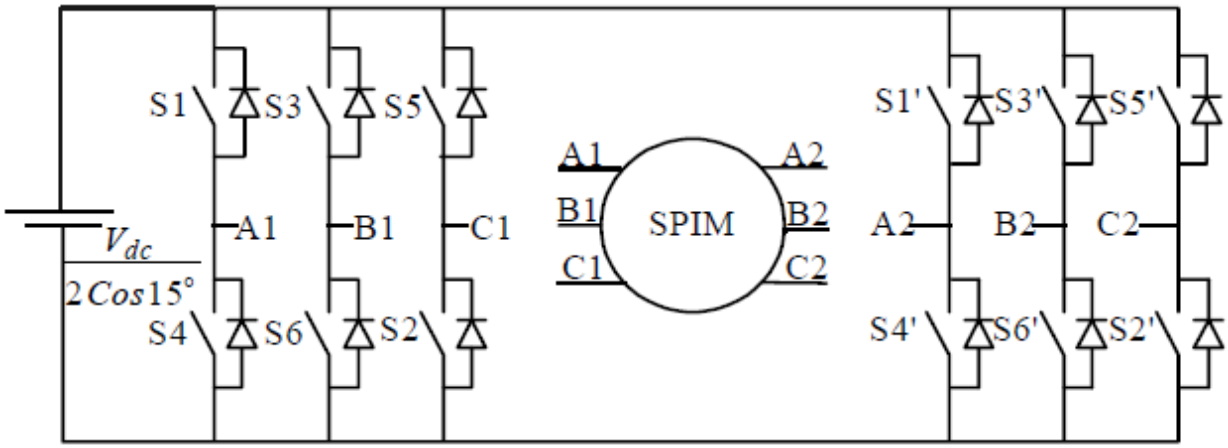

Figure 2.3. SPIM drive[6]

The resultant flux method of direct torque control in SPIM has some advantages and disadvantages.

i. Advantages

The use of vectors from the outermost twelve-sided polygon, higher speed range can be achieved with rated flux. In comparison to three-phase DTC, the angular separation between active voltage vectors and stator flux for traditional three-phase DTC ranges from 90^o to 30^o or 90^o to 150^o. However, the variations of this system are from 90^o to 60^o or 90^o to 120^o. As a result, when compared to three-phase DTC, the torque response in the Resultant flux control method is faster.

ii. **Disadvantages**

The lack of direct control over individual fluxes. As a result, they have a dc drift tendency. to solve this problem, a low pass filter is used instead of a pure integrator.

Low order harmonics, especially the 5th and 7th, can be found in both fluxes. The 5th and 7th harmonic impedances are negligible in SPIM. As a result, the machine draws a lot of stator harmonic currents, increasing stator harmonic loss.

Both inverters are moved from their respective hexagonal space vector positions in the Individual flux control method to keep the individual and resultant flux magnitudes constant at their respective reference values.

The stator resistance and leakage reactance of the DTIM are lower than those of the three-phase machine, according to Chinmaya K. A et al [15] in their research on "Analysis of space vector PWM techniques for dual three-phase induction machine", which reduces the capacity to restrain stator harmonic currents. Using pulse width modulation (PWM) techniques to monitor the harmonic spectrum of the output voltage, inverter output performance may be enhanced. Space vector pulse width modulation (SVPWM) methods can be utilized to improve the inverter's output voltage spectrum while reducing stator harmonic currents and torque pulsation.

Despite the fact that sinusoidal pulse width modulation (SPWM) is the most common switching technique due to its ease of implementation, it is unable to fully exploit the available DC bus voltage. This technique can also be used to increase DC bus usage by injecting sufficient harmonics into the arbitrated signal, similar to third harmonic injection PWM in three-phase inverters. However, as the number of phases increases, the effect becomes weaker. Space vector pulse width modulation (SVPWM) is a typical control method for voltage source inverters.

A space vector modulation method should fulfil certain requirements, such as keeping a constant switching frequency and preventing undesired converter switching, in order to decrease switching losses. It is necessary to make full use of the available DC bus voltage. In order to reach the maximum level of sinusoidal voltage, lower order harmonics in the output voltage must be reduced. The author concluded that the conventional SVPWM method includes lower order harmonics in the phase current since only two active vectors are chosen for synthesising the reference voltage after comparing the SVPWM technique methods. while the vector space decomposition method effectively removes lower order harmonics, its implementation can be very difficult because computation requires either the inverse calculation of a 5×5 matrix or the use of a large look up table. In terms of DC bus use and removal of lower order harmonics, the vector classification SVPWM approach is very well, and the volt-second balance of the d2-q2 plane inherently becomes zero, which is similar to VSD SVPWM. As a result, this method's implementation is simple and convenient.

Igor Bolvashenkov et.al [15] in their "Methodology for Selection and Application of Vehicle Propulsion Systems," study found that the ongoing need of electrical drive trains demands that electric machines be appropriately selected for application. The comparison took into consideration applications like aircraft, cars, ships and trains and the need for various weighted criteria for each electric vehicle. The study found that they do not produce very much noise and vibration compared to other machine types, starting with the induction motors. However, production costs are comparatively small and there is a high capacity to operate in hostile areas. In addition, the power operation is limited, which means that efficiency at lower speeds is lower and power at higher speeds is lower. The rotor without excitation coils or permanent magnets (PMs) in the rotor is fitted with self-reluctance motors (SRMs). Some of the benefits of SRM are low maintenance and low cost of production, since the rotor does not require excitement, thus reducing rotor losses. Furthermore, the control is easy and the reliability compared to the other machines is high. Furthermore, SRMs provide thermal stability and have a reasonably high capacity for overload. SRMs, on the other hand, have high torque ripples and hence produce more noise and vibrations. Permanent internal magnets are used in permanent magnet synchronous machines (PMSM). In comparison to all other machine types, the PMSM has a high power density and nominal speed efficiency. Furthermore, because there are no copper losses owing to the absence of rotor windings, less cooling is required. A PMSM may be implemented in a smaller volume while delivering the same speed and power as an SRM. Because of the utilization of rare earths, the price is high. When considering the modes of service, design characteristics, and technological specifications of electric drive trains, the criteria for railway application fall somewhere between car and ship application. The weight, volume, size, and noise specifications are more stringent than the requirements imposed on the ship's traction motors. At the same time, they are softer than cars. The study's findings indicate that, despite the very similar total values of complex indices, the PMSM outperforms the IM and SRM. However, in today's world of mass manufacturing, PMSMs (Alstom) and IMs (Siemens) are used as traction motors. Induction motors are commonly used in industries, transportation systems, and other real life applications for a variety of reasons, including high reliability, robustness, low cost effectiveness, higher torque, and low maintenance as opposed to other rotating machines.

R. S. Miranda et al. [17] conducted research on the “modelling and analysis of a six-phase induction machine under fault condition.” The study of the six-phase motor drive induction system was presented, with a focus on inverter electrical faults. To analyze the dynamic behavior of a multi-phase machine in a fault condition, a simple model was defined.

Despite the fact that many modern drives are extremely reliable, the inverter can produce a number of faults. The power converter is highly vulnerable to short and open circuit faults in various parts of the converter. The faults considered in this study were switch short circuit analysis, open switch fault analysis, and open phase analysis, in which the short-circuit state is followed by excessive power dissipation in the switch due to a rise in temperature, causing the device to stay closed.

This failure is mostly caused by a short circuit at the load end. Depending on the failure mode of the device, the processes that lead to a switch breakdown can differ. When this malfunction happens, the other switch in the same leg must be automatically turned off to prevent it from passing through. When a switch is open or one of the inverter switches fails, the engine phase is only connected to the DC bus through free-wheeling diodes. This error might be caused by damage to the base drive device. The misfiring of the switch reduces the topology of the pole inverter, and the voltage in phase is determined by the phase current and the switching pattern of the second switch in the same inverter leg. When one of the motor phases fails due to an open circuit, the phase is completely removed from the DC bus.

A mechanical failure of the machine terminal connector, an internal winding rupture, or an electrical failure in one of the inverter phase legs may all cause this form of fault. After six phase simulation under fault conditions, it was discovered that the fault, whether short circuit or open circuit, reflects an undesirable operating state, causing low-frequency torque oscillations and possibly causing significant harm to the drive device. However, the presence of more than three phases allows for the implementation of various techniques for post-fault operation in order to enhance system stability.

CHAPTER 3: METHODOLOGY

3.1 Introduction

This chapter describes methods used to study the applicability of multiphase induction motor technology in DC electrified railway in which the Matlab/Simulink was used. To get matlab models, the following steps were followed.

Step1: Data collection about the three phase induction motor specifications

According to three phase induction motor, the simulation was done by using HP (Horse power) shaft output, supply voltage, current, mechanical speed, coil resistance at a certain temperature, inductances (stator and rotor), frequency, inertia etc. [16][17] obtained from addis ababa light rail corporation, Kality deport as presented by **Yared Kassahun Abadi** in table 3.1 below.

Table 3.1Sample motor Parameters

Parameter	**Value**	**Parameter**	**Value**
Rated power	130KW	Rated efficiency	0.924
Rated voltage	500V	Weight	440±3%kg
Rated current	215A	Rs (stator coil resistance)	0.1968 ohms
Rated frequency	91Hz	Ls (stator coil inductance)	0.00182 henry
No of Poles	6	Xs(stator coil reactance)	0.10400936 ohms
Rated rotating speed	1800r/min	Rr'(rotor coil resistance)	0.164 ohms
Rated rotating speed	188.4 rad/s	Lr'(rotor coil inductance)	0.00152 henry
Synchronous Speed	1820r/min	Xr (rotor coil reactance)	0.08686496 ohms
Synchronous Speed	190.5 rad/sec	Lm(core inductance)	0.001599henry
Rated torque	689N·m	Llm(stator Mutual leakage inductance)	0.0001599henry
DC voltage	750V	Moment of inertia	0.089kg.m^2
Reference speed	600rpm		
Load torque	30N.m		

Step2: Three and six phase induction motor mathematical model

The dynamic analysis of both motors was performed and used to generate matlab models to be simulated in order to get the results. Here the squirrel cage motor was used.

Step3: V/f control method

The v/f as one of motor speed control methods, was chosen to be used due to its simplistic structure, easy to implement and it is the one currently in use by addis ababa light rail transit(AALRT) company.

Step4: PWM (Pulse Width Modulation)

Pulse width modulation was chosen as the inverter output voltage control technique i.e to generate a gate pulse signal.

Step5: Inverter

The type of inverter was chosen according to the type of load (180^o conduction mode), the switches to be used were also chosen for getting higher efficient, reliable and faster dynamic response.

3.2 Mathematical model for both three and six phase induction motors

3.2.1 Three phase induction motor

Torque and Speed Calculations

An induction motor is a kind of Ac motor in which power is transferred to the rotor by the phenomena of Faraday law of electromagnetic induction. The induction motor rotates due to the force among the stator and rotor's magnetic field. The squirrel cage induction motor was used as it is cheapest, easy to repair and consistent[18]. The figure 3.1 portrays the three phase induction motor equivalent circuit

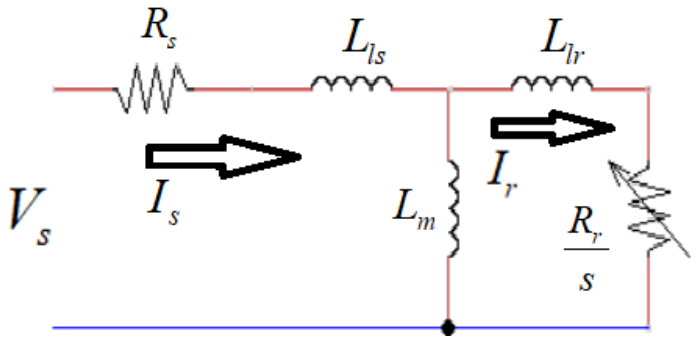

Figure 3.1. Three phase induction motor

$$n_{slip} = n_{sync} - n_m \qquad f_e = \frac{p}{120} n_{sync} \quad \text{..... (1)}$$

$$S = \frac{n_{sync} - n_m}{n_{sync}} = \frac{\omega_e - \omega_r}{\omega_e} = \frac{\omega_{sl}}{\omega_e} \qquad f_r = \frac{p.n_{slip}}{120} \quad \text{..... (2)}$$

$$f_r = \frac{p(n_{sync} - n_m)}{120} = \frac{p.s.n_{sync}}{120} = sf_e \quad \text{..... (3)}$$

$$T_{load} = \frac{P_{out}}{\omega_m}(N.m) \qquad \text{and} \qquad \omega_m = \frac{2\pi n_m}{60} \quad \text{..... (4)}$$

$$P_{in} = \sqrt{3} V_L I_L \cos\theta = 3 V_{ph} I_{ph} \cos\theta \quad \text{..... (5)}$$

$$P_{SCL} = 3 I_s^2 R_s \quad \text{..... (6)}$$

$$P_{AG} = P_{in} - (P_{SCL} + P_{core}) = P_{conv} + P_{RCL} = 3 I_r^2 \frac{R_r}{s} = \frac{P_{RCL}}{s} \quad \text{..... (7)}$$

$$P_{RCL} = 3 I_r^2 R_r$$

$$P_{conv} = P_{AG} - P_{RCL} = 3I_r^2 \frac{R_r(1-s)}{s} = \frac{P_{RCL}(1-s)}{s} \quad \text{(8)}$$

$$P_{conv} = (1-s)P_{AG} \quad \text{(9)}$$

$$P_{out} = P_{conv} - (P_{f+w} + P_{stray}) \quad \text{(10)}$$

$$\tau_{ind} = \frac{P_{conv}}{\omega_m} = \frac{(1-s)P_{AG}}{(1-s)\omega_s} \quad \text{(11)}$$

In the horse power machine, $R_s + j\omega_e L_{ls} << \omega_e L_m$ i.e. the voltage in R_s and L_{ls} are negligeable.so, the voltage in L_m is equal to V_s. the figure 3.2 below illustrates the simplified three phase induction motor equivalent circuit.

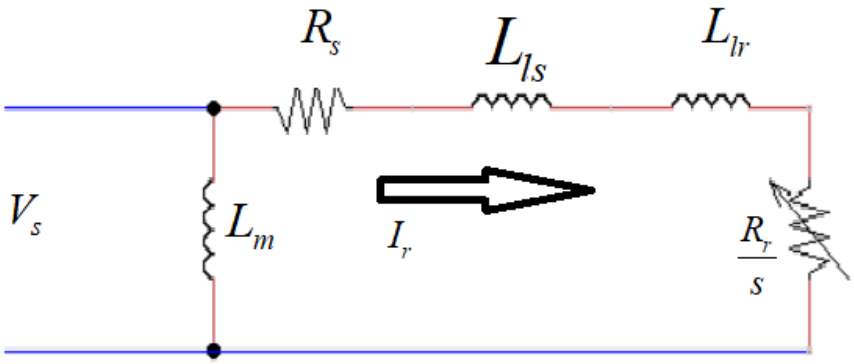

Figure 3.2. Simplified three phase induction motor equivalent circuit

$$S = \frac{\omega_e - \omega_m}{\omega_e} = \frac{\omega_{sl}}{\omega_e} \qquad s\omega_e = \omega_e - \omega_m \quad \text{(12)}$$

$$\omega_m = \omega_e - s\omega_e = \omega_e(1-s) \quad \text{(13)}$$

$$T_e = \frac{P_o}{\omega_m} = \frac{3}{\omega_m} I_r^2 R_r \left(\frac{1-s}{s}\right) = 3\left(\frac{p}{2}\right) I_r^2 \frac{R_r}{s\omega_e} \quad \text{(14)}$$

$$I_r = \frac{V_s}{\sqrt{\left(R_s + \frac{R_r}{s}\right)^2 + \omega_e^2 (L_{ls} + L_{lr})^2}} \quad \text{(15)}$$

$$T_e = 3\left(\frac{p}{2}\right) \frac{R_r}{s\omega_e} \frac{V_s^2}{\left(R_s + \frac{R_r}{s}\right)^2 + \omega_e^2 (L_{ls} + L_{lr})^2} \quad \text{(16)}$$

$$T_e = 3\left(\frac{p}{2}\right) \left(\frac{V_s}{\omega_e}\right)^2 \left(\frac{\omega_{sl} R_r}{R_r^2 + \omega_{sl}^2 L_{lr}^2}\right) \quad \text{(17)}$$

Where p is the number of poles

3.2.2 Six phase induction motor

A dynamic model of the six phase induction motor has been developed in d-q synchronously rotating reference frame[19]. To develop this model some assumptions have made as follow.

i. The air gap is uniform and the winding are sinusoidally distributed around the air gap
ii. There is no friction and winding loss in the system
iii. There is no core losses and magnetic saturation in the core
iv. Mutual inductances are equal
v. The harmonics in voltages and currents are neglected.
vi. Saturation, hysteresis and eddy current effects are negligible.

The mathematical model of six-phase induction motor is composed of four equations: flux equation, voltage equation, torque equation and equation of motion.[20]

The voltage equations of a split phase induction motor are:

$$V_a = V_m \cos(\omega t) \quad \text{..... (18)}$$

$$V_b = V_m \cos(\omega t - \frac{2\pi}{3}) \quad \text{..... (19)}$$

$$V_c = V_m \cos(\omega t + \frac{2\pi}{3}) \quad \text{..... (20)}$$

$$V_x = V_m \cos(\omega t - \alpha) \quad \text{..... (21)}$$

$$V_y = V_m \cos(\omega t - \frac{2\pi}{3} - \alpha) \quad \text{..... (22)}$$

$$V_z = V_m \cos(\omega t + \frac{2\pi}{3} - \alpha) \quad \text{..... (23)}$$

where $\alpha=30^o$ electrical degrees

Then, these six-phase voltages are transferred to a synchronously rotating reference frame in only two phases (d-q axis transformation) [21]

Voltage equations

$$V_{qs1} = r_s i_{qs1} + \omega\lambda_{ds1} + p\lambda_{qs1} \quad \text{..... (24)}$$

$$V_{ds1} = r_s i_{ds1} - \omega\lambda_{qs1} + p\lambda_{ds1} \quad \text{..... (25)}$$

$$V_{qs2} = r_s i_{qs2} + \omega\lambda_{ds2} + p\lambda_{qs2} \quad \text{..... (26)}$$

$$V_{ds2} = r_s i_{ds2} - \omega\lambda_{ds2} + p\lambda_{ds2} \quad \text{..... (27)}$$

$$V_{qr} = 0 = r_r i_{qr} + (\omega - \omega_r)\lambda_{dr} + p\lambda_{qr} \quad \text{..... (28)}$$

$$V_{dr} = 0 = r_r i_{dr} - (\omega - \omega_r)\lambda_{qr} + p\lambda_{dr} \quad \text{..... (29)}$$

Where $(\omega - \omega_r)$ is denoted as ω_e

Where $p = \frac{d}{dt}$

For the squirrel cage induction motor, The rotor voltages V_{qr} and V_{dr} are set to zero since the rotor cage bars are shorted[22] [8] [23]

Flux Linkage equations

$$\lambda_{qs1} = i_{qs1}L_{ls} + L_{lm}(i_{qs1} + i_{qs2}) + L_m(i_{qs1} + i_{qs2} + i_{qr}) \quad (30)$$

$$\lambda_{ds1} = i_{ds1}L_{ls} + L_{lm}(i_{ds1} + i_{ds2}) + L_m(i_{ds1} + i_{ds2} + i_{dr}) \quad (31)$$

$$\lambda_{qs2} = i_{qs2}L_{ls} + L_{lm}(i_{qs1} + i_{qs2}) + L_m(i_{qs1} + i_{qs2} + i_{qr}) \quad (32)$$

$$\lambda_{ds2} = i_{ds2}L_{ls} + L_{lm}(i_{ds1} + i_{ds2}) + L_m(i_{ds1} + i_{ds2} + i_{dr}) \quad (33)$$

$$\lambda_{qr} = i_{qr}L_{lr} + L_m(i_{qs1} + i_{qs2} + i_{qr}) \quad (34)$$

$$\lambda_{dr} = i_{dr}L_{lr} + L_m(i_{ds1} + i_{ds2} + i_{dr}) \quad (35)$$

Current equations

$$i_{ds1} = \frac{1}{X_{ls}}(\lambda_{ds} - \lambda_{dm}) \quad (36)$$

$$i_{ds2} = \frac{1}{X_{ls}}(\lambda_{ds} - \lambda_{dm}) \quad (37)$$

$$i_{qs1} = \frac{1}{X_{ls}}(\lambda_{qs} - \lambda_{dm}) \quad (38)$$

$$i_{qs2} = \frac{1}{X_{ls}}(\lambda_{qs} - \lambda_{dm}) \quad (39)$$

$$i_{dr} = \frac{1}{X_{ls}}(\lambda_{dr} - \lambda_{dm}) \quad (40)$$

$$i_{qr} = \frac{1}{X_{ls}}(\lambda_{qr} - \lambda_{dm}) \quad (41)$$

Torque equation

$$T_{em} = \frac{3}{2}\frac{P}{2}\frac{L_m}{L_r}[\lambda_{dr}(i_{qs1} + i_{qs2}) - \lambda_{qr}(i_{ds1} + i_{ds1})] \quad (42)$$

Equivalent circuit of Asymmetrical six phase Motor

The d-q axis dynamic equivalent per phase circuits of six phase induction motor are represented in figure 3.3 and 3.4 respectively.

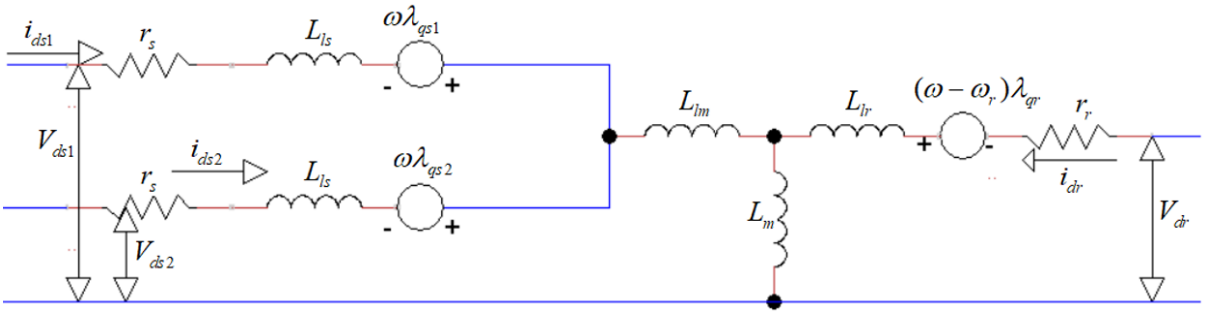

Figure 3.3. d-axis dynamic equivalent per phase circuits of six phase induction motor

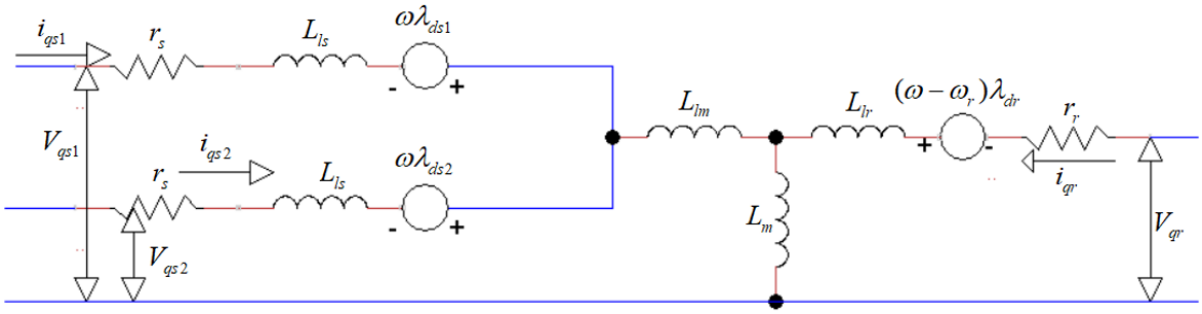

Figure 3.4. q-axis dynamic equivalent per phase circuits of six phase induction motor

3.3 Matlab/simulink model of three and six phase induction motor

3.3.1 Three phase induction motor

Voltage Source inverter (VSI) fed three phase induction motor

In this scheme, a 750V three phase inverter was used and each switch conducts 180^0 hence the name 180^0 type. Switching for this type is carried out without an off period, that is, each switch is always on either the positive or negative terminal, but the situation to avoid is having all three on the positive or negative terminal simultaneously. At any given instant, three switches are conducting, say S1, S2, and S3. After a period of 60°, S2, S3, and S4 will be conducting. The conduction period for each switch is 180°, so that no two switches in the same leg conduct simultaneously.

Six distinct 60° intervals exist for one output cycle, and the rate of sequencing these intervals specifies the inverter output frequency. The complete switching pattern for the six intervals is shown in Table 1 below. The six-step sequence creates a cyclic pattern: 1-2-3, 2-3-4, 3-4-5, 4-5-6, 5-6-1, 6-1-2… It can be seen that each switch conducts for a period of 180°.

Table 3.2. Switching pattern of power devices

Interval	**S1**	**S2**	**S3**	**S4**	**S5**	**S6**
0 to 60°	On	Off	Off	Off	On	On
60 to 120°	On	On	Off	Off	Off	On
120 to 180°	On	On	On	Off	Off	Off
180 to 240°	Off	On	On	On	Off	Off
240 to 300°	Off	Off	On	On	On	Off
300 to 360°	Off	Off	Off	On	On	On

The three output voltage waveforms can now be derived by assuming a balanced, Y-connected resistive load R. The phase voltages for the various 60° intervals can be obtained by considering the equivalent circuit for each interval, as shown in Figure 3.5 below. From these equivalent circuits, the voltages associated with each phase of the load can be determined. A summary of the results is given in Table 3.3 below. the phase voltages have six discontinuities per cycle, corresponding to the six switching points per cycle. The line voltages can be obtained from the following relationships:

$\mathbf{V_{AB} = V_{AN} — V_{BN}}$

$\mathbf{V_{BC} = V_{BN} — V_{CN}}$

$V_{CA} = V_{CN} — V_{AN}$

and the phase voltages are calculated depending on conduction angle as shown in figure 3.5 and the results obtained are illustrated in table 3.3 below;

Table 3.3. Phase voltages according to conduction angle

Interval	V_{AN}	V_{BN}	V_{CN}	V_{AB}	V_{BC}	V_{CA}
0 to 60°	*E/3*	*-2E/3*	*E/* 3	*+E*	*-E*	0
60 to 120°	*2E/3*	*-E/*3	*-E/3*	*+E*	0	*-E*
120 to 180°	*E/3*	*E/* 3	*-2E/3*	*0*	*+E*	*-E*
180 to 240°	*-E/3*	*+2E/3*	*-E/3*	*-E*	*+E*	0
240 to 300°	*-2E/3*	*E/3*	*E/3*	*-E*	*0*	*+E*
300 to 360°	*-E/3*	*-E/* 3	*+2E/3*	0	*-E*	*+E*

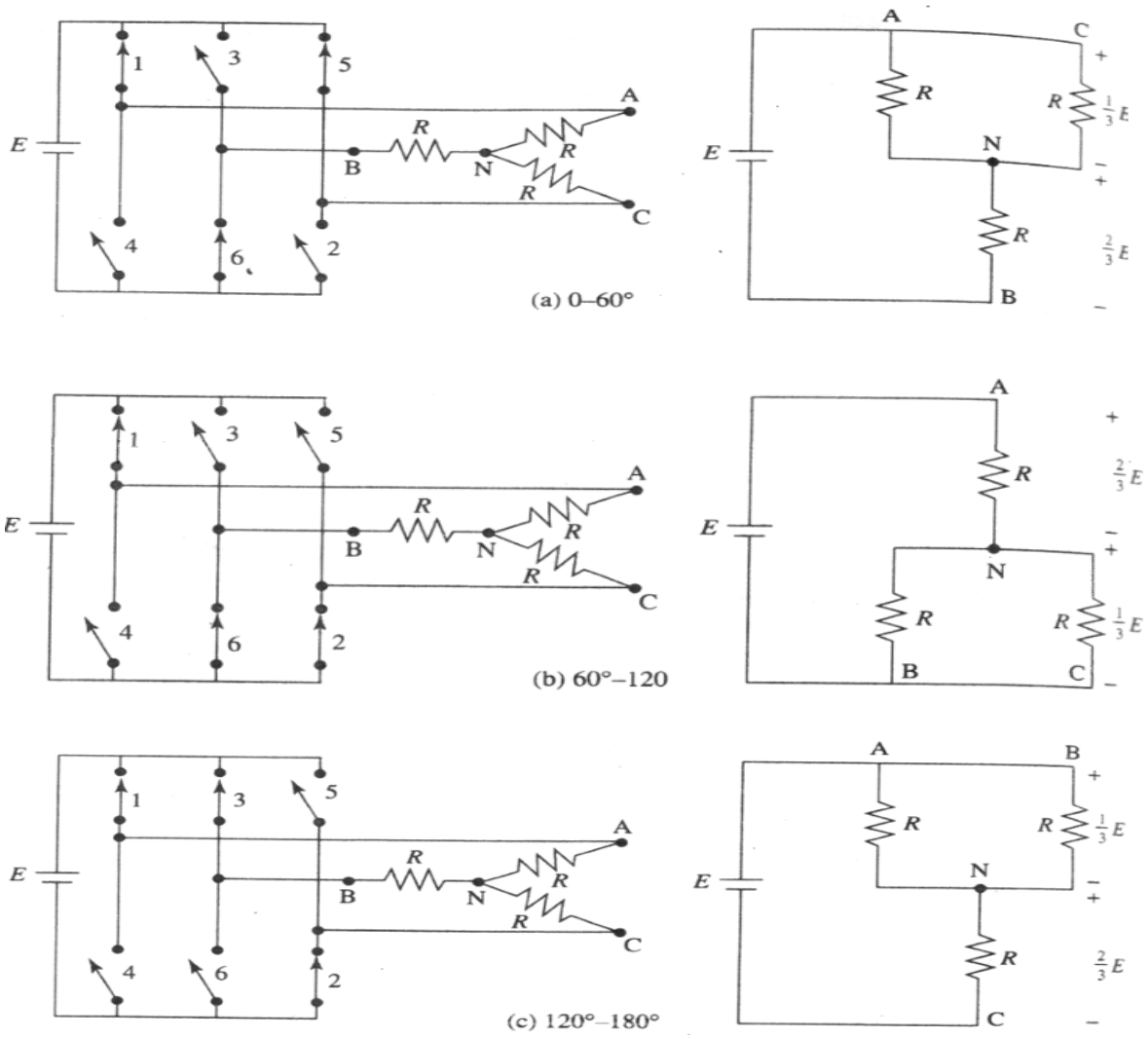

Figure 3.5Three-phase bridge inverter equivalent circuits

In the subsequent simulation, the Insulated Gate Bipolar Transistor (IGBT) is used as a switch device due to combined efficiency and speed properties as portrayed in figure 3.6 below.

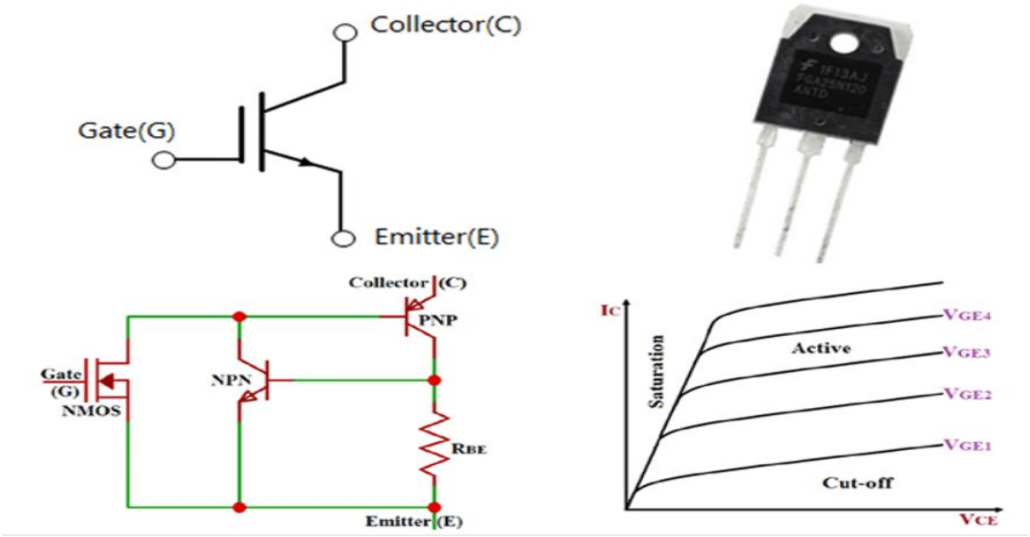

Figure 3.6. IGBT Symbol and internal structure[24]

It is a three-terminal semiconductor switching device that may be utilised in many different types of electronic devices for quick switching with great efficiency. These devices are typically employed in amplifiers to switch/process complicated wave patterns with pulse width modulation (PWM).

Because the IGBT possesses output of a combination of the PNP transistor, NPN transistor, and MOSFET, it may be built using the equivalent circuit of two transistors and a MOSFET. The low saturation voltage of a transistor is combined with the high input impedance and switching speed of a MOSFET in an IGBT. This combination produces the output switching and conduction properties of a bipolar transistor while controlling the voltage like a MOSFET.

The switches used are IGBTs and the settings of the pulse generators are shown in table 3.4 below:

Table 3.4. Pulse generator settings

No	Switch	Period(seconds)	Pulse width(%period)	Phase delay(seconds)	Signal Amplitude (Volts)
1	S1	0.02	33	0	1
2	S2	0.02	33	0.0033	1
3	S3	0.02	33	0.0066	1
4	S4	0.02	33	0.01	1
5	S5	0.02	33	0.0133	1
6	S6	0.02	33	0.0166	1

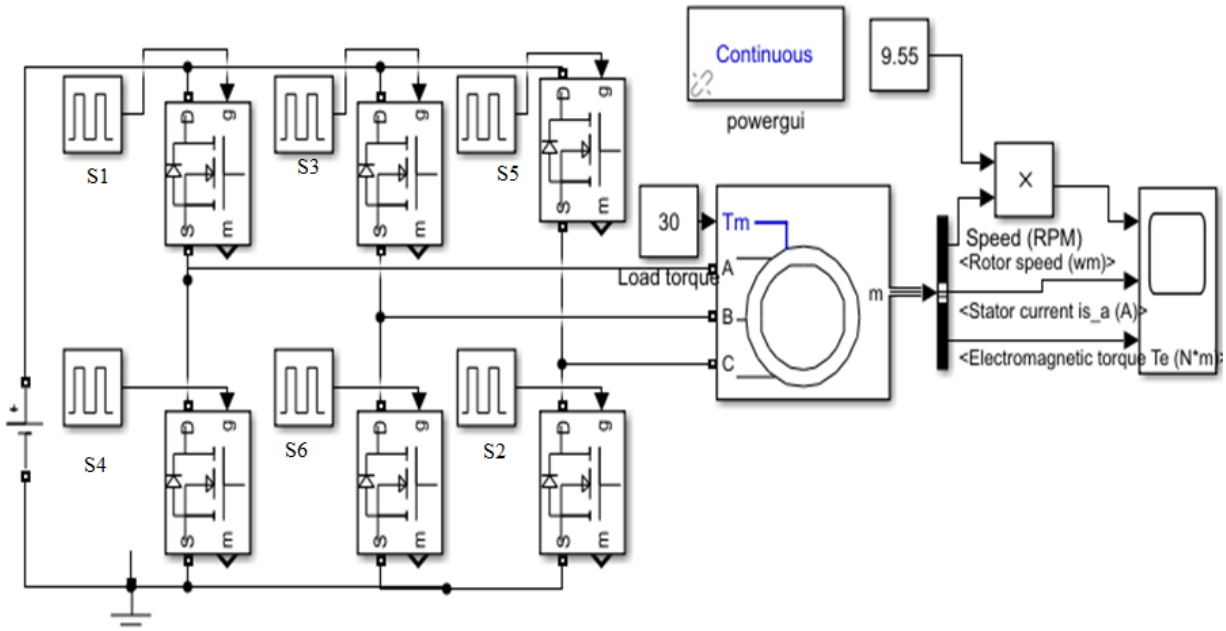

Figure 3.7. VSI fed induction motor

V/F with SPWM control method at various Load condition

The air gap flux will tend to saturate if the supply frequency is reduced while maintaining the rated supply voltage. This will result in excessive stator current and stator flux wave distortion. Therefore, the stator voltage should be reduced according to the frequency in order to keep the air-gap flux constant.

The magnitude of the stator flux is proportional to the stator voltage-to-frequency ratio. As a result, if the voltage-to-frequency ratio is kept constant, the flux remains constant. Furthermore, by keeping V/F constant, the produced torque remains roughly constant. This method improves run-time efficiency. As a result, the majority of AC speed drives use the constant V/F approach (or variable voltage, variable frequency method) to control the speed. This technology provides a 'soft start' capability in addition to a wide range of speed control. A pulse width modulated inverter is used for V/F speed control. The inverter is powered by a direct current voltage and has three phase legs, each of which contains two transistors and two diodes.

PWM comes in a variety of topologies, however in this simulation, SPWM (sine-triangle pulse width modulation) control is employed. The switches of the inverter are controlled by SPWM control, which compares a sinusoidal control signal with a triangle switching signal. The triangle waveform establishes the inverter's switching frequency, while the sinusoidal control waveform establishes the required fundamental frequency of the inverter output. The

modulation frequency ratio is defined as the ratio of the triangle wave and the sinusoid frequencies.

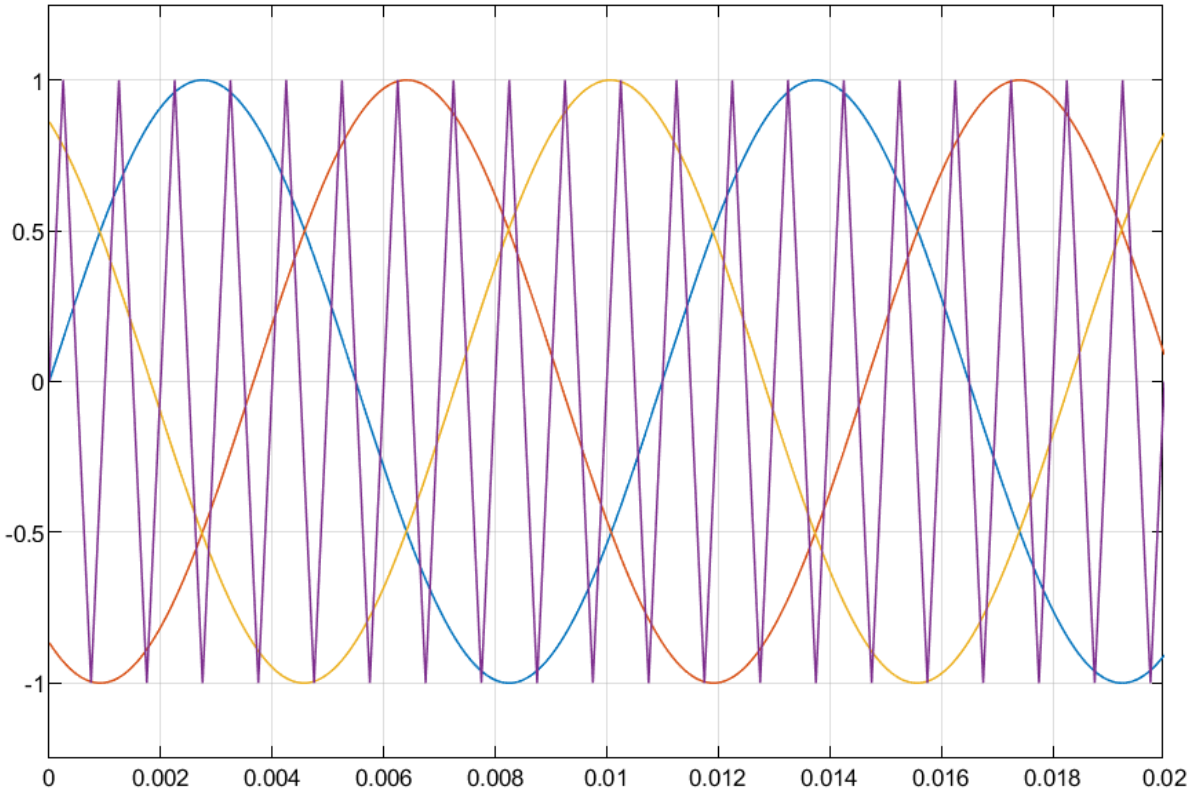

Figure 3.8. SPWM Signals

The switches in each leg are never on or off at the same time in principle, therefore the phase voltages oscillate between the input voltage (Vdc) and zero. The line-line inverter output voltages are ac, with a fundamental frequency matching to the frequency of the sinusoidal control voltage, because the switches are controlled in this way. In most cases, the triangle wave's magnitude is kept constant. Adjusting the amplitude of the sinusoidal control voltages controls the amplitude of the inverter output voltages. The amplitude modulation ratio is the ratio of the amplitude of the sinusoidal waveforms to the amplitude of the triangular wave. The inverter must source power in all four quadrants in systems where inductive loads are used.

When a transistor is gated on but unable to conduct the polarity of the load current, the diodes provide current routes.

The graphs under the following configuration are plotted on a carrier frequency of 1000Hz and by decreasing this frequency, the speed can be decreased and vice versa as shown in figure 3.9 below;

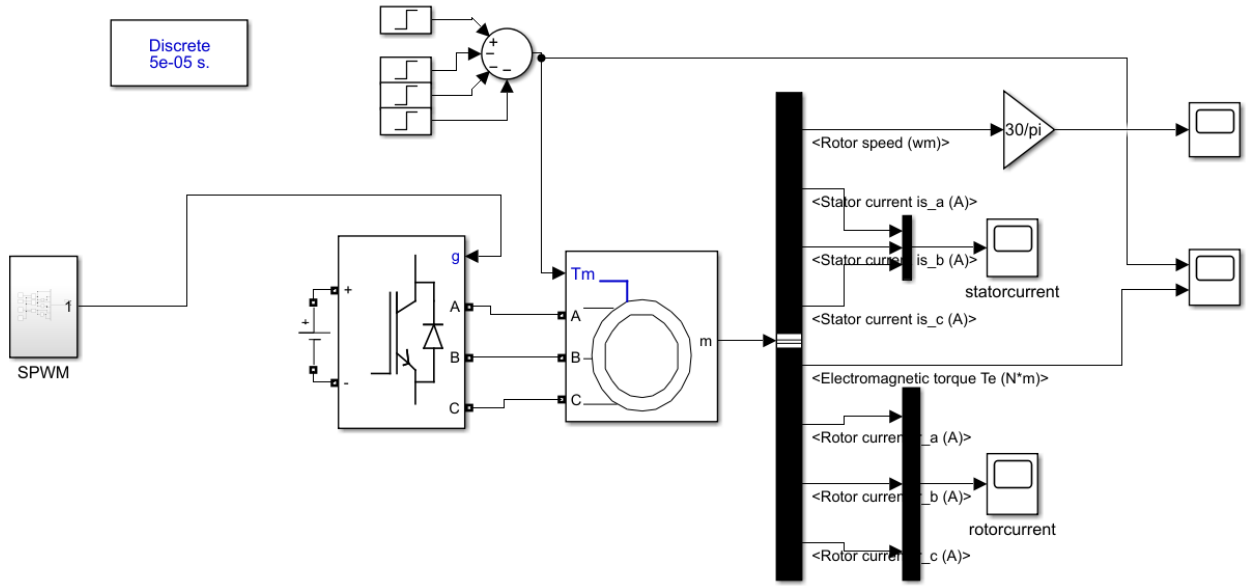

Figure 3.9. VF control at various load conditions

In this simulation, the motor is directly on an AC supply of the inverter output and the load is varied at different step times. The initial torque is 70Nm which is taken to 30Nm after two seconds as shown in the table 3.5 below:

Table 3.5. Variable torque with step time

No	Step time(seconds)	Torque(Nm)
1	3	70
2	5	40
3	10	30
4	13	15
5	15	15

3.3.2 Six phase induction motor simulink implementation

Motor

The equations have been organised into four main blocks in order to implement the six phase induction motor in Simulink.

a. Inputs: voltages, and load torque
b. Outputs: currents, electromagnetic torque and speed
c. Electrical parts of the machine
d. Mechanical part of the machine

The model was created in matlab Simulink environment by using the functions, signal routing, sensors for measurement and other multiple blocks obtained from Simulink commonly used blocks. In this research, the asymmetrical six phase (30^0 phase shift) was used.

The steps followed in modelling the six phase induction motor in matlab are as follow:

a. Calculate the V_{abc} ,V_{xyz} to $V_{\alpha\beta}$ i.e. Clarke transformation
b. Calculate the $V_{\alpha\beta}$ to V_{dq} i.e. park transformation
c. Calculate stator flux and rotor flux
d. Calculate stator currents
e. Calculate electromagnetic torque and inverse currents (dq to $\alpha\beta$ to abcxyz form i.e. inverse park and Clarke transformation)

The voltages block is obtained by conversion of six input voltages to two phase voltages using Clarke's transformation as represented in matrix form as follow [25] ;

$$\begin{bmatrix} V_{\alpha s1} \\ V_{\beta s1} \end{bmatrix} = \sqrt{\frac{2}{3}} \begin{bmatrix} 1 & -\frac{1}{2} & -\frac{1}{2} \\ 0 & \frac{\sqrt{3}}{2} & -\frac{\sqrt{3}}{2} \end{bmatrix} \begin{bmatrix} V_a \\ V_b \\ V_c \end{bmatrix} \quad \text{..... (43)}$$

$$\begin{bmatrix} V_{\alpha s2} \\ V_{\beta s2} \end{bmatrix} = \sqrt{\frac{2}{3}} \begin{bmatrix} \frac{\sqrt{3}}{2} & -\frac{\sqrt{3}}{2} & 0 \\ \frac{1}{2} & \frac{1}{2} & -1 \end{bmatrix} \begin{bmatrix} V_x \\ V_y \\ V_z \end{bmatrix} \quad \text{..... (44)}$$

The figure 3.10 portrays the conversion of ABC XYZ voltages to αβ stationary axis i.e clark transformation.

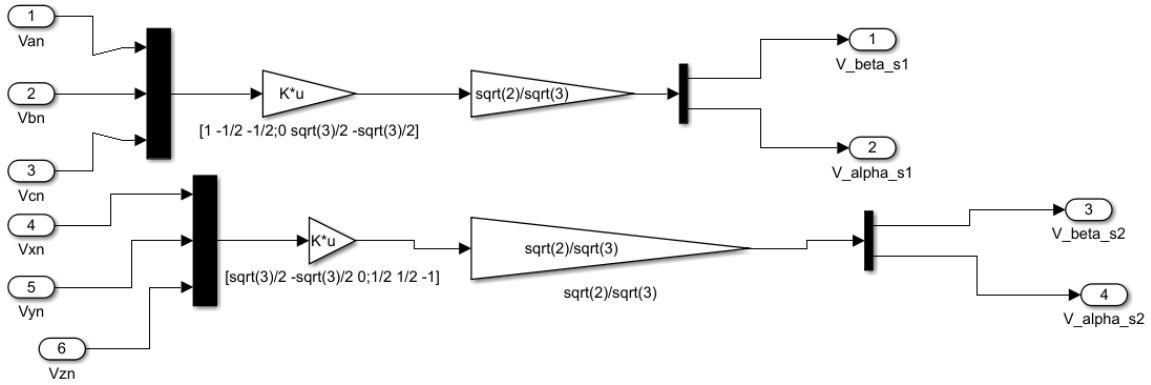

Figure 3.10. ABC and XYZ to αβ (stationary axis) conversion

Voltage conversion from $V_{\alpha\beta}$ to V_{dq} i.e. park transformation is demonstrated in figure 3.11 and 3.12 for two sets of windings respectively.

$$V_{qs1} = V_{\beta s1}\cos\theta + V_{\alpha s1}\sin\theta \quad \text{..... (45)}$$

$$V_{ds1} = V_{\alpha s1}\cos\theta - V_{\beta s1}\sin\theta \quad \text{..... (46)}$$

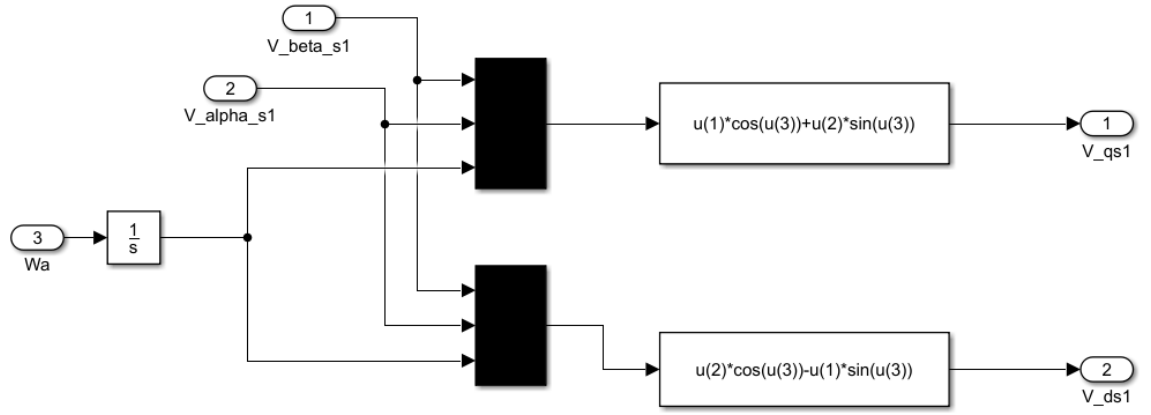

Figure 3.11. Voltage conversion from $V_{\alpha\beta}$ to V_{dq} for first set of windings

$$V_{qs2} = V_{\beta s2}\cos\theta + V_{\alpha s2}\sin\theta \quad \text{..... (47)}$$

$$V_{ds2} = V_{\alpha s2}\cos\theta - V_{\beta s2}\sin\theta \quad \text{..... (48)}$$

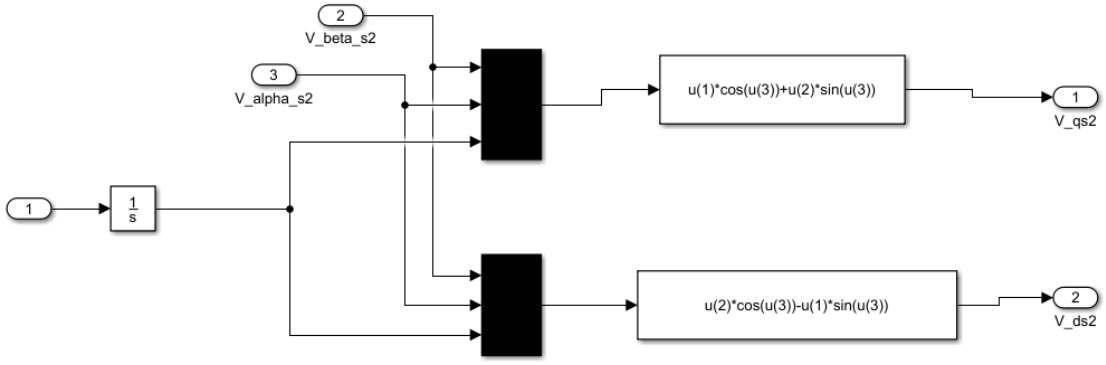

Figure 3.12. Voltage conversion from $V_{\alpha\beta}$ to V_{dq} for the second set of windings

And here below is the figure 3.13 which shows the Combination of voltage conversion for both sets of windings.

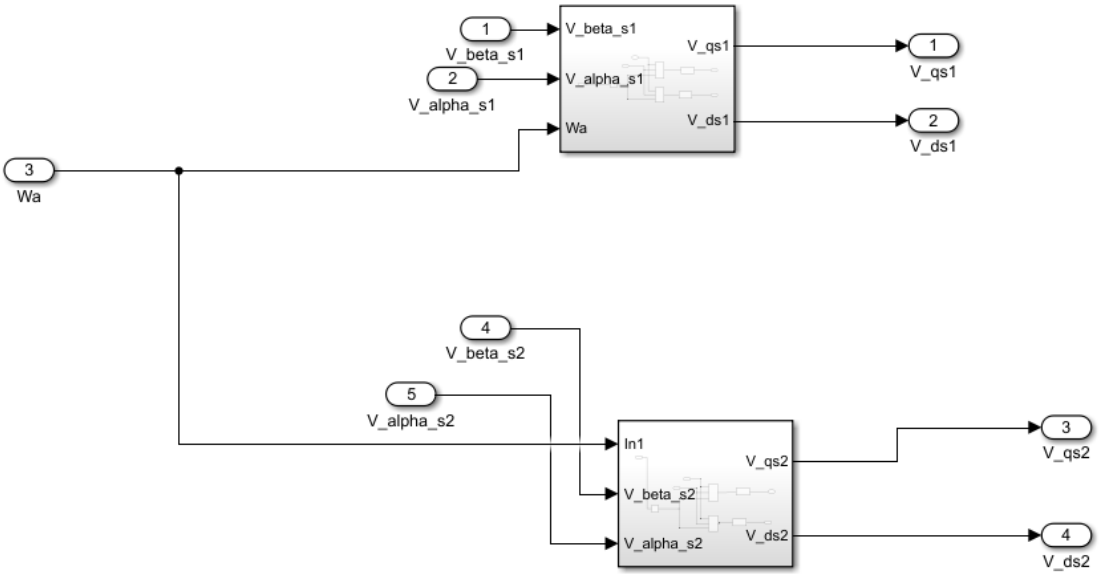

Figure 3.13. Combination of voltage conversion for both sets of windings

The figure 3.14 demonstrates the combination of both Clarke and park transformation

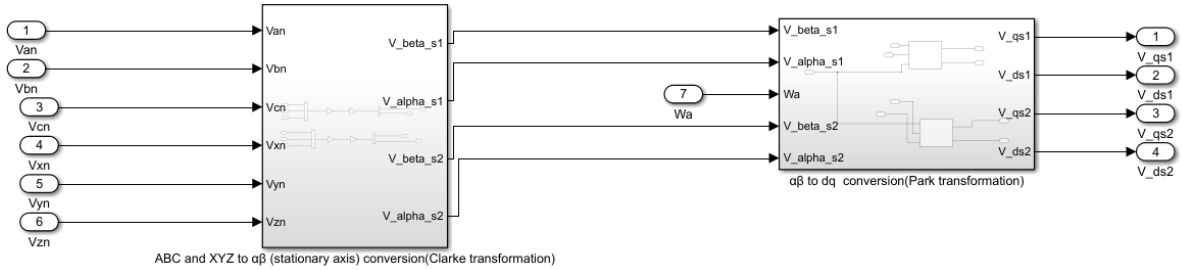

Figure 3.14. Clarke and park transformation for both stator windings

Rotor flux blocks are obtained as follows;

$$\lambda_{dr} = i_{dr}L_{lr} + L_m(i_{ds1} + i_{ds2} + i_{dr}) \quad \text{..... (49)}$$

The rotor d-q flux blocks were built on the basis of mathematical model (eq.49 and 50) as represented on figure 3.15 and 3.16 respectively.

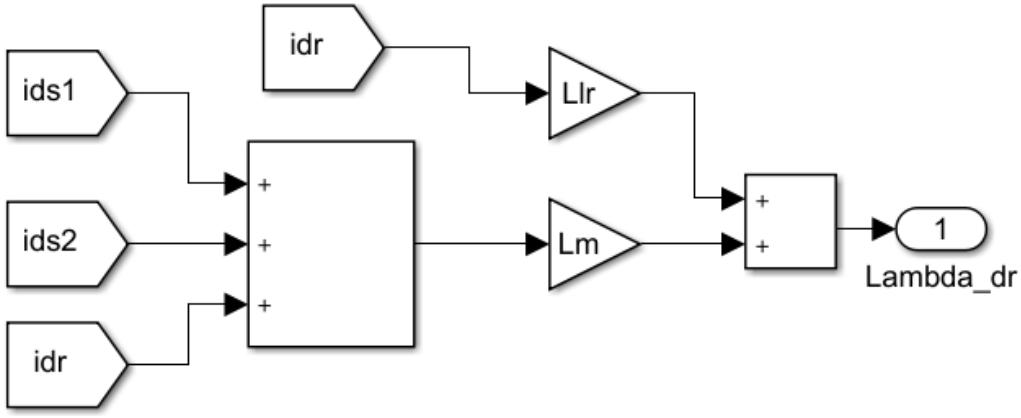

Figure 3.15. D-axis rotor flux

$$\lambda_{qr} = i_{qr}L_{lr} + L_m(i_{qs1} + i_{qs2} + i_{qr}) \quad \text{..... (50)}$$

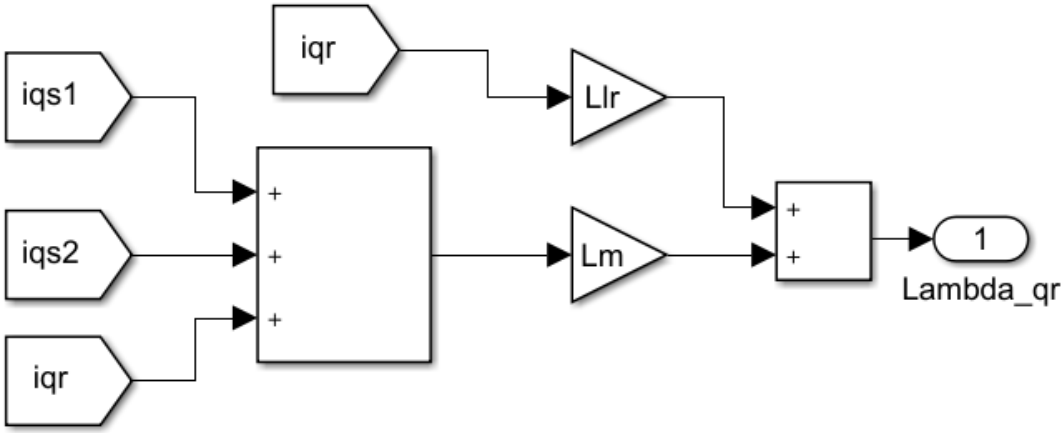

Figure 3.16. Q- axis rotor flux

Mechanical blocks(Electromagnetic Torque and Rotor speed) are obtained using these equations(51 and 52) [26] and the Matlab blocks are portrayed on figure 3.17 and 3.18 respectively.

$$T_{em} = \frac{3}{2}\frac{P}{2}\frac{L_m}{L_r}[\lambda_{dr}(i_{qs1} + i_{qs2}) - \lambda_{qr}(i_{ds1} + i_{ds1})] \quad \text{..... (51)}$$

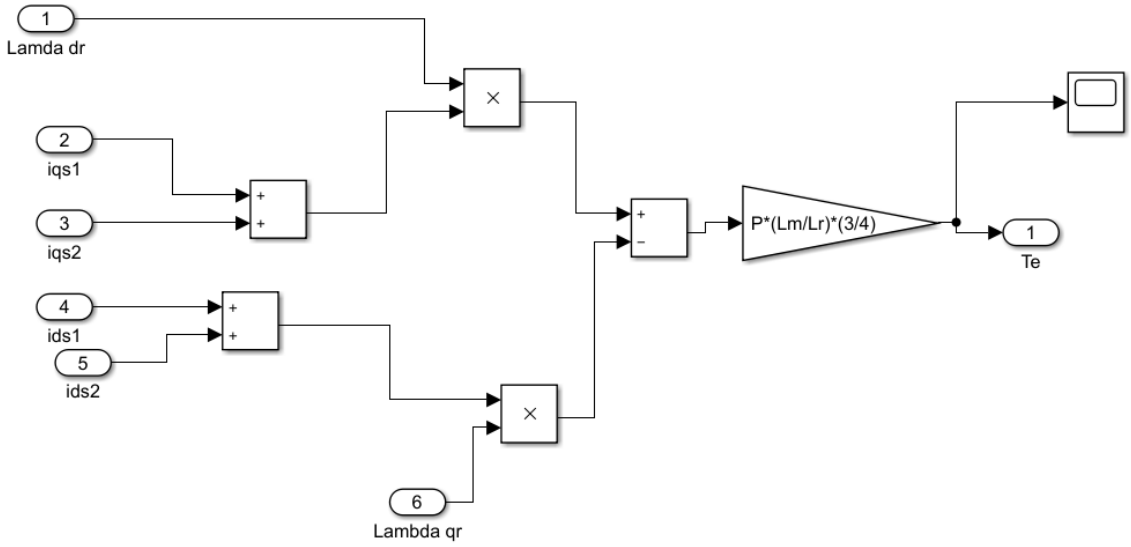

Figure 3.17. Electromagnetic Torque

$$\omega_r = \int \frac{1}{J}(T_{em} - T_L) \quad \text{..... (52)}$$

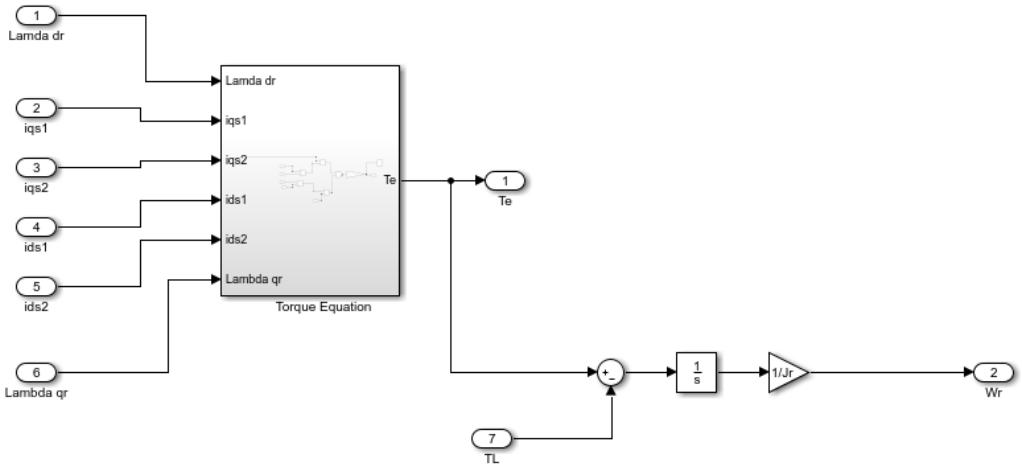

Figure 3.18. Rotor speed

$$\omega_e = \omega_r \times \frac{p}{2} \quad \text{..... (53)}$$

Current blocks are as follows[21]

$$i_{qs1} = \int \frac{1}{L_{ls} + L_{lm} + L_m} \left\{ V_{qs1} - r_s i_{qs1} - p(L_{lm} + L_m) i_{qs2} - pL_m i_{qr} - \omega \left[(L_{ls} + L_{lm} + L_m) i_{ds1} - (L_{lm} + L_m) i_{ds2} - L_m i_{dr} \right] \right\}$$

..... (54)

The figure 3.19 and 3.20 represents the q-axis stator currents blocks for both first and second sets of winding as of equations 54 and 55.

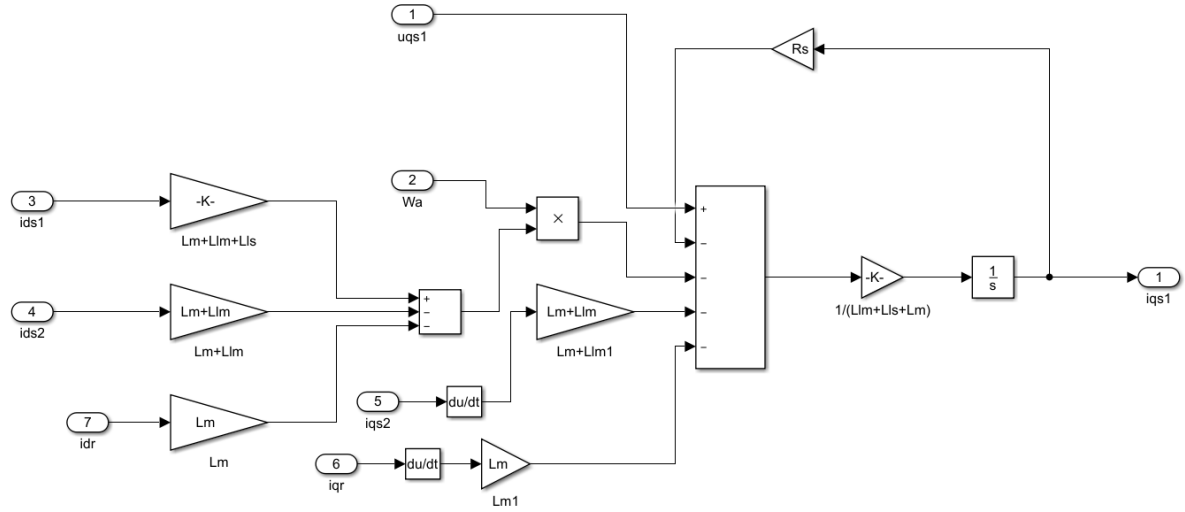

Figure 3.19. q-axis currents for the first set of winding

$$i_{qs2} = \int \frac{1}{L_{ls} + L_{lm} + L_m} \left\{ V_{qs2} - r_s i_{qs2} - p(L_{lm} + L_m) i_{qs1} - pL_m i_{qr} - \omega \left[(L_{ls} + L_{lm} + L_m) i_{ds2} - (L_{lm} + L_m) i_{ds1} - L_m i_{dr} \right] \right\}$$

……..…….... (55)

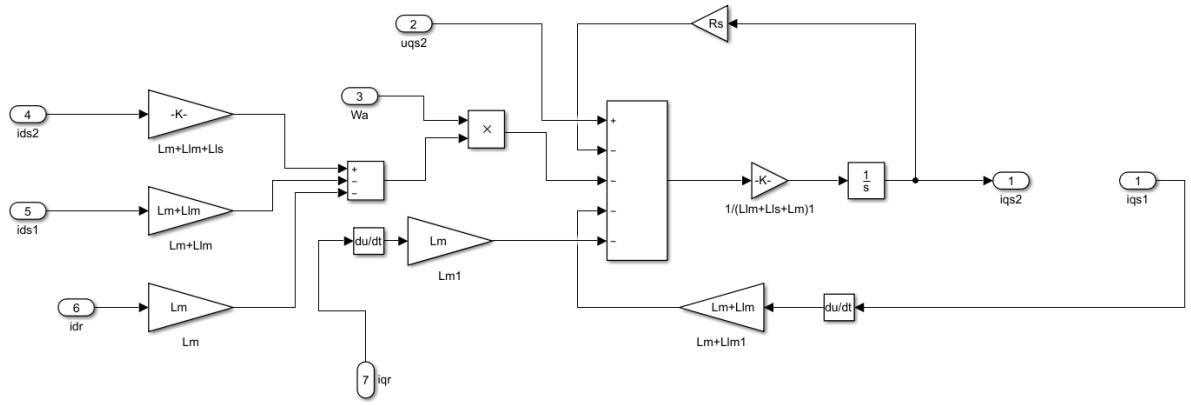

Figure 3.20. q-axis currents for the second set of winding

The figure 3.21 and 3.22 demonstrates the d-axis stator current blocks for both first and second sets of winding as of equation 56 and 57.

$$i_{ds1} = \int \frac{1}{L_{ls} + L_{lm} + L_m} \left\{ V_{ds1} - r_s i_{ds1} - p(L_{lm} + L_m) i_{ds2} - pL_m i_{dr} + \omega \left[(L_{ls} + L_{lm} + L_m) i_{qs1} + (L_{lm} + L_m) i_{qs2} + L_m i_{qr} \right] \right\}$$

……..…….... (56)

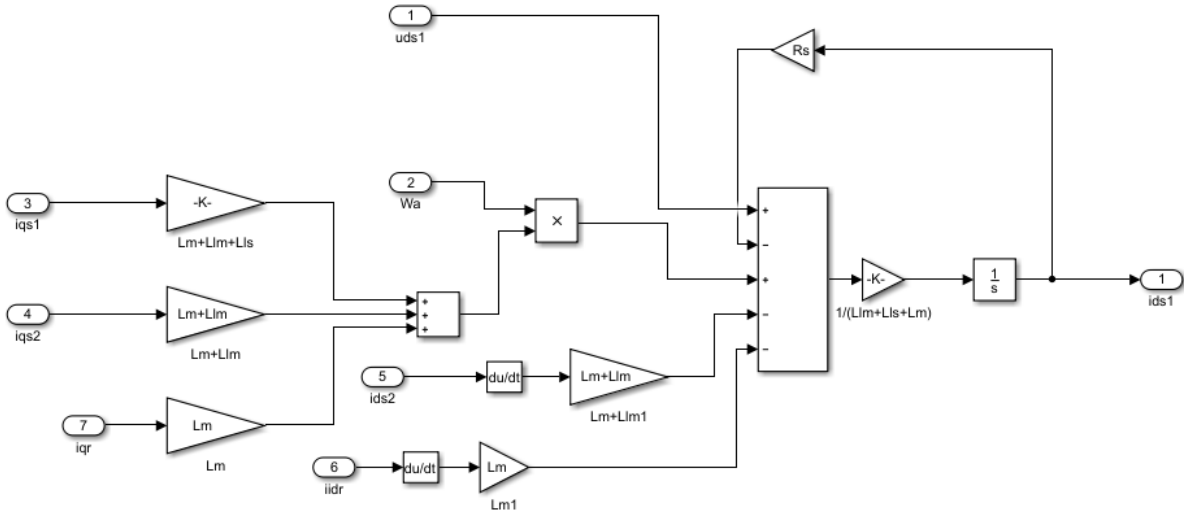

Figure 3.21. D-axis currents for the first set of winding

$$i_{ds2} = \int \frac{1}{L_{ls} + L_{lm} + L_m} \left\{ V_{ds2} - r_s i_{ds2} - p(L_{lm} + L_m) i_{ds1} - pL_m i_{dr} + \omega \left[(L_{ls} + L_{lm} + L_m) i_{qs2} + (L_{lm} + L_m) i_{qs1} + L_m i_{qr} \right] \right\}$$

……..…….... (57)

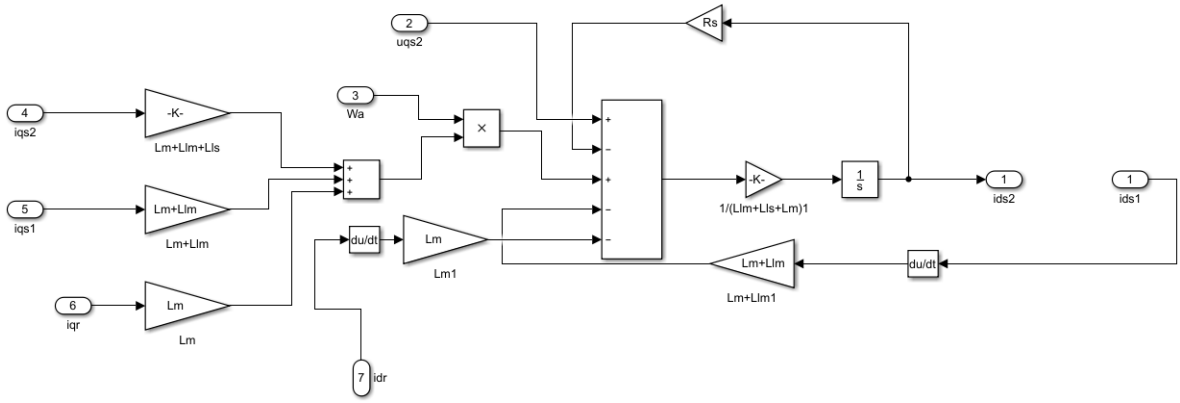

Figure 3.22. D-axis currents for the second set of winding

The figure 3.23 and 3.24 represents the q-d axis rotor currents respectively and were built on basis of equations 58 and 59 respectively.

$$i_{qr} = \int \frac{1}{L_{lr} + L_m} \left\{ V_{qr} - r_r i_{qr} - pL_m (i_{qs1} + i_{qs2}) - (\omega - \omega_r) \left[(L_{lr} + L_m) i_{dr} + L_m (i_{ds1} + i_{ds2}) \right] \right\} \text{…….. (58)}$$

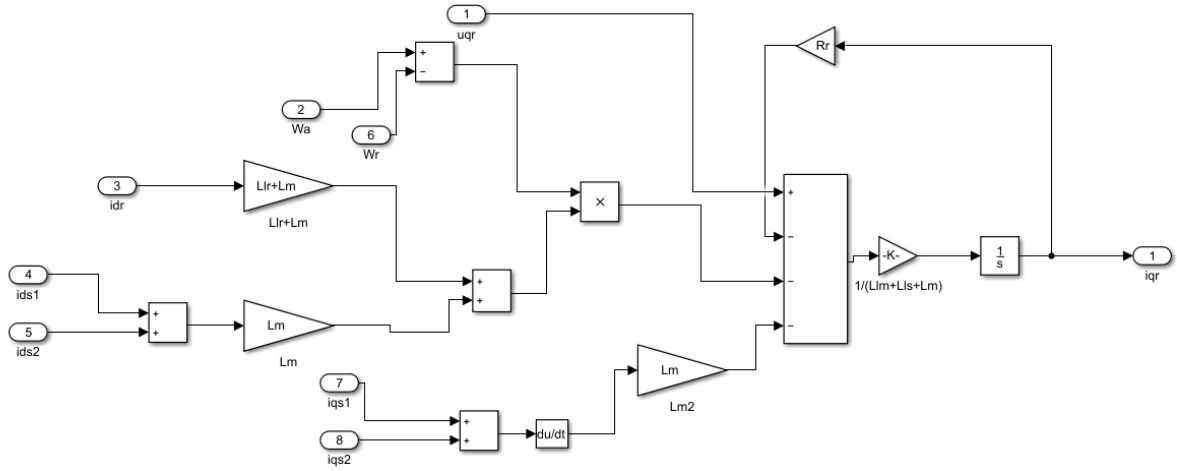

Figure 3.23. Q- axis rotor current

$$i_{dr} = \int \frac{1}{L_{lr} + L_m} \left\{ V_{dr} - r_r i_{dr} - pL_m (i_{ds1} + i_{ds2}) + (\omega - \omega_r) \left[(L_{lr} + L_m) i_{qr} + L_m (i_{qs1} + i_{qs2}) \right] \right\} \ldots\ldots\ldots (59)$$

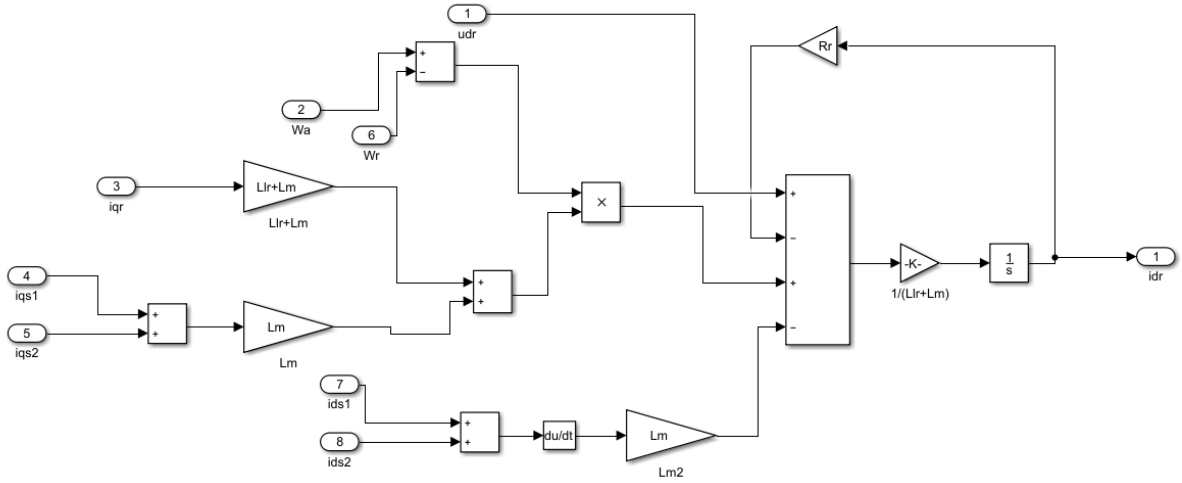

Figure 3.24. D- axis rotor current

Inverse Park and Clarke Transformation

In order to get stator ABCXYZ currents, we first use the inverse park transformation as demonstrated on figure 3.25 and 3.26 for the first and second winding respectively. and the blocks were built on basis of equations 60 to 63.

Stator currents from dq to alpha beta using inverse Park transformation

$$i_{\beta s1} = i_{qs1} \cos\theta - i_{ds1} \sin\theta \ldots\ldots\ldots (60)$$

$$i_{\alpha s1} = i_{ds1} \cos\theta + i_{qs1} \sin\theta \ldots\ldots\ldots (61)$$

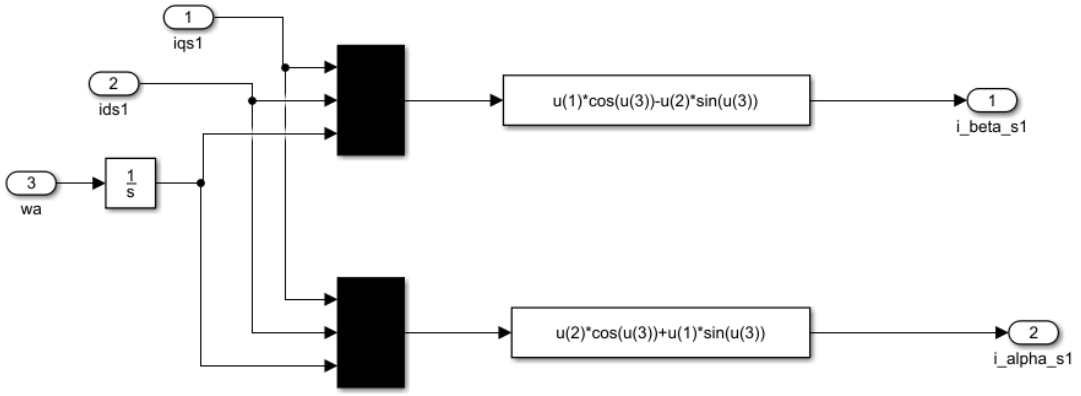

Figure 3.25. First winding inverse park transformation

$$i_{\beta s2} = i_{qs2}\cos\theta - i_{ds2}\sin\theta \quad \ldots\ldots (62)$$

$$i_{\alpha s2} = i_{ds2}\cos\theta + i_{qs2}\sin\theta \quad \ldots\ldots (63)$$

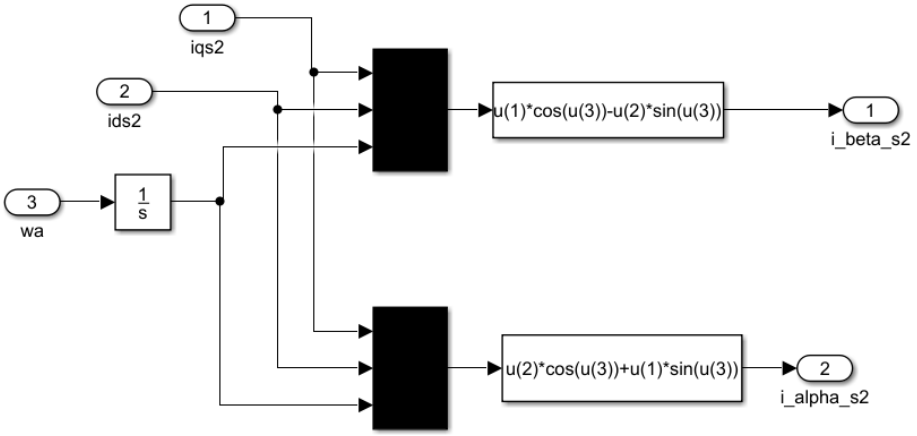

Figure 3.26. Second winding inverse park transformation

And then inverse Clarke transformation was finally used to get ABCXYZ currents as represented on figure 3.27 and 3.29 below. These figures were built on the basis of equations 64 and 65.

Stator currents transformation from $\alpha\beta$ to abcxyz using inverse Clarke transformation

For the first winding is as follow:

$$\begin{bmatrix} i_a \\ i_b \\ i_c \end{bmatrix} = \sqrt{\frac{2}{3}} \begin{bmatrix} 1 & 0 \\ \frac{-1}{2} & \frac{\sqrt{3}}{2} \\ \frac{-1}{2} & -\frac{\sqrt{3}}{2} \end{bmatrix} \begin{bmatrix} i_{\beta s1} \\ i_{\alpha s1} \end{bmatrix} \quad \ldots\ldots (64)$$

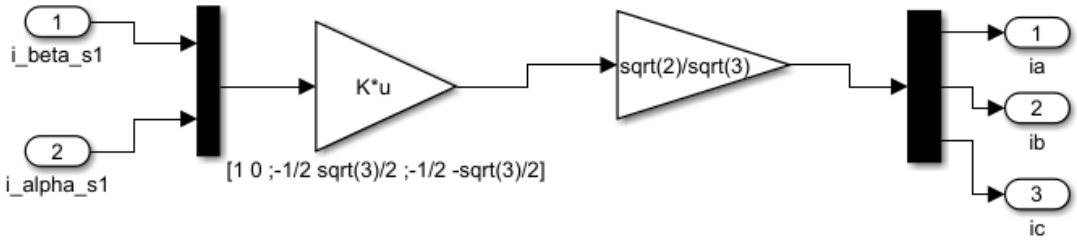

Figure 3.27. First winding inverse Clarke transformation

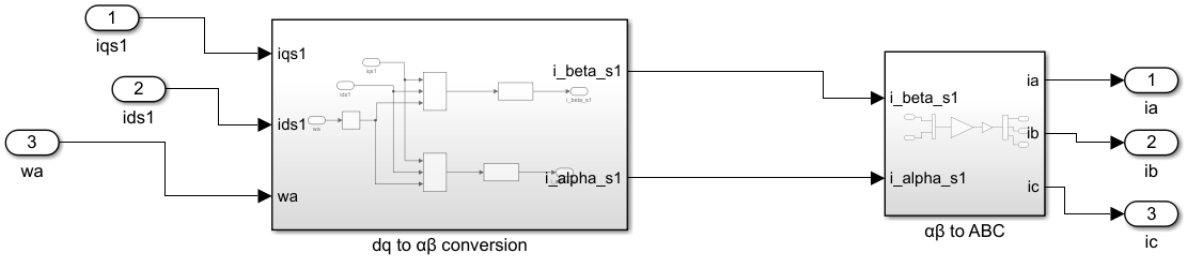

Figure 3.28. Combination of both inverse park and Clarke transformation for first winding

ω_a is the same as ω

For the second winding is as follow:

$$\begin{bmatrix} i_x \\ i_y \\ i_z \end{bmatrix} = \sqrt{\frac{2}{3}} \begin{bmatrix} \frac{\sqrt{3}}{2} & \frac{1}{2} \\ -\frac{\sqrt{3}}{2} & \frac{1}{2} \\ 0 & -1 \end{bmatrix} \begin{bmatrix} i_{\beta s2} \\ i_{\alpha s2} \end{bmatrix} \quad \text{(65)}$$

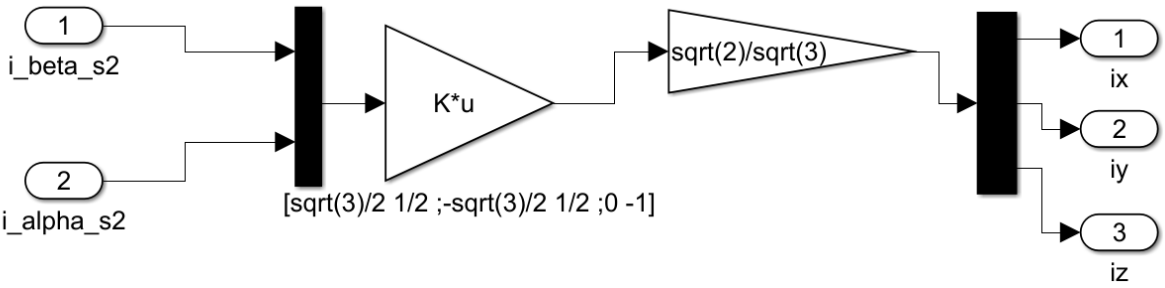

Figure 3.29. Second winding inverse Clarke transformation

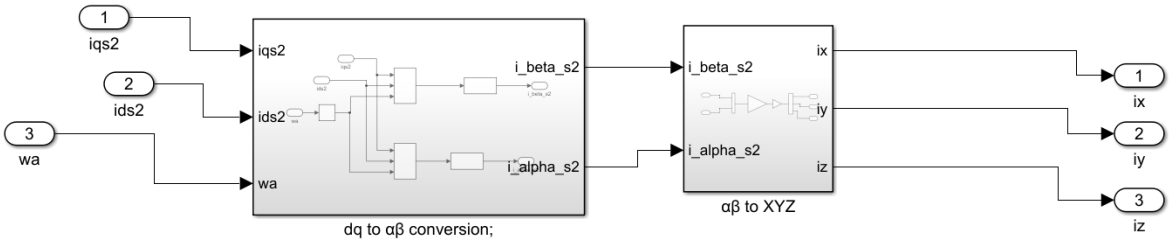

Figure 3.30. Combination of both inverse park and Clarke transformation for second winding

Rotor currents from dq **to abcdef using inverse Clarke transformation** [27]

In order to get the ABCXYZ rotor currents, the inverse Clarke transformation was employed as of equation 66 and the Matlab model is demonstrated on figure 3.31.

$$\begin{bmatrix} i_{ar} \\ i_{br} \\ i_{cr} \\ i_{dr} \\ i_{er} \\ i_{fr} \end{bmatrix} = \begin{bmatrix} 1 & 0 \\ \frac{1}{2} & \frac{\sqrt{3}}{2} \\ -\frac{1}{2} & \frac{\sqrt{3}}{2} \\ -1 & 0 \\ -\frac{1}{2} & -\frac{\sqrt{3}}{2} \\ \frac{1}{2} & -\frac{\sqrt{3}}{2} \end{bmatrix} \begin{bmatrix} i_{dr} \\ i_{qr} \end{bmatrix} \quad \text{..... (66)}$$

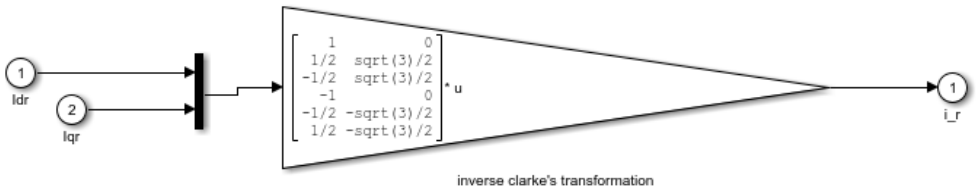

Figure 3.31. Rotor currents

And the final model of six phase split winding induction motor was represented on figure 3.32 below;

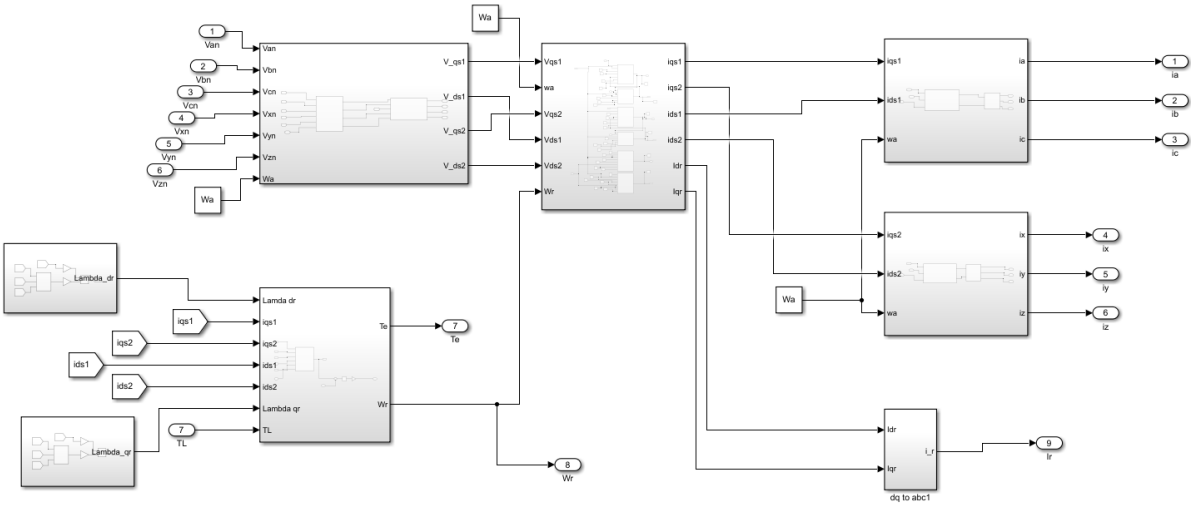

Figure 3.32. Six phase split winding induction motor

Space vector pulse width modulation(SVPWM)

A step input was used to implement the reference speed signal. The speed conversion block, shown in Figure 3.33, converted the speed signal to frequency. The voltage was converted from the frequency. The alpha and beta component vectors for the SVPWM generator were computed using both voltage and frequency, as shown in Figures 3.34 and 3.35. The Space Vector Pulse Width Modulation (SVPWM) technology was used to create pulses for PWM inverters using alpha beta vectors [28].

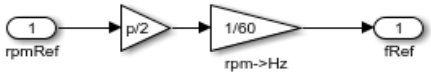

Figure 3.33. RPM conversion

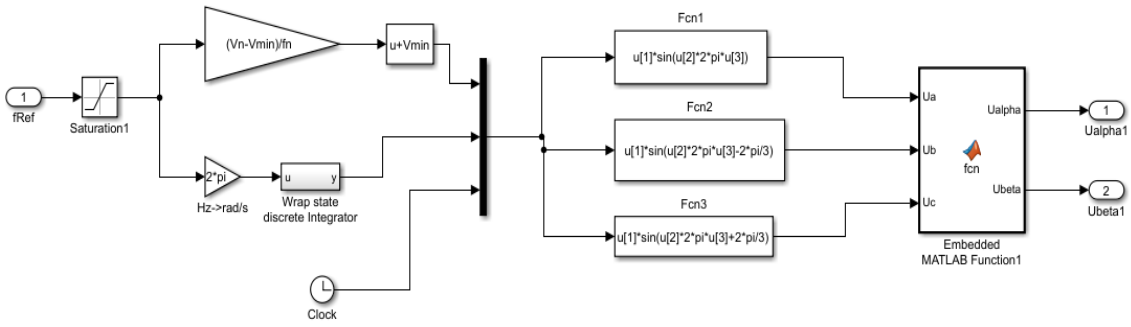

Figure 3.34. Alpha and beta calculation 1

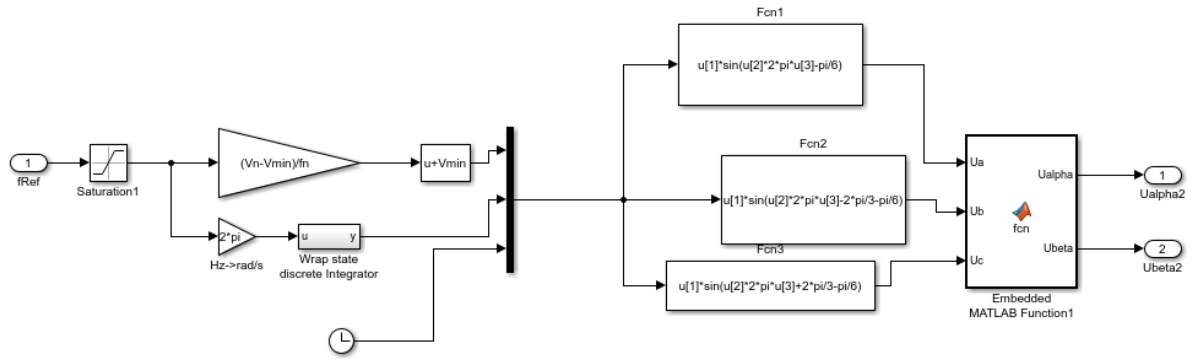

Figure 3.35. Alpha and beta calculation 2

Space vector pulse width modulation was implemented using the SVPWM generator from Matlab's library. The alpha and beta signals are used as inputs to this block. As shown in Figure 3.36, the PWM frequency and switching pattern were set to 2000HZ and pattern#1, respectively. This block's output, a six-pulse signal, was fed into the two-level inverter.

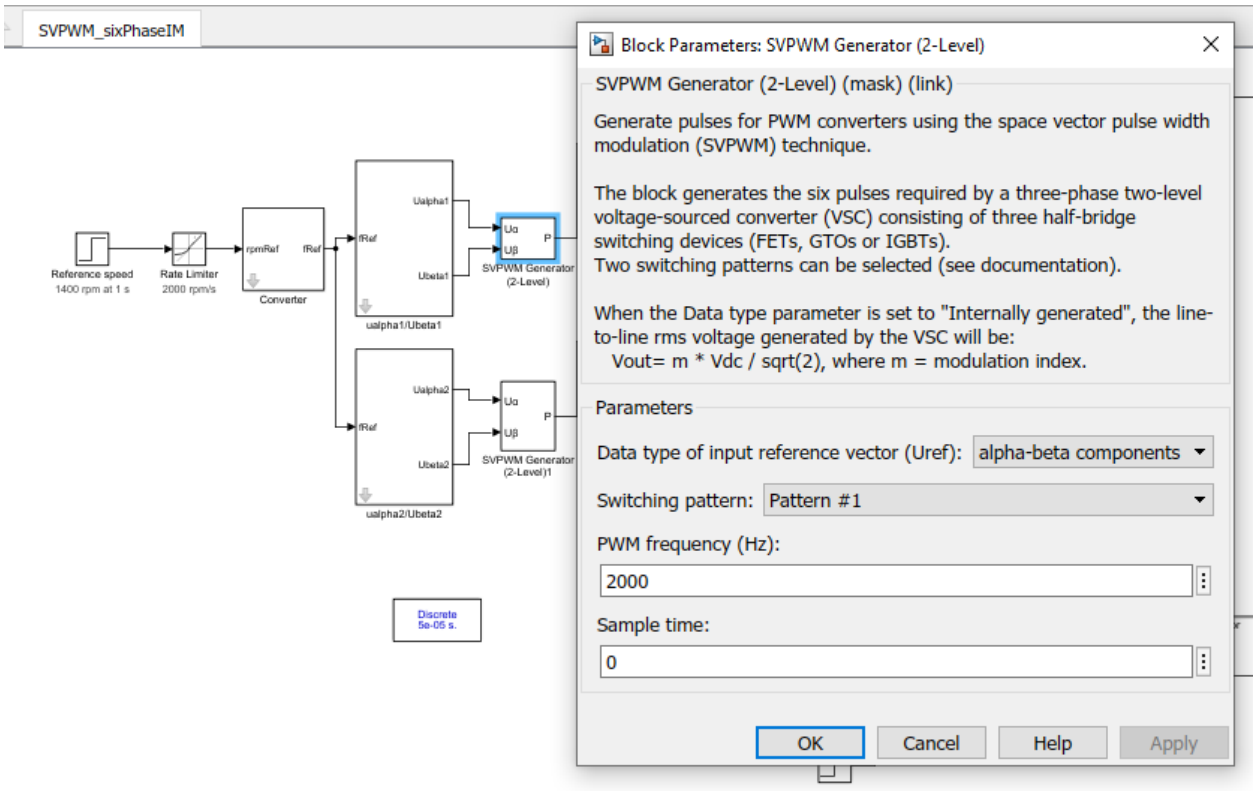

Figure 3.36. SVPWM generator

Inverter model

The inverters were powered from a single DC voltage source of 750V indicated by figure 3.37

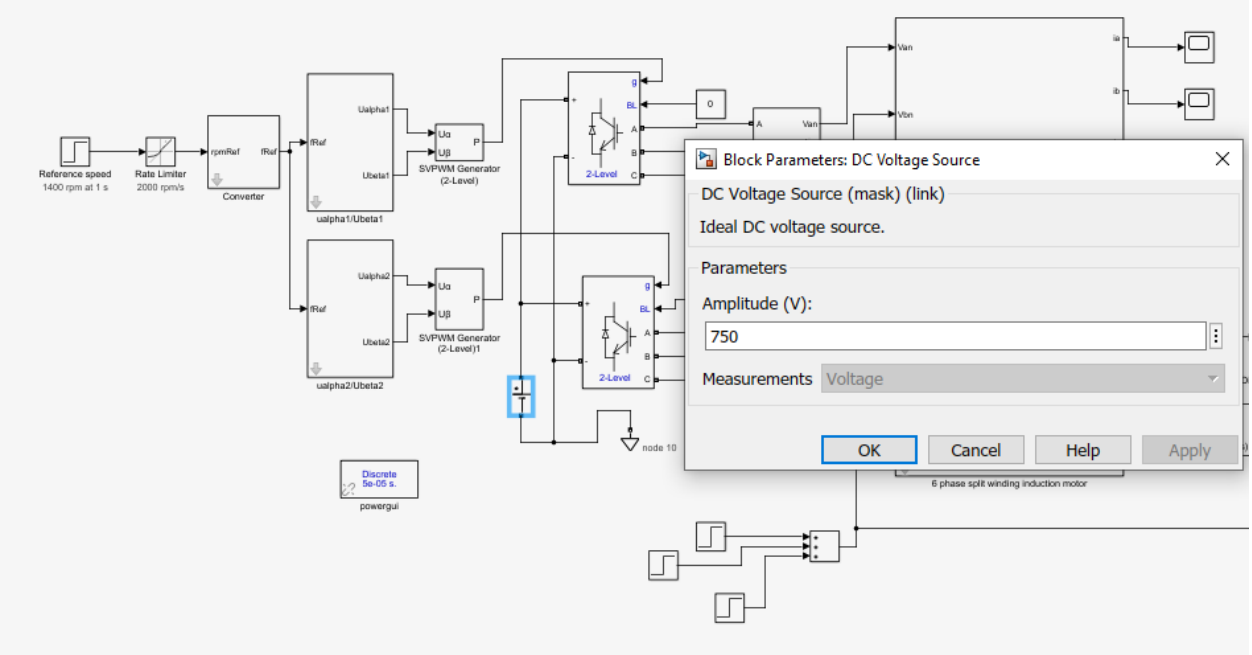

Figure 3.37. Inverter power source

The figure 3.38 and 3.39 represents the Line to neutral voltage calculations for both sets of winding.

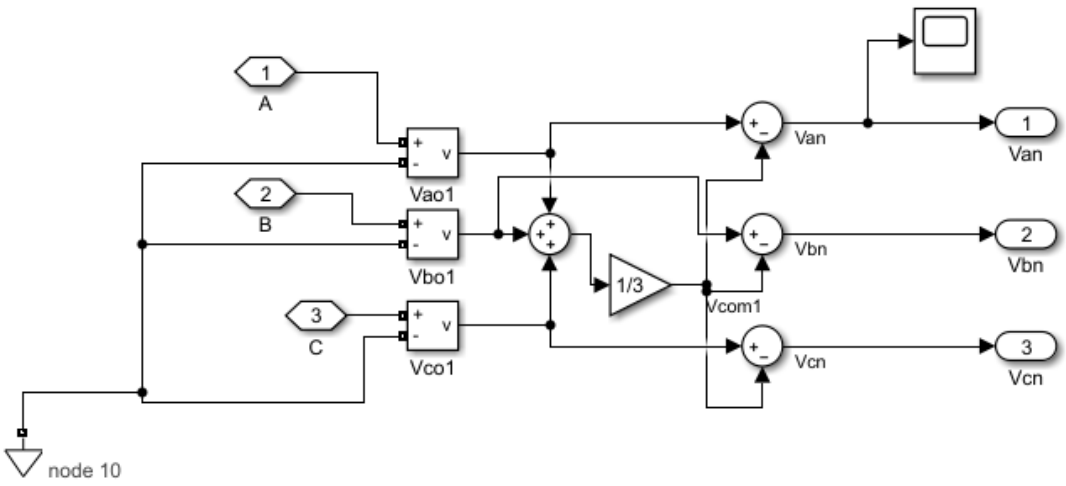

Figure 3.38. Line to neutral voltage calculation for first winding

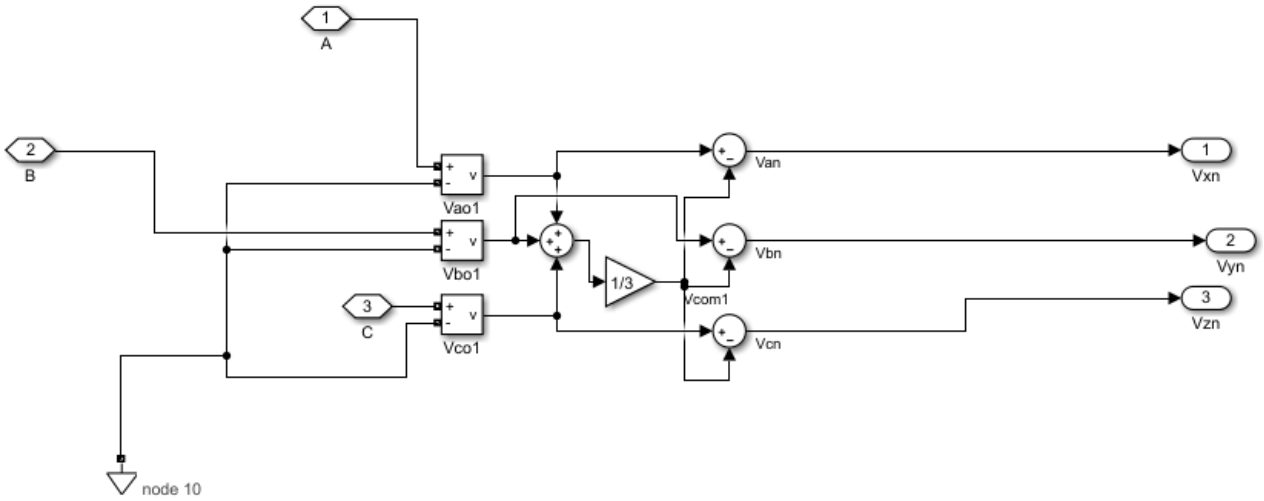

Figure 3.39. Line to neutral voltage calculation for second winding

According to the definition of common-mode voltage in converter, we can know V_{com} is the common-mode voltage of converter. The expression of the V_{com} is shown as follows:

$$Vcom1 = \frac{Vao + Vbo + Vco}{3} \quad \text{(67)}$$

$$Vcom2 = \frac{Vxo + Vyo + Vzo}{3} \quad \text{(68)}$$

$$Van = Vao - Vcom1 \quad \text{(69)}$$

$$Vbn = Vbo - Vcom1 \quad \text{(70)}$$

$$Vcn = Vco - Vcom1 \quad \text{(71)}$$

$$Vxn = Vxo - Vcom2 \quad \text{(72)}$$

$$Vyn = Vyo - Vcom2 \quad \text{(73)}$$

$$Vzn = Vzo - Vcom2 \quad \text{(74)}$$

Scalar Control of six phase induction motor

The Scalar Control is implemented using the V/f or V/Hz, control structure [29]. The open-loop V/f control structure that the block implements is depicted in figure 3.40. This approach, often known as scalar control, does not employ the field orientation of the motor. Instead, the key control variables are frequency and voltage, which are applied to the stator's windings. The rotor's status is disregarded, which means that no speed or position signal is fed back.

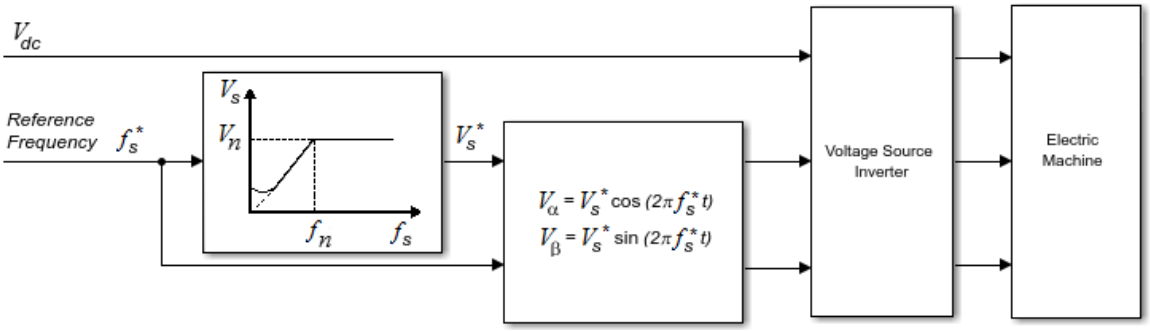

Figure 3.40. Implementation of scalar control

The Induction Machine Scalar Control block computes the magnitude of the stator voltage based on the reference frequency, f_{*S}, as:

$$V^*_s = \left(\frac{V_n - V_{\min}}{f_n - f_{\min}} \right) * f^*_s \quad \text{..... (75)}$$

where:

- V_n is the rated voltage.
- V_{min} is the minimum voltage.
- f_n is the rated electrical frequency.
- f_{min} is the minimum frequency.

The voltage components in the stationary reference frame [29]are:

$$V_\alpha = V^*_s * \cos(2\pi f^*_s * t) \quad \text{..... (76)}$$

And

$$V_\beta = V^*_s * sin(2\pi f^*_s * t) \quad \text{..... (77)}$$

The block obtains V_{abc} from V_α and V_β by using an inverse Clarke transformation is represented on figure 3.41.

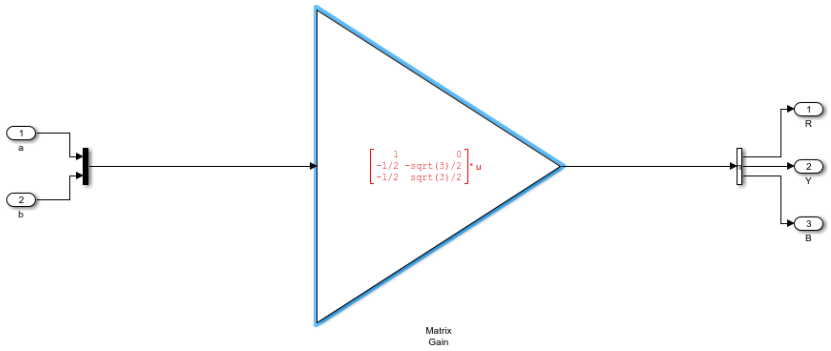

Figure 3.41. Phase conversion

The step by step subsystem model of the V/f method is shown in figure 3.42 to 3.44. The six phase motor was modelled as discussed in [30].

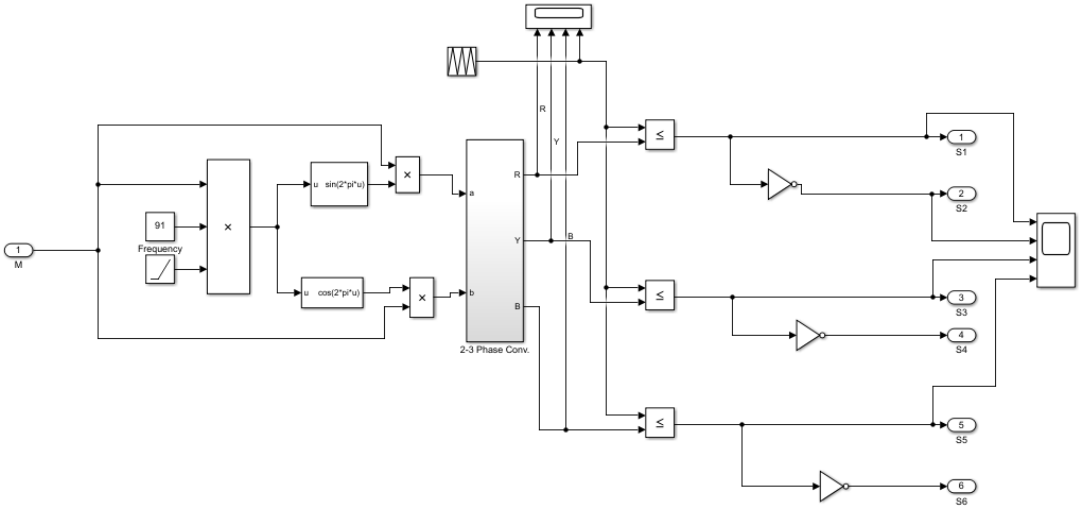

Figure 3.42. PWM1 and V/F1 block

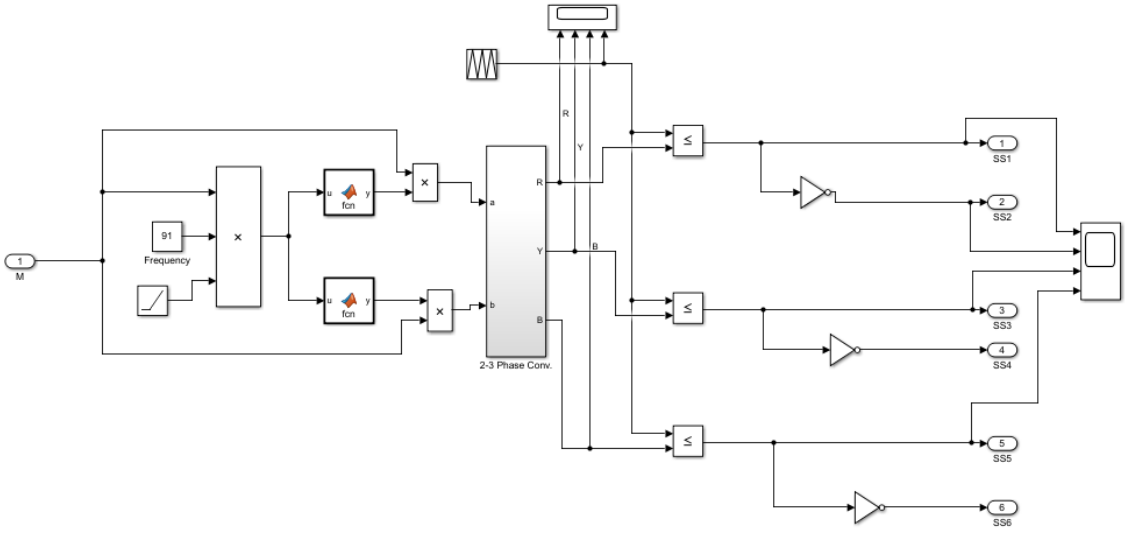

Figure 3.43. PWM2 and V/F2 block

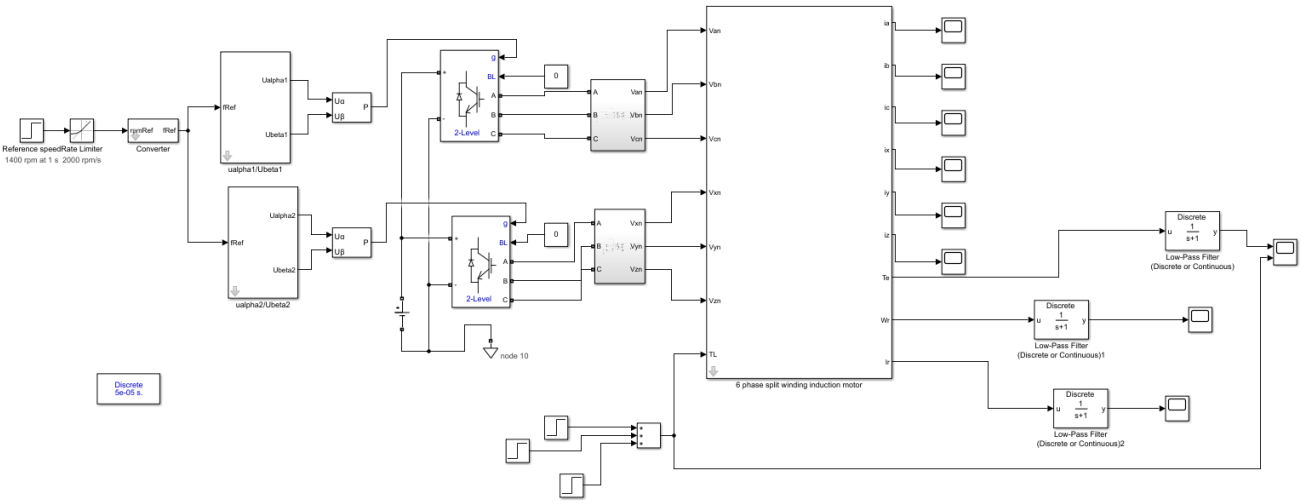

Figure 3.44. Completed V/F model of six phase Motor

CHAPTER 4: SIMULATION RESULTS AND DISCUSSION

4.1 Introduction

Simulations using the matlab/simulink simulation tool were performed to examine the starting and operating performance of three phase and six phase induction motors when subjected to traction. To compare simulation results, the kality deport sample motor specification was used, and simulations were done by running both three and asymmetrical six phase induction motors.

4.2 SPWM voltage source inverter

The switching sequence of gate pulses is presented on the figure 41 below;

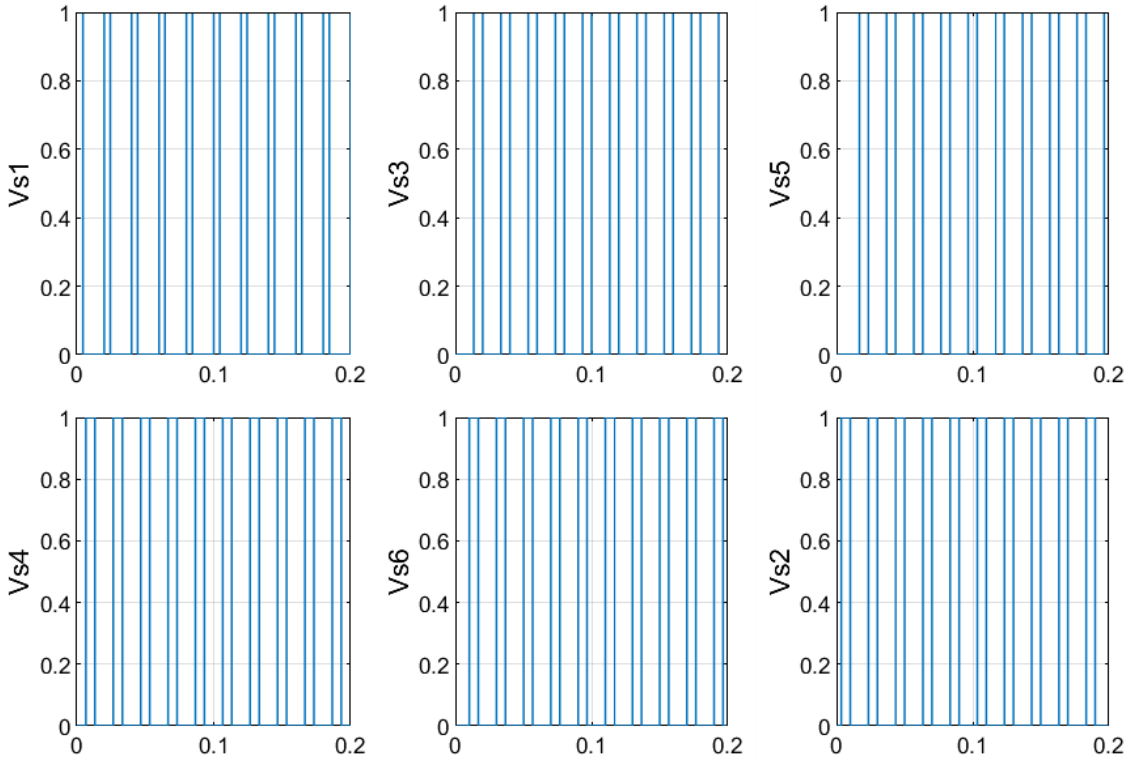

Figure 4.1. Gate signal

The graphs under the following configuration were plotted on a carrier frequency of 1000Hz and by decreasing this frequency, the speed can be decreased and vice versa. The switches in each leg are never both on or off simultaneously; therefore, the phase voltages fluctuate between voltages $\frac{2v_{dc}}{3}$ and zero as the RMS block was employed. The line-line inverter output voltages are ac, with a fundamental frequency corresponding to the frequency of the sinusoidal control voltage, because the switches are controlled in this way. The inverter output voltages are shown in figure 4.2 below,

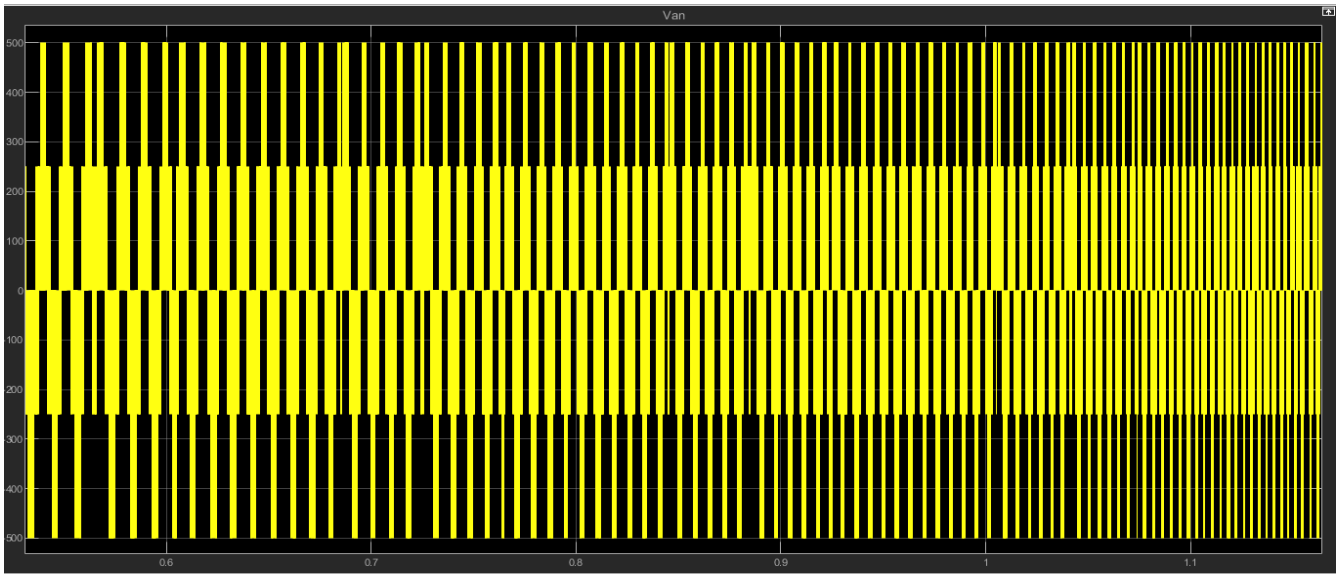

Figure 4.2. Inverter phase voltages

4.3 Stator and Rotor Currents

The figure 4.3 to 4.6 represents the stator and rotor currents for three and six phase induction motor respectively;

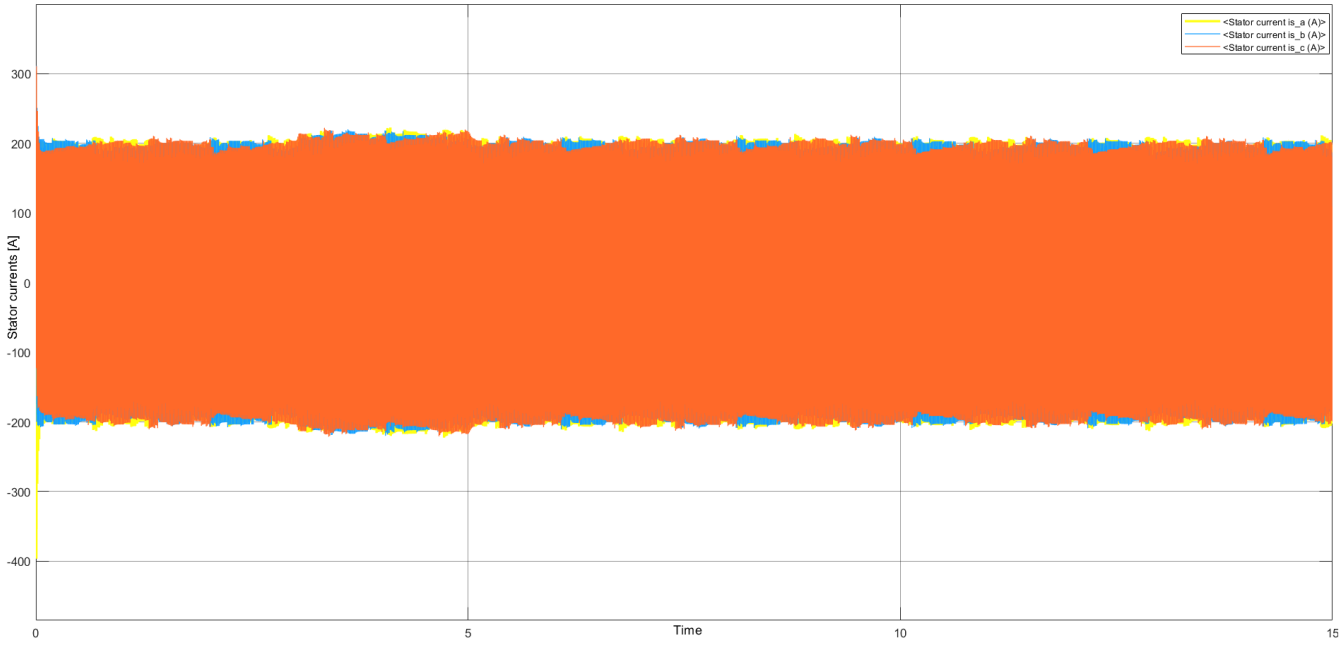

Figure 4.3Stator currents waveforms for TPIM

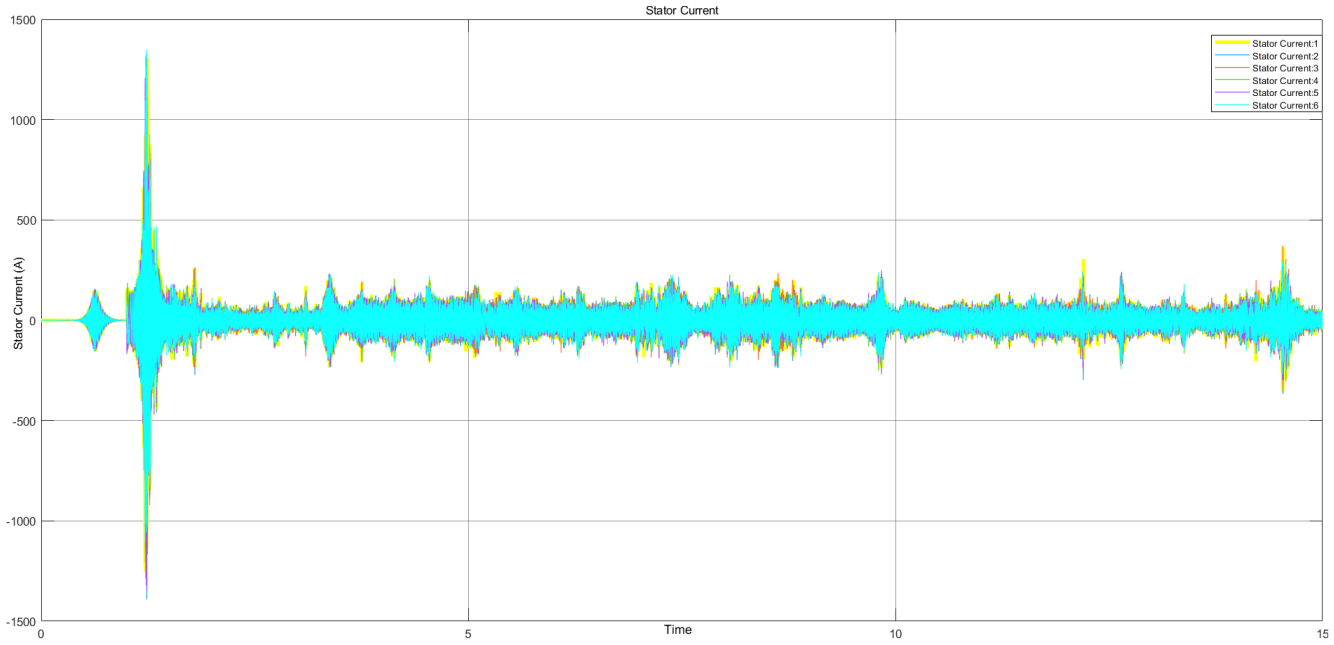

Figure 4.4stator currents waveforms for SPIM

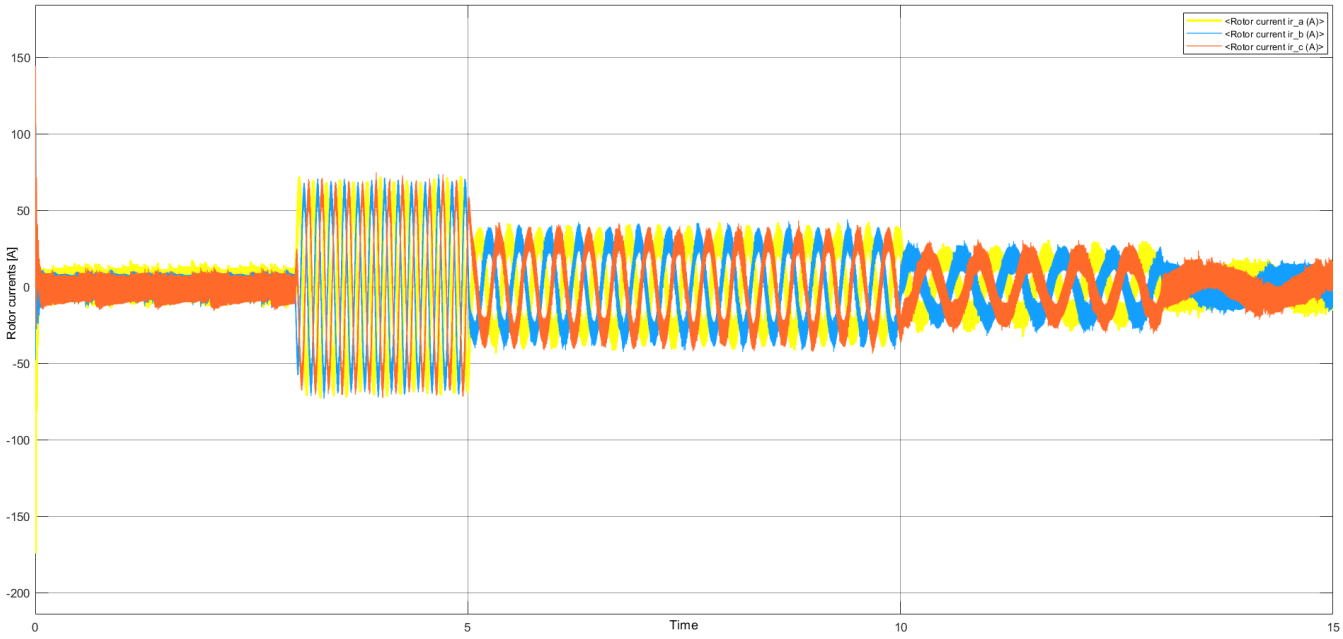

Figure 4.5. rotor currents waveforms for TPIM

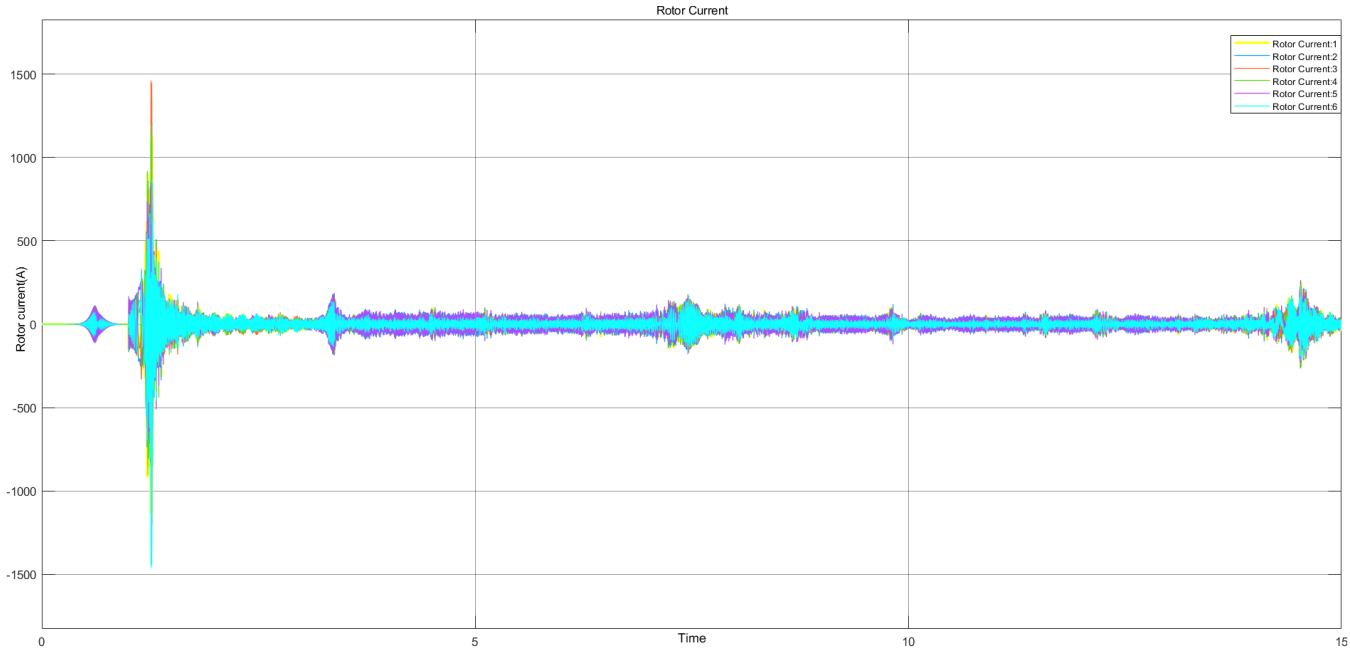

Figure 4.6. rotor currents waveforms for SPIM

As can be observed from the graph, the motor has a high initial starting current for every torque variation. Because induction motors have a high inrush current when they start, this happens.

The actual starting current curve is determined by the motor's design and the voltage supplied. It is absolutely unaffected by the load on the motor. The time it takes for the motor to accelerate to full speed, and the duration of the high starting current, is affected by the motor load.

4.4 FFT Analysis

Figure 4.7 to 4.14 demonstrates fourier analysis for stator and rotor currents in order to measure how much the distortion of a current is due to harmonics in the signal. The cycles are 100

4.4.1 Stator currents

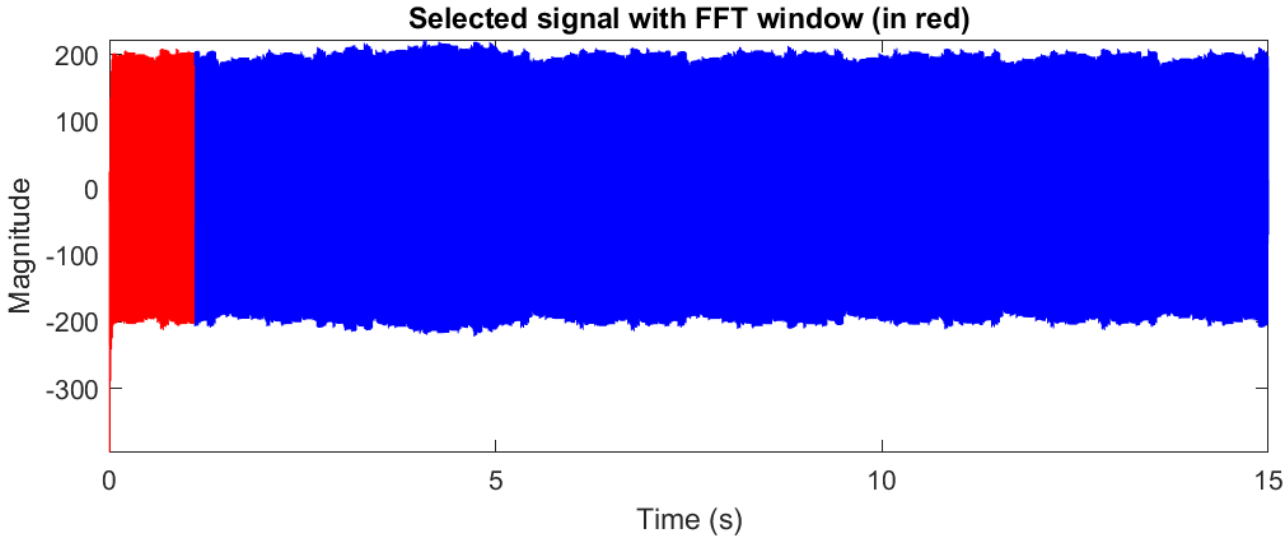

Figure 4.7. Stator currents signal for TPIM

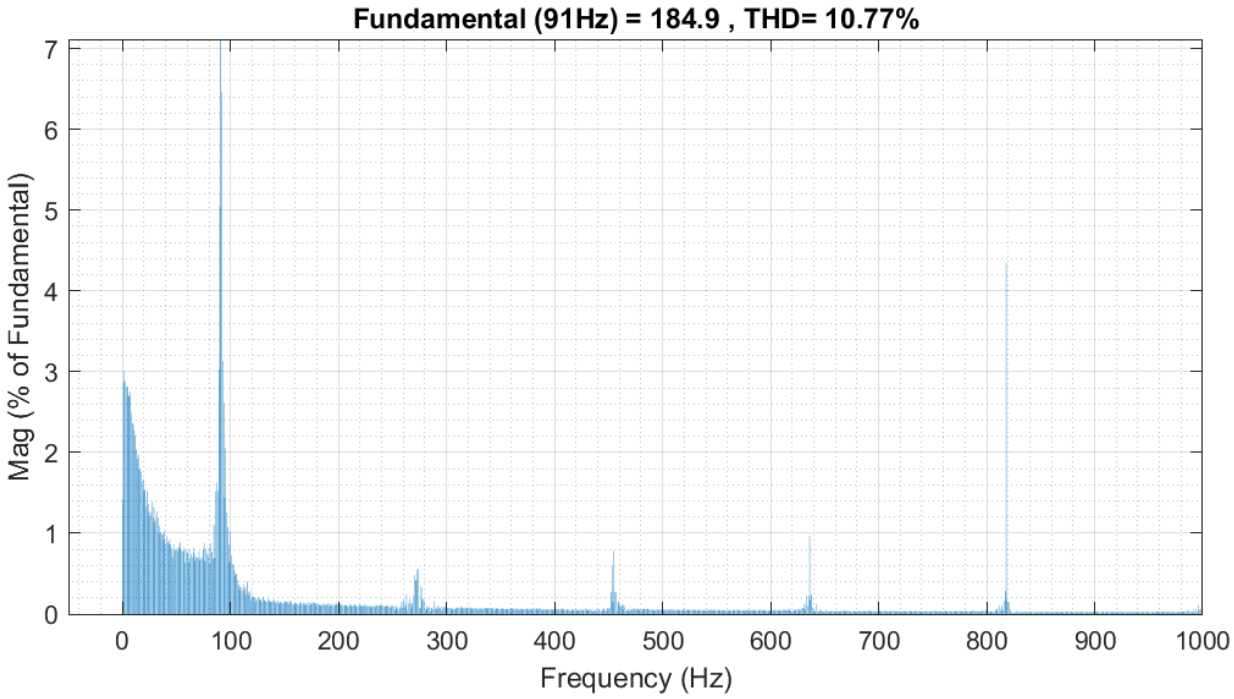

Figure 4.8. FFT analysis for stator current (THD of 10.77%) for TPIM

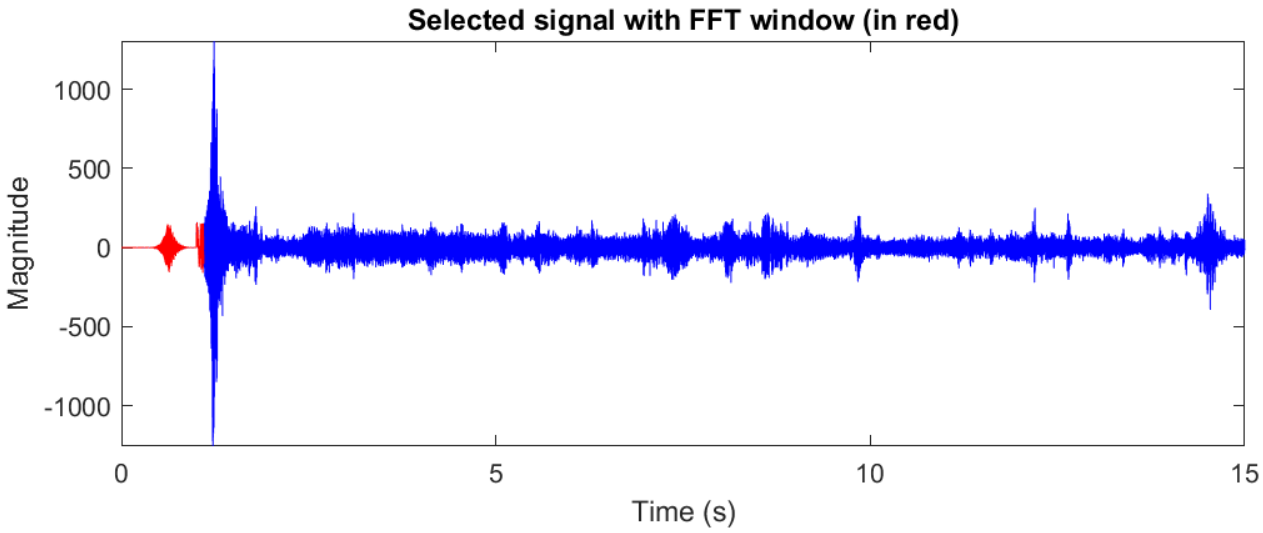

Figure 4.9. Stator currents signal for SPIM

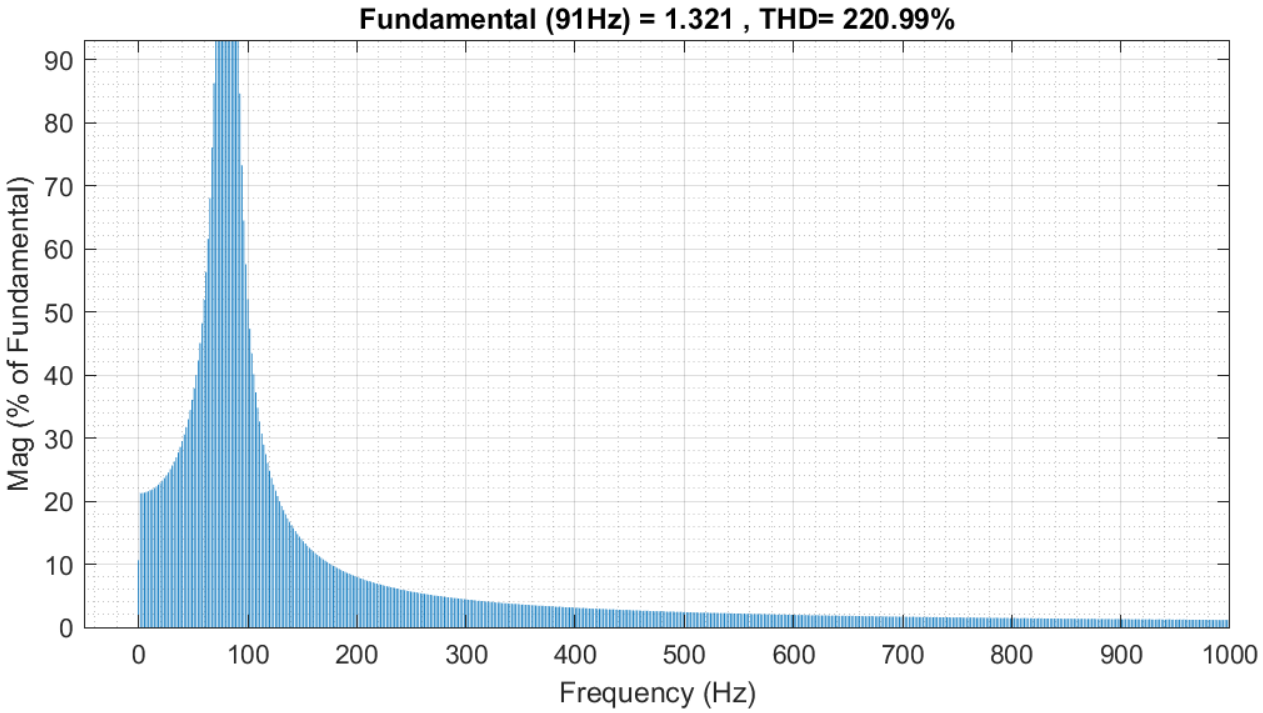

Figure 4.10. FFT analysis for stator current (THD of 220.99%) for SPIM

4.4.2 Rotor currents

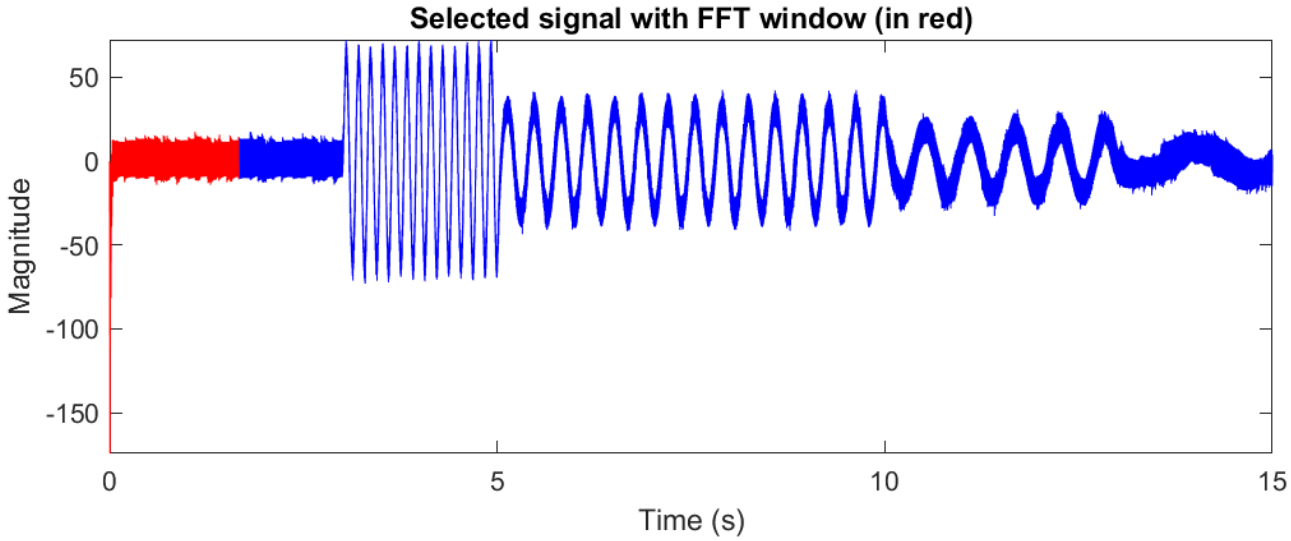

Figure 4.11. Rotor currents signal for TPIM

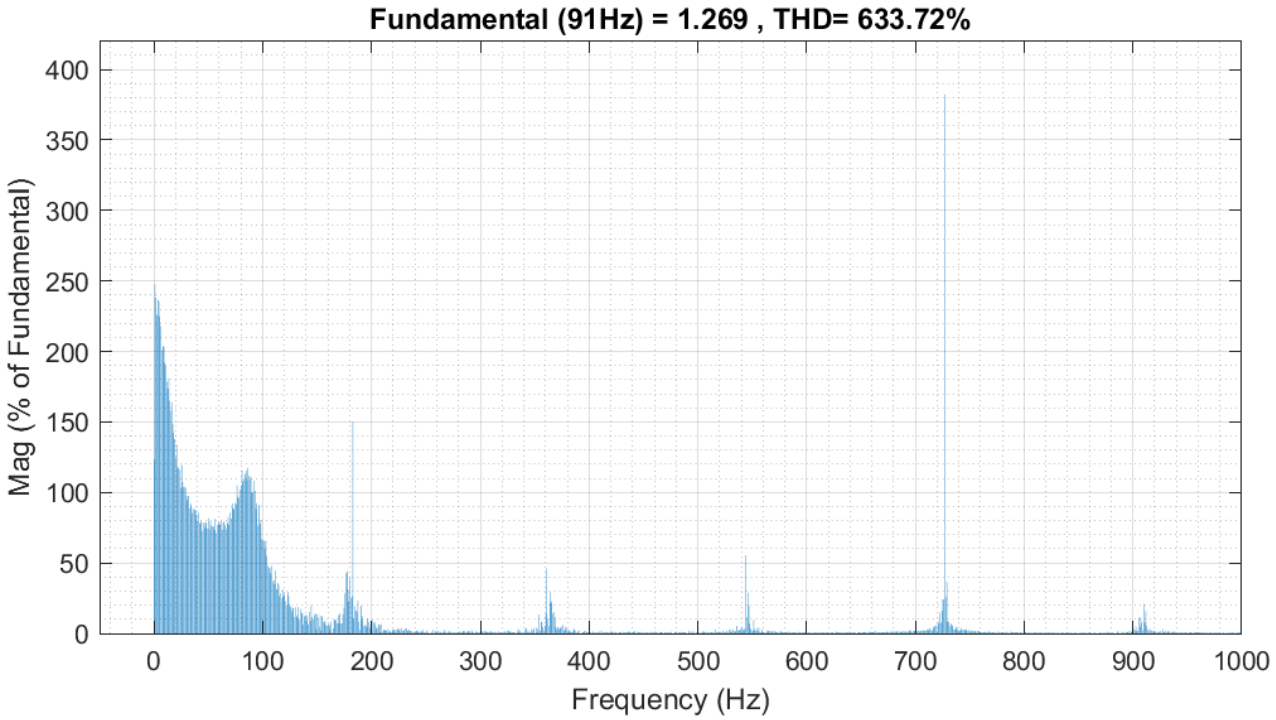

Figure 4.12. FFT analysis for rotor current (THD of 633.72%) for TPIM

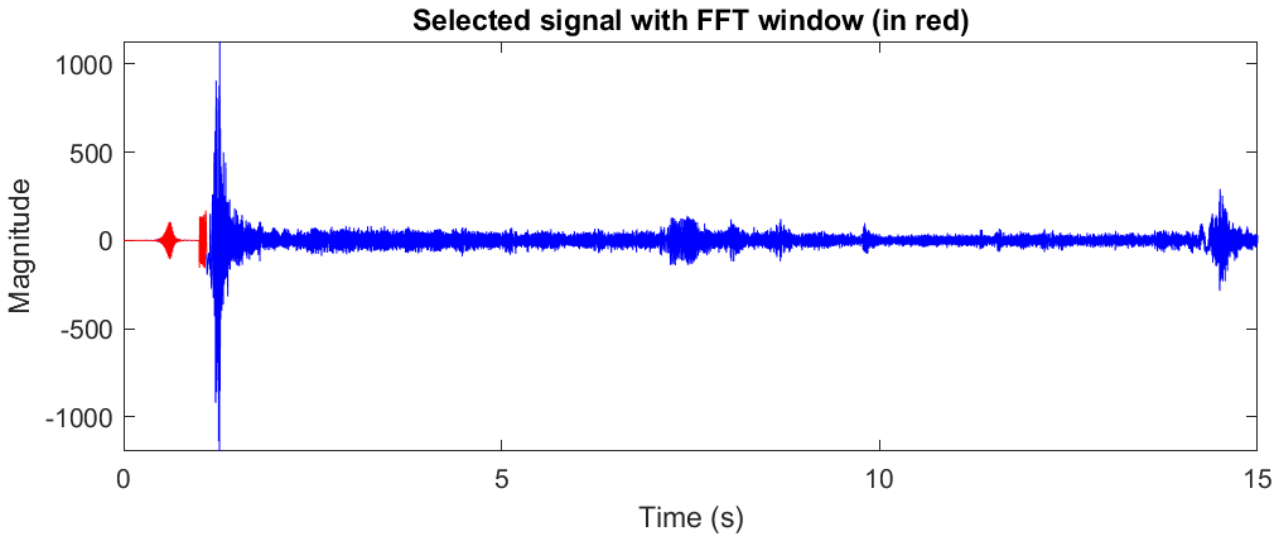

Figure 4.13. Rotor currents signal for SPIM

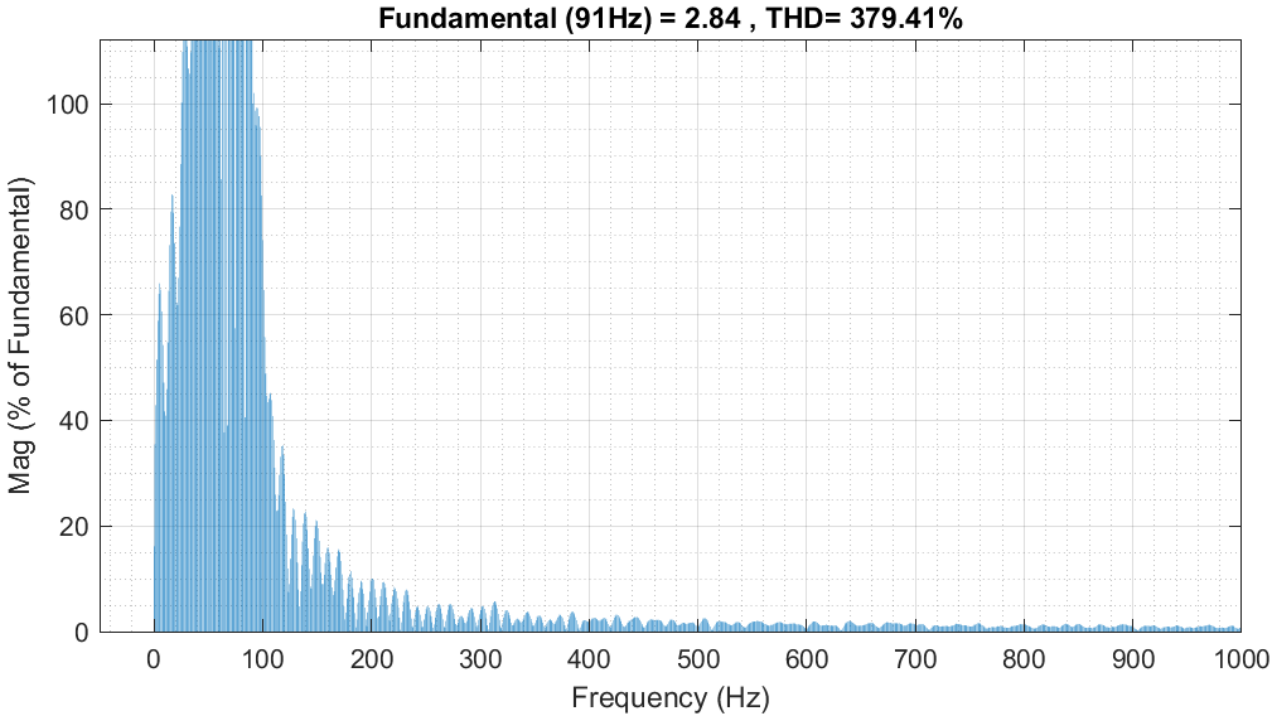

Figure 4.14. FFT analysis for rotor currents (THD of 379.41%) for SPIM

A periodic function's Fourier analysis is the extraction of the series of sines and cosines that, when superimposed, reproduce the function. The harmonic distortion factor can be calculated by analyzing a segment of the signal. Total harmonic distortion (THD) is a measurement that indicates how much a voltage or current is distorted as a result of harmonics in the signal. Harmonics, also known as harmonic frequencies, are frequency components of a signal that are integer multiples of the main signal's frequency.

A purely sinusoidal signal has no harmonic distortion, whereas a square wave, which is periodic but does not look sinusoidal, has a lot. Of course, in the real world, sinusoidal voltages and currents are not completely sinusoidal, and there will be some harmonic distortion.

THD is defined as the ratio of the equivalent root mean square (RMS) voltage of all harmonic frequencies (from the second harmonic) to the RMS voltage of the fundamental frequency (The fundamental frequency is the main frequency of the signal, i.e., the frequency that you would identify if examining the signal with an oscilloscope).

$$THD = \frac{\sqrt{\sum_{n=2}^{\infty} V_{n\_rms}^2}}{V_{fund\_rms}}$$ where,

Vn~rms: is the RMS voltage of the nth harmonic

$V_{fund\text{-}rms}$: is the RMS voltage of the fundamental frequency [31]

The simulation of the induction motor supplied from inverter for the above simulation shows that over 100 cycles of FFT analysis, the rotor current is much distorted compared to stator current.

4.5 Mechanical and Electromagnetic torque

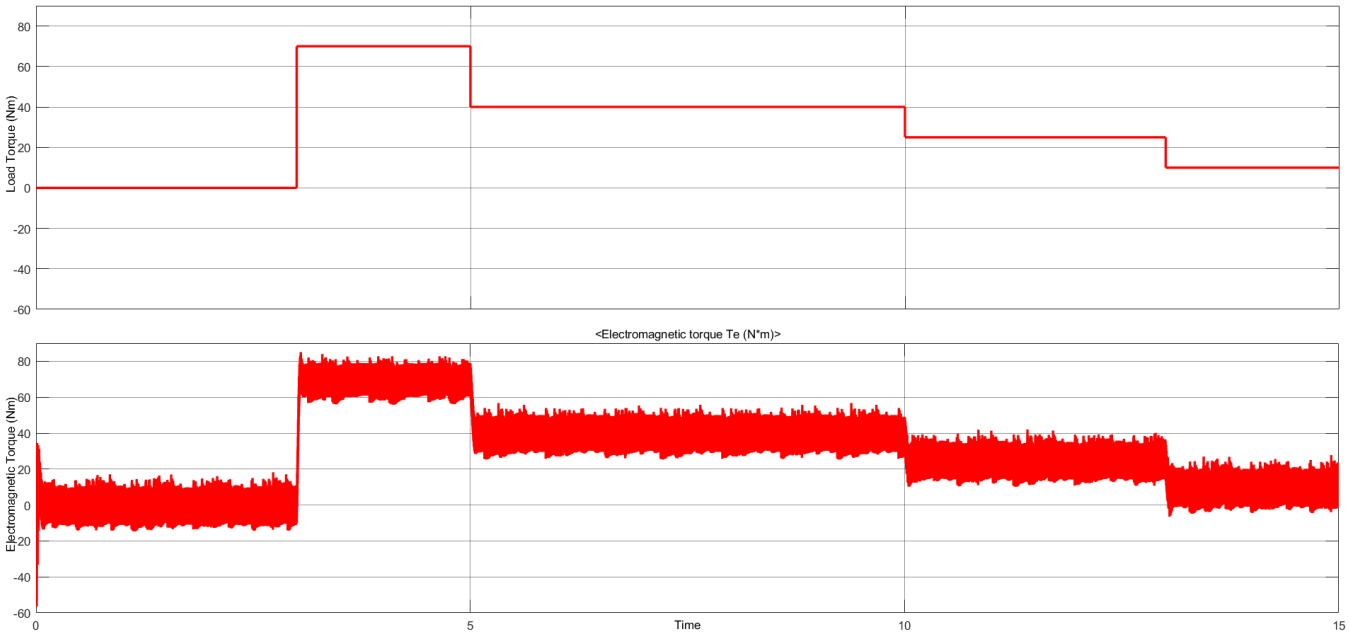

Figure 4.15. Mechanical torque, electromagnetic torque for TPIM

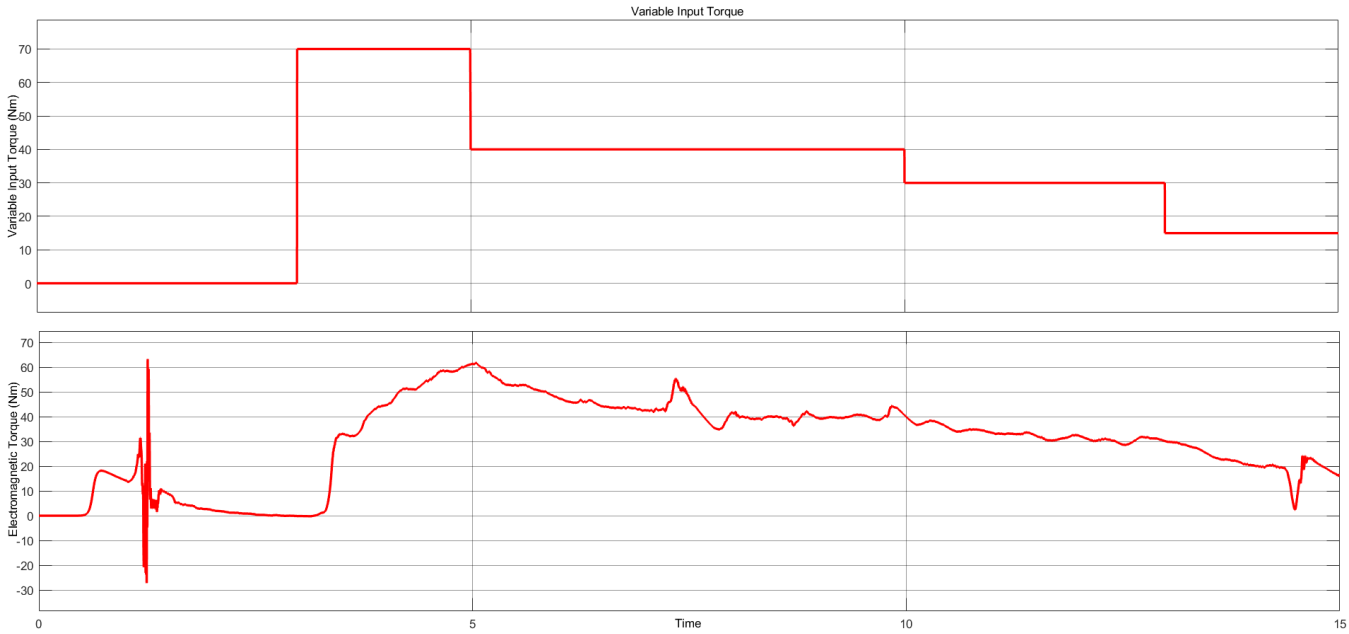

Figure 4.16. Mechanical torque, electromagnetic torque for SPIM

4.6 Rotor speed

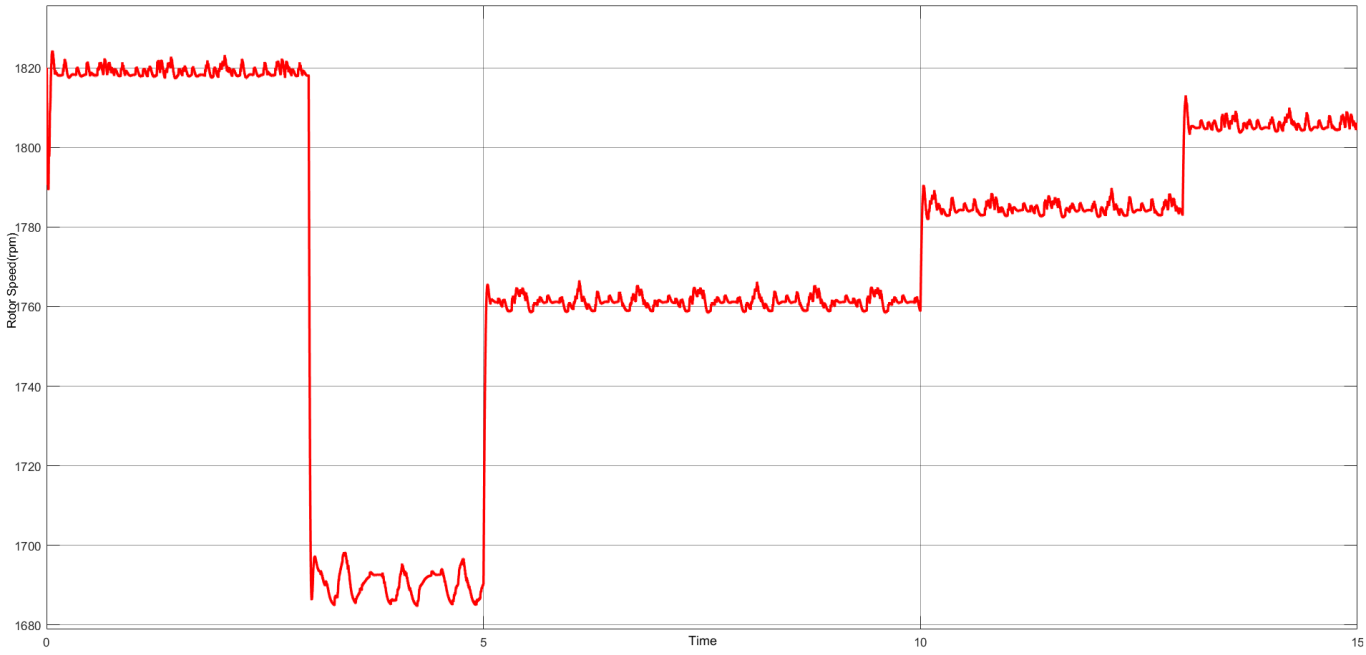

Figure 4.17. rotor speed variation for TPIM

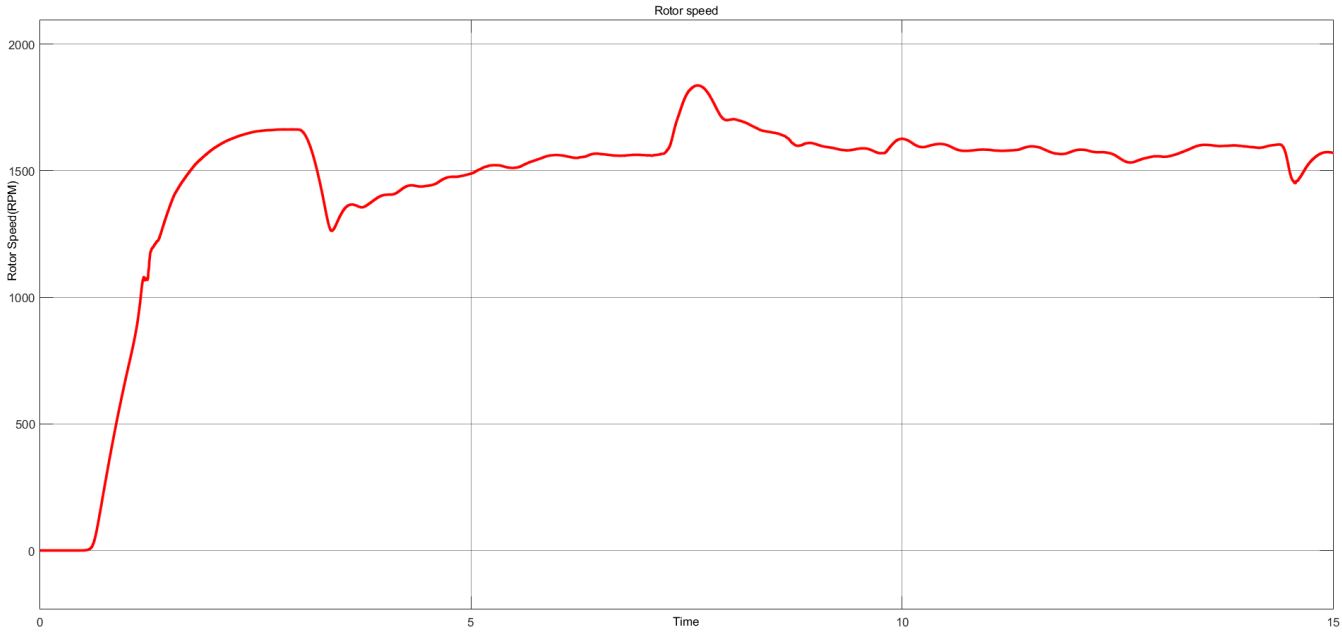

Figure 4.18. rotor speed variation for SPIM

Both parameters have a higher starting value, as demonstrated by the torque and current variations. This occurs because induction motors draw a large starting current, up to 5 to 7 times the full load current. Induction motors are regarded short-circuited secondary transformers, and their equivalent circuit consists of two parallel branch circuits: magnetizing current and resistance, and reactance circuit.

The magnetic component of current flowing through an induction motor is proportionate to the applied voltage and is unaffected by the motor's load. The slip will be unit when the motor starts. As a result, the resistance offered to current (for both stator and rotor) will be minimal, resulting in a high initial inrush current. The current drawn by the machine reduces as the rotor picks up speed. The starting torque is high because the torque is proportional to the current.

The motor will attain full speed if the torque developed by the motor exceeds the load torque at all speeds during the starting cycle. During the starting cycle, if the motor's torque is less than the load's torque at any speed, the motor will stop accelerating. The acceleration torque is the difference between the motor's produced torque and the load torque, and it changes as the motor accelerates due to the motor's speed-torque curve and load/speed load curve.

4.7 Discussions

It has been discovered that three phase induction motors have substantially higher rotor harmonics than six phase induction motors, resulting in increased rotor heating and pulsing or reduced torque. Acoustic noise is also reduced as a result of this.

Table 4.1.Three to six phase parameters comparison

Parameters	SPIM	TPIM
Torque(Nm)	14.22	7.649
Speed(rpm)	689.2	1818
THD in stator(%)	220.99	10.77
THD in rotor(%)	379.41	633.72

SPIM outperforms conventional TPIM, according to the research findings. Some of the advantages of SPIM over traditional TPIM are as follows.

The torque per ampere is improved as the required power is divided into several phases, resulting in an increase in power handling capability.

Harmonic distortion is lower in rotor current.

The speed variation from no load to maximum load is smaller than that for a three-phase induction motor.

Economic analysis of the motors

In the motor design the best one is the one which attains the maximum advantage of better performance and high efficiency in the least possible cost. This is due to the fact that the stator excitation in a multiphase machine produces a field with a lower space-harmonic content, so the efficiency is higher than in a three-phase machine.

For the case of this research, in order to sustain the same rating for both six phase and three phase induction motors the following equation has to be performed;

$P_{in} = mV_{ph}I_{ph}10^{-3}$ [30] Where m is the number of phases

$3V_{ph(3\phi)}I_{ph(3\phi)} = 6V_{ph(6\phi)}I_{ph(6\phi)}$

Knowing that the phase currents are the same, we get

$$V_{ph(6\phi)} = \frac{3V_{ph(3\phi)}I_{ph(3\phi)}}{6I_{ph(6\phi)}} = \frac{1}{2}V_{ph(3\phi)}$$

The power requirement of the multiphase machine per phase decreases as the overall power is divided by the number of phases; hence, the current-voltage values of the semiconductor switching elements that provide this power decrease.

This means that the phase voltage in six phase system is a half of its three phase counterpart which results in reduced power ratings, cost and losses of supply converters and in low capacity insulation materials [32] . Cost wise, as the number of phases increase for the same motor capacity, the motor cost decreases. For example, a 5 hp NEMA AC Induction Motor, 2 pole three phase, 3450 rpm costs $972.22 while a 5 hp NEMA AC Induction Motor, 2 pole single phase,3450 rpm costs $1,049.21[33].

Increased torque per ampere in six phase motor for the same three phase volume machine, results in reduced stator copper losses and reduced rotor harmonic currents[34]
As current frequency increases, current tends to flow at the outer edge of the wires while avoiding the centre area. The larger the cable and higher the frequency, the more pronounced the skin effect. Typical electrical systems have maximum fundamental frequencies up to 1 to 1.5 kHz which are sufficient to produce significant skin effect in large cables. The table 4.2 below compares 3 to 9phases motor in terms of efficient use of cable cross-sectional area.

Table 4.2. Comparison of 3 to 9 phases motor in terms of cable cross-sectional area usages

	3-phases	9-phases
Phase current	555A	185A
Conductor size	120mm^2	25mm^2
Cabling loss	353W	572W
Cabling temperature elevation	60^{0}C	55^{0}C
Cable diameter	22.6mm	11.2mm
Total cabling weight	10.97kg	7.31kg
Minimum bending radius	Easier to route near the motor and drive	
	90.4mm	44.8mm

This results in an overall reduction of copper surface and weight.

However, as smaller gage cables and associated components are more readily available, the overall impact of multi-phase systems yields a small reduction in price as shown in the following table (low prices are for low volumes);

Table 4.3. The overall impact of multi-phase systems yields in a small reduction in price [35]

	3Phase Motor			**3*3Phase Motor**			
	Quantity	**$/unit**	**$total**	Quantity	$/unit	$total	**Variation**
wire	3*2.5m	$36.14	$271.05	9*2.5m	$8.53	$191.92	-41%
Terminal lug	6	$5.30	$31.80	18	$1.04	$18.72	-69%
Cable gland	6	$34.00	$204.00	18	$15.00	$270.00	24%
			$536.85			$480.64	-11%

The number of stator and rotor slots increases as the number of phases increase and this yields in increased starting torque and current. [36]

The six-phase induction motor is a failsafe and fault-tolerant system that allows a six-phase machine to operate as a six-phase machine at low speed with high torque while still operating as a three-phase machine at higher speed. The three-phase motor, on the other hand, necessitates the use of a modular parallel switch redundant system to provide fault tolerance, which necessitates the use of an appropriate control architecture, which includes a monitoring system, fault detection strategy, and controller reconfiguration for fault handling and subsequent post-fault operation for the detection of a single switch short-circuit, phase-leg short-circuit, single switch open-circuit, and single-phase open-circuit. Furthermore, there are significant costs associated with providing fault-tolerant operation, as all topologies necessitate additional components in the form of silicon switches and/or fuses to provide capacity in the case of a fault that would not otherwise be present in a standard three-phase inverter drive.[37]

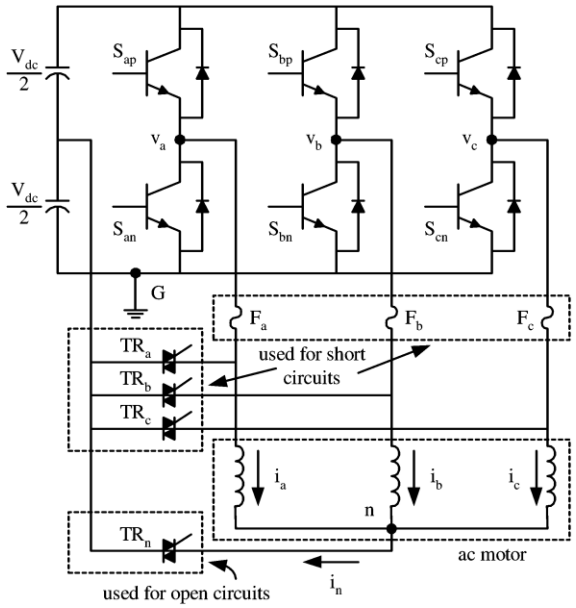

Figure 4.19. Topology of three phase induction motor fault tolerant operation

CHAPTER 5: CONCLUSION AND RECOMMENDATION

5.1 Conclusion

Thanks to their superior nature of robust construction and low maintenance requirements, induction motors are widely used in drive applications in transport. In order to obtain variable supply frequency and terminal voltage, the speed of an induction motor was controlled using an inverter.

The speed of an induction motor is controlled by an inverter in order to achieve variable supply frequency and terminal voltage. Induction motor designs for railway traction are frequently targeted at reducing machine size, which can be desirable or even essential due to space constraints, and must meet higher efficiency, reliability, and a wider range of speed controllability.

According to the findings of this study, which compared the performance of six phase induction motor to that of three phase induction motor, the six phase induction motor meets all of the requirements to replace the traditional three phase motor since torque is high at low speeds. The distortion was shown to be higher in three phase motors (633.72) than in six phase motors (379.41), despite the fact that the six phase induction motor is more cost-effective, failsafe, and fault-tolerant technology.

The torque in six phase was seen to be 1.86 times that of three phase induction motor while the speed in three phase induction motor is 2.6 times that of six phase induction motor.

The overall impact of multi-phase systems yields in a small reduction in price (-11%) according to economic analysis.

Six phase induction motors are the ideal choice for railway traction systems since an electric vehicle drive system must have a fast torque response, reasonable cost, reliability, and durability.

5.2 Recommendation

The type of six phase induction motor used in this research was asymmetrical six phase (30^0 phase shift between two successive phases of two different windings). The six phase induction motor has shown a good performance in a railway industry compared to its three phase counterpart (conventional). The further research work could be carried out in the areas of multiphase induction motor by:

a. Considering the symmetrical induction motor.
b. Using Lab method in comparison with matlab results
c. Using closed loop speed control system
d. Evaluating many control technics, especially vector control

References

[1] G. D. Friedlander, “Railroad electrification: Past, present, and future: History of systems in the United States,” *IEEE Spectr.*, vol. 5, no. 7, pp. 50–65, 1968.

[2] S. Ravindra Jape and A. Thosar, “Comparison of Electric Motors for Electric Vehicle Application,” *Int. J. Res. Eng. Technol.*, vol. 06, no. 09, pp. 12–17, 2017.

[3] H. A. T. and S. W. E. Levi, R. Bojoi, F. Profumo, “Multiphase induction motor drives – a technology status review.”

[4] A. Thaduri, A. Garmabaki, and U. Kumar, “Impact of climate change on railway operation and maintenance in Sweden : A State-of-the-art review,” pp. 1–19, 2021.

[5] M. M. Bakran, A. Marz, B. Laska, E. Krafft, O. Korner, and A. Nagel, “Latest developments in increasing the power density of traction drives,” *2014 Int. Power Electron. Conf. IPEC-Hiroshima - ECCE Asia 2014*, pp. 2113–2119, 2014.

[6] K. Gopakumar, “Elect.Engg. Indjan Institute of Science Bangalore 560 012,.”

[7] K. S. Aher and A. G. Thosar, “Modeling and Simulation of Five Phase Induction Motor using MATLAB / Simulink,” vol. 6, no. 5, pp. 1–8, 2016.

[8] A. E. James, L. Anih, and O. Okoro, “Transient Analysis and Modelling of Sixphase Asynchronous Machine,” vol. 4, no. 6, pp. 77–83, 2015.

[9] E. Levi, “Multiphase electric machines for variable-speed applications,” *IEEE Trans. Ind. Electron.*, vol. 55, no. 5, pp. 1893–1909, 2008.

[10] R. O. C. Lyra and T. A. Lipo, “Torque density improvement in a six-phase induction motor with third harmonic current injection,” *IEEE Trans. Ind. Appl.*, vol. 38, no. 5, pp. 1351–1360, 2002.

[11] J. M. Apsley and S. Williamson, “Analysis of multi-phase induction machines with winding faults,” pp. 249–255, 2005.

[12] P. Venter, A. A. Jimoh, and J. L. Munda, “Realization of a ‘ 3 & 6 Phase ’ Induction Machine,” no. July 2014, 2012.

[13] A. Fathy, I. Larrazabal, D. Ortega, I. Larrazabal, and F. Briz, “Strategies for for Induction Induction Motors Motors in in Railway,” *MDPI*, 2019.

[14] K. Hatua and V. T. Ranganathan, “Direct Torque Control Schemes for Split-phase Induction Machine,” *IEEE Ind. Electron. Mag.*, pp. 615–622, 2004.

[15] I. Bolvashenkov, J. Kammermann, and H. G. Herzog, “Methodology for selecting electric traction motors and its application to vehicle propulsion systems,” *2016 Int. Symp. Power Electron. Electr. Drives, Autom. Motion, SPEEDAM 2016*, no. c, pp.

1214–1219, 2016.

[16] Yared Kassahun Abadi, “Development of Adaptive Control for Railway Vehicles Braking System,” Addis Ababa Institute of Technology, 2017.

[17] D. Verma, “Performance Evaluation of Asymmetrical Multiphase Induction Motor Using Matlab / Simulink,” pp. 1–6, 2016.

[18] S. R. Nelatury, “Uniqueness of Torque-Speed Characteristics of an Induction Motor,” *IEEE Trans. Magn.*, vol. 40, no. 5, pp. 3431–3433, 2004.

[19] R. J. Lee, P. Pillay, R. G. Harley, and K. G. V Avenue, “D, Q Reference Frames for the Simulation of Induction Motors,” vol. 8, pp. 15–26, 1984.

[20] C. Tuo, “Analysis on the Mathematical Model of the Six-Phase,” pp. 303–310, 2011.

[21] E. Engineering, “Model of Six-Phase Induction Motor Roma RINKEVIČIENĖ 1,” vol. 221, pp. 510–514, 2015.

[22] B. Kundrotas, S. Lisauskas, and R. Rinkeviciene, “Model of Multiphase Induction Motor Model of Multiphase Induction Motor,” no. May, 2014.

[23] P. Kumar and K. B. Yadav, “Modelling and Analysis of Asymmetrically wound 6-phase Induction Motor for improve performance,” vol. 4, no. 5, pp. 39–47, 2016.

[24] “A Brief Overview of IGBT - Insulated Gate Bipolar Transistor.” [Online]. Available: https://components101.com/articles/what-is-igbt-working-operation-symbol-and-types. [Accessed: 10-Apr-2020].

[25] S. Mandal, “Performance Analysis of Six-Phase Induction Motor Performance Analysis of Six-Phase Induction Motor,” *Int. J. Eng. Res. Technol.*, vol. Vol. 4, pp. 589–593, 2015.

[26] E. K. Appiah, G. M, A. A. Jimoh, J. L. Munda, and A. S. O. Ogunjuyigbe, “Symmetrical Analysis of a Six-Phase Induction Machine Under Fault Conditions,” *Int. J. Electr. Comput. Eng.*, vol. 7, no. 3, pp. 324–331, 2013.

[27] S. E. Iduh, “3.11. Dynamic Modeling and Simulation with MATLAB Simulink The simulation of the developed mathematical model of the SPIM in MATLAB/Simulink is done using,” pp. 35–43, 2020.

[28] A. Gündoğdu and R. Çelİkel, “Performance Analysis of Open Loop V / f Control Technique for Six-Phase Induction Motor Fed By A Multiphase Inverter Çok Fazlı İnverterden Beslenen Altı Fazlı İndüksiyon Motorun Açık Çevrim V / f Kontrol Tekniğinin Performans Analizi,” vol. 15, no. 2, pp. 111–125, 2020.

[29] Gundogdu A and Celikel R, “Performance Analysis of Open Loop V/f Control Technique for Six-Phase Induction Motor Fed By A Multiphase Inverter,” *Turkish J.*

Sci. Technol., no. September, 2020.

[30] F. O. F. Engineering, "SIX-PHASE INDUCTION MOTOR THESIS BY DEPARTMENT OF ELECTRICAL / ELECTRONIC ENGINEERING FACULTY OF ENGINEERING," no. June, pp. 1–77, 2020.

[31] David Williams, "Understanding, Calculating, and Measuring Total Harmonic Distortion (THD)," 2017. [Online]. Available: https://www.allaboutcircuits.com/technical-articles/the-importance-of-total-harmonic-distortion/. [Accessed: 20-Oct-2020].

[32] M. H. A. Yazdian and V. M. Mohamadian, "Three-phase dual-output six-switch inverter," vol. 5, no. May, pp. 1634–1650, 2012.

[33] "Induction Motor Price List," *ATO*, 2019. [Online]. Available: https://www.ato.com/induction-motor-price-list. [Accessed: 05-Apr-2020].

[34] B. Kundrotas, S. Lisauskas, and R. Rinkeviciene, "Model of Multiphase Induction Motor," vol. 5, no. 5, pp. 111–114, 2011.

[35] E. Toussaint, "5 benefits of multi-phase motors and inverters," 2016.

[36] K. N. Gyftakis and J. Kappatou, "The Impact of the Rotor Slot Number on the Behaviour of the Induction Motor," vol. 2013, 2013.

[37] B. A. Welchko, T. A. Lipo, L. Fellow, T. M. Jahns, S. E. Schulz, and S. Member, "Fault Tolerant Three-Phase AC Motor Drive Topologies : A Comparison of Features , Cost , and Limitations," vol. 19, no. 4, pp. 1108–1116, 2004.

Appendix

Glossaries

V_a, V_b, V_c **:** Phase a, b, c stator voltages respectively for 1st set

V_x, V_y, V_z **:** Phase x, y, z stator voltages respectively for 2nd set

λ_{qs2} λ_{qs1}**:** Stator flux linkages on q- axis

λ_{ds1} , λ_{ds2} **:** Stator flux linkages on d- axis

i_{qs1} i_{qs2} i_{ds1} i_{ds2} : Stator currents components on d- and q-axis

i_{qr} i_{dr} : Rotor d-axis and q-axis currents components

V_{qs1} V_{qs2} V_{ds1} V_{ds2} : Stator winding voltages on d-axis and q-axis

V_{qr} V_{dr} : Rotor winding voltages on d-axis and q-axis

L_{ls} : Stator leakage inductance

L_m : Air gap inductance

L_{lm} : Stator mutual leakage inductance

L_{lr} : Rotor leakage inductance

d : Direct axis

q : Quadrature axis

V_{rms} : Induced voltage in the stator

ω_r : Rotor angular speed

p : Number of pole

T_L : Load torque

T_{em} : Electromagnetic torque